CALCIUM-ION EXCHANGE OF COAL FOR RETENTION OF SULFUR DURING COMBUSTION

Thesis By

Karl Kho-Chung Chang

In Partial Fulfillment of the Requirements

for the Degree of

Doctor of Philosophy

California Institute of Technology

Pasadena, California

1985

(Submitted January 7, 1985)

This thesis is dedicated to my parents,

who always knew that I was headed for graduate school.

ACKNOWLEDGMENTS

It is with my deepest appreciation that I acknowledge my thesis advisor, Professor George R. Gavalas, for his thoughtful suggestions and guidance throughout the second half of this project. He provided direction to my research, while allowing me the latitude to be creative. I would like to express my gratitude to my former advisor, the late Professor William H. Corcoran, who patiently guided me through difficult times. His ideas on professional and personal conduct will always be an inspiration to me. I would also like to acknowledge Professor Richard C. Flagan for his invaluable advice and contributions on the second half of this project.

The financial support of the California Institute of Technology and the Department of Energy is gratefully acknowledged.

I wish to express my warm thanks to Donna Johnson and Kathy Lewis for helping me prepare this thesis at moment's notice.

I thoroughly enjoyed the open and friendly atmosphere created here at Caltech by my fellow graduate students. In particular, I thank Murray, Puvin, Teri and Phil.

I would like to thank Hank Blauvelt and Alex Ortiz, whose years of companionship made life at Caltech more bearable. Special thanks go to Kwang-I Yu, who was always around when I needed advice and counseling. I also gratefully thank Ellen Johnson, who helped with my experiments and helped to keep me sane during the rigors of my last years at Caltech.

Most of all I want to thank my parents for their love and support for making all this possible.

Abstract

The kinetics of calcium-ion exchange of coal and the combustion of calcium-exchanged coals in a laminar flow furnace were investigated. Particle diffusion was found to be the rate-determining step for the process of ion exchange. A diffusion model gave good agreement with observed rates of ion exchange. Diffusion of ions in PSOC 680, a bituminous coal, was observed to be much slower than in PSOC 623, a lignite.

Retention of sulfur during combustion of calcium-exchanged coals was observed to increase with increasing particle residence and oxygen concentration in the combustion gas. Chemical reaction was found to be the rate-determining step in the capture of SO_2 by CaO in coal ash. The results of this study were interpreted in a proposed mechanism for the release and capture of SO_2.

Table of Contents

List of Tables

List of Figures

CHAPTER 1

INTRODUCTION

In the wake of world energy crises in the 1970's, coal has become an increasingly important source of energy. However, coal utilization gives rise to a number of ecological problems, among which are air pollution from particulates, nitrogen oxides and sulfur dioxide produced by combustion in utility boilers. Efforts to control sulfur emission during coal combustion have led to various commercial processes of post-combustion scrubbing. Because of the high cost and complex operation of these scrubbing processes, alternative methods of sulfur removal have been under active investigation. The most successful of these, fluidized combustion in a bed of calcined limestone or dolomite, is already commercial in industrial boilers and might soon become commercialized in utility boilers. At the relatively low temperatures of fluidized combustion, sulfur oxides combine with the calcium or magnesium oxide particles to form stable sulfates. Fluidized combustion has several other advantages as well, but its application is limited to new power plants. Other methods of sulfur control suitable for existing pulverized coal-fired boilers rely on injecting the calcium sorbent with the coal and removing the spent sorbent with the ash. At the high temperatures of the pulverized coal flame, calcium sulfate is not thermodynamically stable. Therefore, sulfur oxide removal must exploit either rate limitations in the release of sulfur oxides or the capture of sulfur oxides in the cooler post-flame part of the furnace, where the equilibrium formation of sulfates becomes thermodynamically favorable.

Two modes of calcium sorbent injection have been investigated. The first involves the injection of ground limestone along with the coal either in a conventional furnace or in a furnace employing staged combustion (Case et al., 1982).

This method has the merit of extreme simplicity and low cost but has yielded sulfur removal in the range of 40-60%, insufficient to meet existing environmental standards. Evidently, the kinetics of sulfur oxide capture in the post-flame region of the furnace are not sufficiently rapid as observed by Borgwardt (1970), perhaps due to the slow diffusion within the partially sintered calcium oxide particles (Pigford and Sliger, 1973; Hartman and Coughlin, 1976).

Another method that has been investigated involves the calcium sorbent in closer association with the coal particles. One version is to impregnate the coal with a calcium solution and precipitate calcium carbonate right in the pores of particles. The other method is to add calcium by exchanging acidic groups in coal with calcium cations, using a suitable solution. This exchange may be represented by

$$2RH + CA^{++} \rightarrow R^{-}Ca^{++}R^{-} + 2H^{+}$$

where RH is a carboxylic or phenolic group in coal. Lignites have sufficient acidic groups for accepting as much as 6-8% calcium by weight. Bituminious coals do not possess sufficient acidic groups but they can acquire the required ion exchange capacity by mild oxidation ($\sim 200°C$) at the cost of losing some heating value. Adding calcium by ion exchange produces very fine, atomic-scale, dispersion in close association with the sulfur source resulting in more rapid kinetics of sulfur capture and reduced diffusional limitations due to deactivation of CaO by solid product layers.

Freund and Lyon (1982) studied the combustion of calcium-exchanged coal as a function of fuel equivalence ratio and found sulfur removal as high as 90% at sufficiently high equivalence ratios. At equivalence ratios used in conventional combustion the sulfur removal fell to 60% or lower. In view of this, they proposed this mode of calcium addition in connection with staged combustion.

In the first fuel-rich stage sulfur would be captured in the form of sulfide. If this fuel-rich stage is followed by an oxygen-rich stage, the sulfide would be converted to sulfate provided the temperature remains sufficiently low.

The present work examines both the kinetics of calcium-ion exchange of coal and the combustion of the calcium-exchanged coals in a laminar flow furnace under extreme fuel-lean conditions. The purpose of this study was to determine the mechanism of ion exchange of coal and the processes of sulfur dioxide release and recapture in the presence of finely dispersed calcium oxide during combustion.

References

Borgwardt, R. H., Env. Sci. Tech. **4**:59-63 (1970).

Case, P. L., Heap, M. P., McKinnon, C. N., Pershing, D. W. and Payne, R., Prepr. ACS Fuel Chemistry Division **27**:158-166 (1982).

Freund, H. and Lyon, R. K., Comb. Flame **45**:191-203 (1982).

Hartman, M. and Coughlin, R. W., AIChE J. **22**:490-498 (1976).

Pigford, R. L. and Sliger, G., Ind. Eng. Chem. Proc. Des. Dev. **12**:85-91 (1973).

CHAPTER 2

CALCIUM-ION EXCHANGE OF COAL

2.1 Introduction

Ion exchange of coal to incorporate calcium into the coal matrix for retention of sulfur during combustion has been shown to be promising in recent investigations by Freund and Lyon (1982), and Chang, Flagan and Gavalas (1984). The concept of ion exchange utilizes the presence of acidic functional groups in coal to exchange the hydrogen ions with calcium ions in an alkali medium. One of the factors that determines the success of the method of ion exchange for sulfur emission control is the ability to incorporate a sufficient amount of calcium into the coal sample so that a desired level of Ca/S molar ratio (Ca/S = 1 for theoretically complete retention of sulfur by exchanged calcium) may be obtained. This criterion, in turn, is dependent on the ion-exchange capacity of the coal and the process of ion exchange.

The characterization of the ion-exchange capacity of coal has been studied in detail (Fuchs and Sandhoff, 1940; Brooks and Sternhell, 1957; Schafer, 1970; Schobert, 1984). It was found that the occurrence of acidic groups increased as the rank (or carbon content) of the coal sample decreased, thus low-rank coals such as lignites generally possess a sufficient content of acidic groups to achieve Ca/S ratios greater than 1 by calcium-ion exchange. Higher-rank coals such as bituminous coals, on the other hand, do not possess sufficient acidic groups, but they can acquire the required ion-exchange capacity by mild oxidation at the cost of losing some heating value (Brooks and Maher, 1957; Kalema, 1985).

A survey on the topic of kinetics of ion exchange revealed that a significant number of studies (Boyd, Adamson and Meyers, 1947; Reichenberg, 1953; Kressman and Kitchener, 1949; Helfferich, 1962) have been conducted on theoretical

and experimental aspects of ion exchange. However, the materials examined in all cases were monofunctional ion-exchange resins whose physical and chemical properties were relatively well characterized. Currently there are no available data on the kinetics of ion exchange of coal, possibly due to the complex nature of the system which involved not only a complicated pore-size distribution but also a range of acidic groups of varying strengths.

In the present work the kinetics of calcium-ion exchange of two different types of coal were studied in a batch reactor. The purpose of this study was to elucidate the mechanism and kinetics of ion exchange of coal in order to utilize the ion-exchange properties of coal to incorporate calcium into the coal structure for possible retention of sulfur during combustion. The effects of chemical kinetics, film diffusion, partial diffusion, pH and partial oxidation were evaluated.

2.2 Experimental

2.2.1 Coal Preparation

Two coals of different rank from the Pennsylvania State University Coal Bank were selected for this study. Elemental analyses for the coals, PSOC 623, a Texas Darco lignite, and PSOC 680, an Indiana No. 6 high volatile B bituminous, are presented in Table 2.1. Since the ion-exchange properties of coal are dependent on oxygen content, an oxygen content of 14.29% for PSOC 623 and 9.53% for PSOC 680 suggests considerable differences in the acid groups present in the coals.

The coal samples were ground to 120x200 U.S. mesh size and treated with dilute acid to remove minerals from the solid. The ground coal was stirred with 1.0 N HCl in a ratio of 10 ml/g for 24 hours at 40°C. The acid treatment was sufficient for the removal of the cations of Ca, Mg, Na, and K associated with the

Table 2.1

Elemental Analyses of PSOC 623 (Darco Lignite) and PSOC 680 (Indiana No. 6) on a Dry Basis Provided by the PSU Coal Bank

	PSOC 623	PSOC 680
% Ash	16.60	11.91
% Carbon	60.67	68.47
% Hydrogen	4.27	4.59
% Nitrogen	1.07	1.52
% Sulfur	1.13	3.58
% Oxygen (diff.)	14.29	9.53

organic acid sites. After the acid wash, the slurry was filtered and rinsed with demineralized water to neutral pH. The powder was then vacuum dried at 105°C for 24 hours.

2.2.2 Experimental Apparatus and Procedure

2.2.2.1 Coal Oxidation

Oxidation of the bituminous coal samples in air was carried out in a fluidized-bed reactor, shown as a block diagram in Fig. 2.1. The reactor was a stainless steel pipe with a length of 58 cm and a diameter of 2.5 cm. The reactor and air preheater were heated externally by semi-cylindrical ceramic elements. The temperature was monitored with an Inconel-sheathed, type K thermocouple probe inserted into the middle of the fluidized-coal bed, as illustrated in Fig. 2.2. Coal samples were introduced into the empty reactor from the feed hopper through the draft tube. The steel wool and glass wool at the top of the reactor serve to contain entrained coal in the exit stream.

At the start of a reaction, the gas line to the draft tube was opened and the flow of fluidizing air was directed through the hopper. The coal was carried down the draft table into the bottom of the reactor. When the hopper was empty, the fluidizing air was switched back to the bottom of the reactor. Each oxidation experiment was conducted with approximately 20 g of coal. The temperature of the reactor was maintained within 5°C of the desired value.

2.2.2.2 Ion Exchange of Coal

The experimental apparatus used in this study is shown in Fig. 2.3. The reactor vessel was a 400 ml beaker placed in a water bath maintained at a constant temperature. The temperature of the reaction mixture was monitored with an immersed thermometer. A stream of nitrogen was used to purge the reactor of air in order to minimize the oxidation of coal in the presence of alkali and to

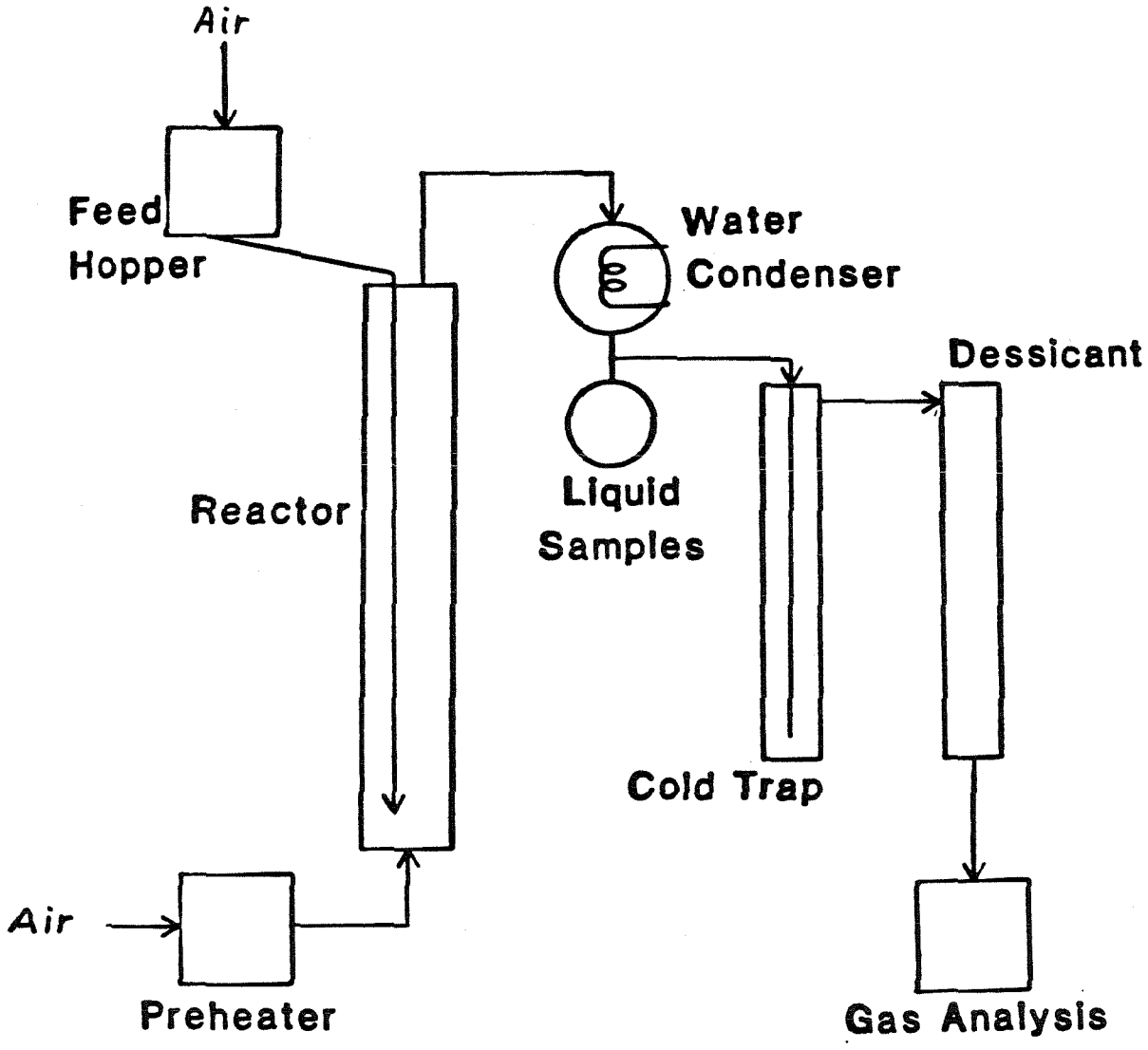

Fig. 2.1 Fluidized-bed reactor.

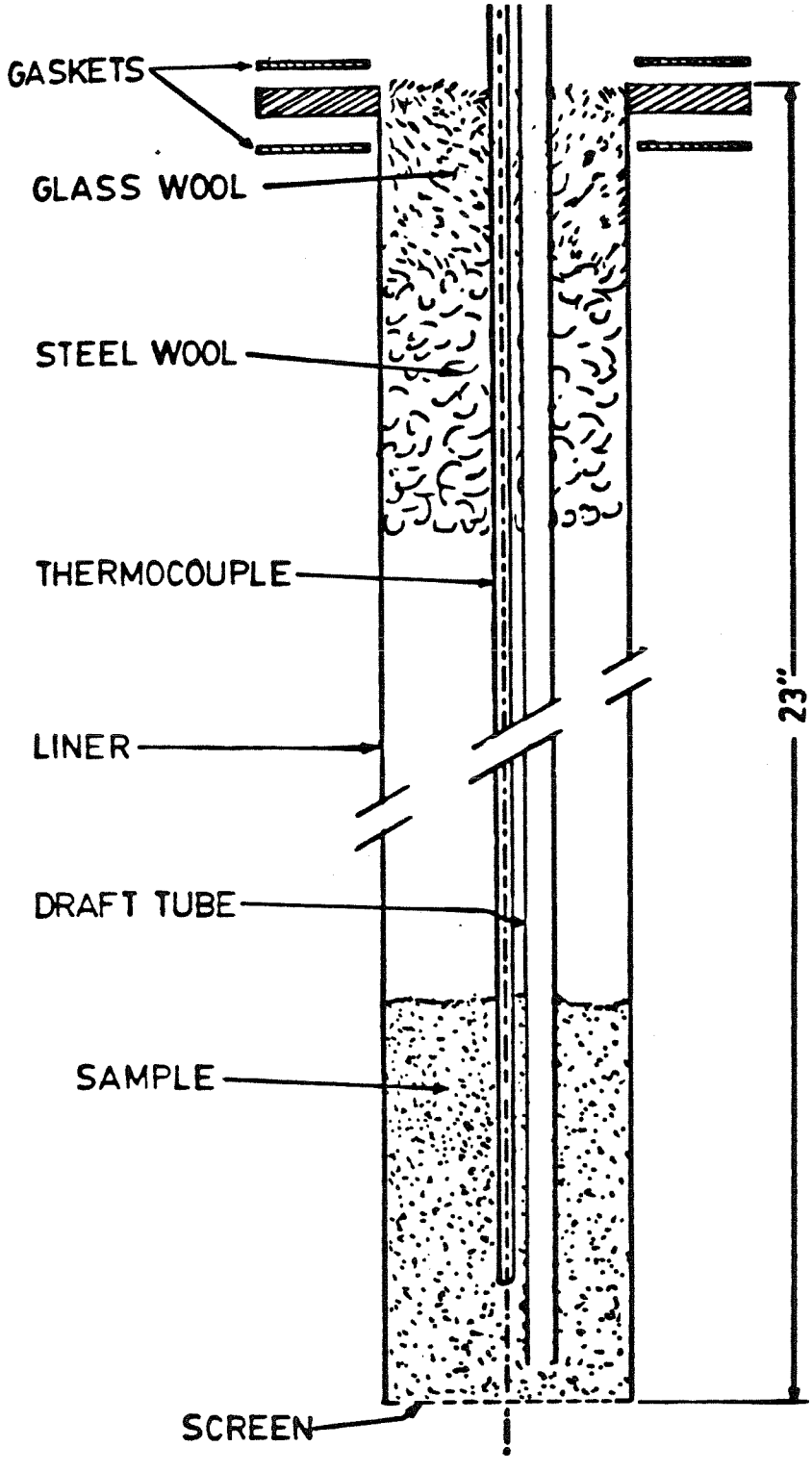

Fig. 2.2 Cross-sectional view of reactor (not to scale).

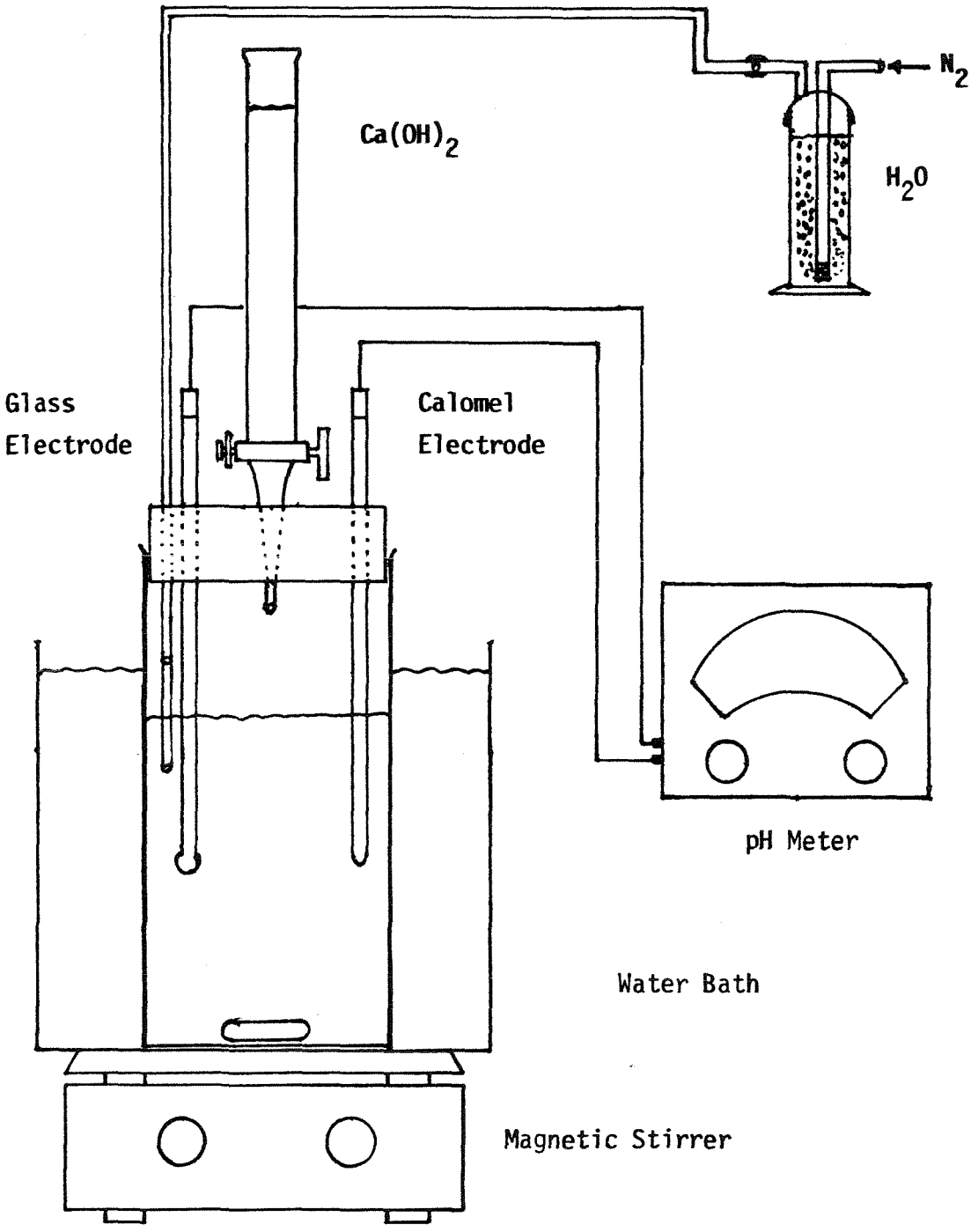

Fig. 2.3 Ion-exchange apparatus.

prevent the absorption of atmospheric CO_2 by the solution. The coal slurry was well mixed with a magnetic stirrer while the water bath was agitated with a variable speed stirrer.

Approximately 0.5 g of coal sample was added to the reactor along with 10 ml of demineralized water. The coal-water slurry was mixed for ten minutes to ensure that the coal particles were wetted thoroughly, thus reducing film-diffusional resistance on the particle surface. At the start of the reaction, 190 ml of pH-adjusted calcium acetate solution was added to the reactor. The reactor was sealed quickly and the reaction slurry was maintained at the initial pH value with the continuous addition of standard 0.03 N $Ca(OH)_2$ solution. The amount of $Ca(OH)_2$ titrant used was recorded at discrete periods of time. The extent of ion exchange at each time interval was then calculated from the volume of titrant as follows:

$$Q_t = \frac{V_{Ca(OH)_2} N_{Ca(OH)_2}}{1000\ w} \qquad (2\text{-}1)$$

where

Q_t = the extent of calcium exchange at time t, g. equiv./g sample.

$V_{Ca(OH)_2}$ = volume of $Ca(OH)_2$ titrant at time t, ml.

$N_{Ca(OH)_2}$ = normality of $Ca(OH)_2$ solution, g.equiv./l.

w = weight of coal sample, g.

Special care was taken to ensure that the pH measurements were accurate and reproducible. The pH was measured with a calomel-glass-electrode pair and a Radiometer pHM-26 pH meter. The calomel electrode was kept filled with saturated-KCl solution in the presence of KCl crystals. The electrode was stored in saturated-KCl solution when not in use. Prior to an experiment, the elec-

trodes were placed in a pH 7 buffer solution for half an hour to equilibrate. At the end of the half hour the meter was calibrated to pH 7. The electrode pair was then immersed in a pH 10 buffer solution to adjust the slope of the meter response. In a well-stirred solution, the response time of the pH meter was approximately five seconds.

2.2.3 Analysis of Ion-Exchange Capacity of Coal

2.2.3.1 Carboxyl Group Determination

The carboxylic-acid-group content of coal was determined by using a procedure developed by Schafer (1970). A 0.5-1.0 g sample of acid-washed 120x200 mesh coal was refluxed for four hours with 75 ml of 1 N barium acetate solution which had been adjusted to pH 8.3 with either dilute $Ba(OH)_2$ or HCl. The refluxed mixture was titrated back to pH 8.3 with 0.1 N $Ba(OH)_2$. The procedure of refluxing and titration was repeated once more to ensure that complete exchange had taken place. During refluxing in a basic solution, carboxylic-acid groups in the coal preferentially picked up barium ions and released hydrogen ions to the solution. Thus, the carboxylic-acid-group content of the coal was calculated from the volume of titrant as follows:

$$n_c = \frac{V_{Ba(OH)_2} N_{Ba(OH)_2}}{1000\ w} \qquad (2\text{-}2)$$

n_c = carboxylic-acid-group content, g. equiv./g sample.

$V_{Ba(OH)_2}$ = volume of $Ba(OH)_2$ titrant, ml.

$N_{Ba(OH)_2}$ = normality of $Ba(OH)_2$ solution, g.equiv./l.

w = weight of sample, g.

2.2.3.2 Total Acid Group Determination

The total acid-group content of coal was determined by adapting a procedure

developed by Blom et al. (1957). A 0.5 g sample of acid-washed 120x200 mesh coal was added to a 150 ml plastic bottle containing 50 ml of 0.1 N barium hydroxide solution. The bottle was purged with nitrogen and then sealed to prevent the oxidation of coal in the presence of alkali and the reaction of $Ba(OH)_2$ with atmospheric CO_2. The mixture was heated for 16 hours and the coal was then filterd and washed. During the alkali treatment at pH 12.5, all acid groups in coal preferentially picked up barium ions and released hydrogen ions. The excess $Ba(OH)_2$ in the filtrate and washings was titrated by 0.1 N HCl. The total acid-group content of the coal was calculated from the volume of $Ba(OH)_2$ and HCl as follows:

$$n_T = \frac{V_{Ba(OH)_2}N_{Ba(OH)_2} - V_{HCl}N_{HCl}}{1000\ w}, \qquad (2\text{-}3)$$

n_T = total acid-group content, g. equiv./g sample.

$V_{Ba(OH)_2}$ = volume of $Ba(OH)_2$, ml.

$N_{Ba(OH)_2}$ = normality of $Ba(OH)_2$ solution. g.equiv./l.

V_{HCl} = volume of HCl titrant, ml.

N_{HCl} = normality of HCl titrant, g.equiv./l.

w = weight of sample, g.

The phenolic-group content of the coal was taken as the difference between the total acid-group content and the carboxylic-acid-group content.

2.3 Results

Analysis of the acid-washed PSOC 623 sample shows that the lignite coal selected for this study has a total acid-group content of 5.16 meq/g. The carboxylic-acid-group content is determined to be 2.46 meq/g, thus the

difference of the two values establishes the phenolic-hydroxyl-group content at 2.70 meq/g.

The effect of particle size on the kinetics of calcium-ion exchange of the lignite coal at pH 8.3 is exhibited in Fig. 2.4. The results reveal a significant increase in the extent of exchange achieved as a function of time as the particle size decreased from 50x80 mesh (177-297 μm) to 120x200 mesh (74-125 μm). Figure 2.5 shows a slight dependence of the extents of exchange on the concentration of calcium ions in the exchange solution. Analysis of the data indicates that as the concentration of calcium ions increases from 0.05 N to 1.0 N, the initial rate of exchange increases, but the final rates of exchange are similar. The same type of behavior is observed in the effect of temperature as shown in Fig. 2.6. Figure 2.7 shows that as the pH of the ion exchange solution is increased, a corresponding increase in the extent of calcium exchange is obtained since some of the phenolic groups are also being exchanged as well as carboxylic-acid groups.

The total acid-group content of PSOC 680, the bituminous coal, is determined to be 2.41 meq/g with 0.41 meq/g of carboxylic-acid groups. Table 2.2 summarizes the results of partial oxidation of the bituminous coal sample at 195°C and 260°C for various periods of time. Both carboxylic-acid-groups and phenolic hydroxyl group contents are observed to reach maximum values as the time of oxidation was increased from 2 to 24 hrs at a reaction temperature of 195°C. Both acid-group contents are also observed to decrease as the reaction time was increased from 2 to 8 hrs at 260°C.

Figure 2.8 shows the experimental data for coal samples oxidized at 195°C. The results indicate that the extent of exchange achieved in a given time increases with the time of oxidation. The rates of calcium-ion exchange are

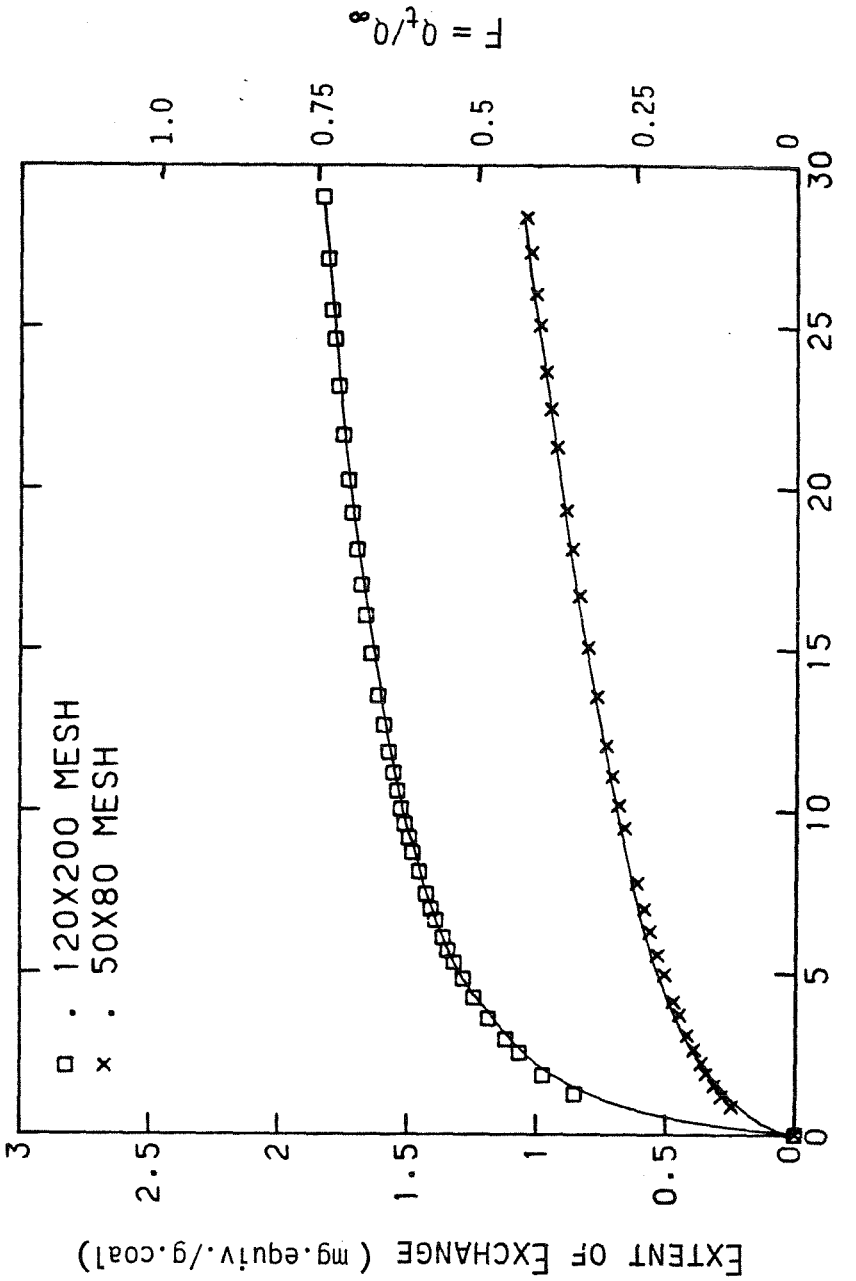

Fig. 2.4 Effect of particle size on the extent of calcium exchange of PSOC 623 at pH 8.3 and 22°C in 0.1 N [Ca^{++}].

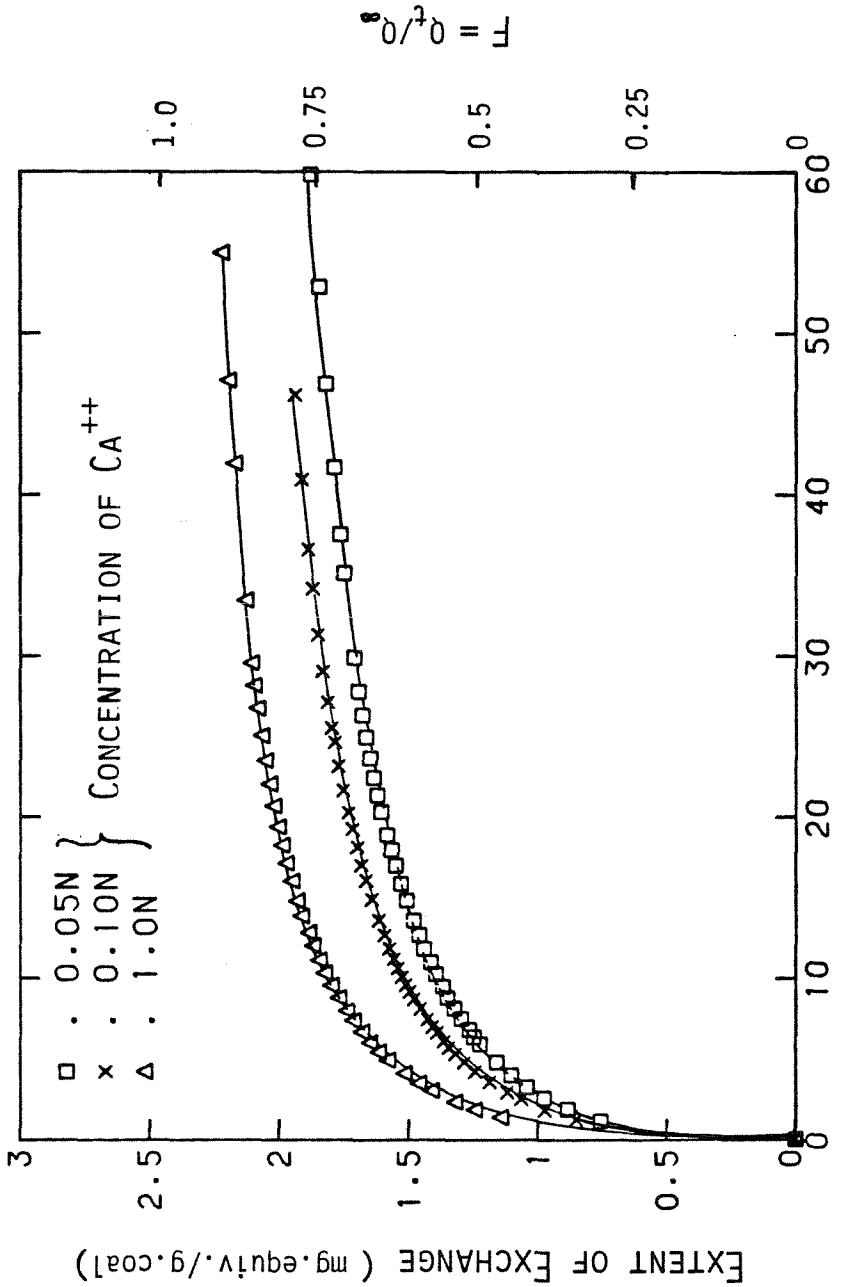

Fig. 2.5 Effect of calcium concentration on the extent of calcium exchange of PSOC 623 (120X200 mesh) at pH 8.3.

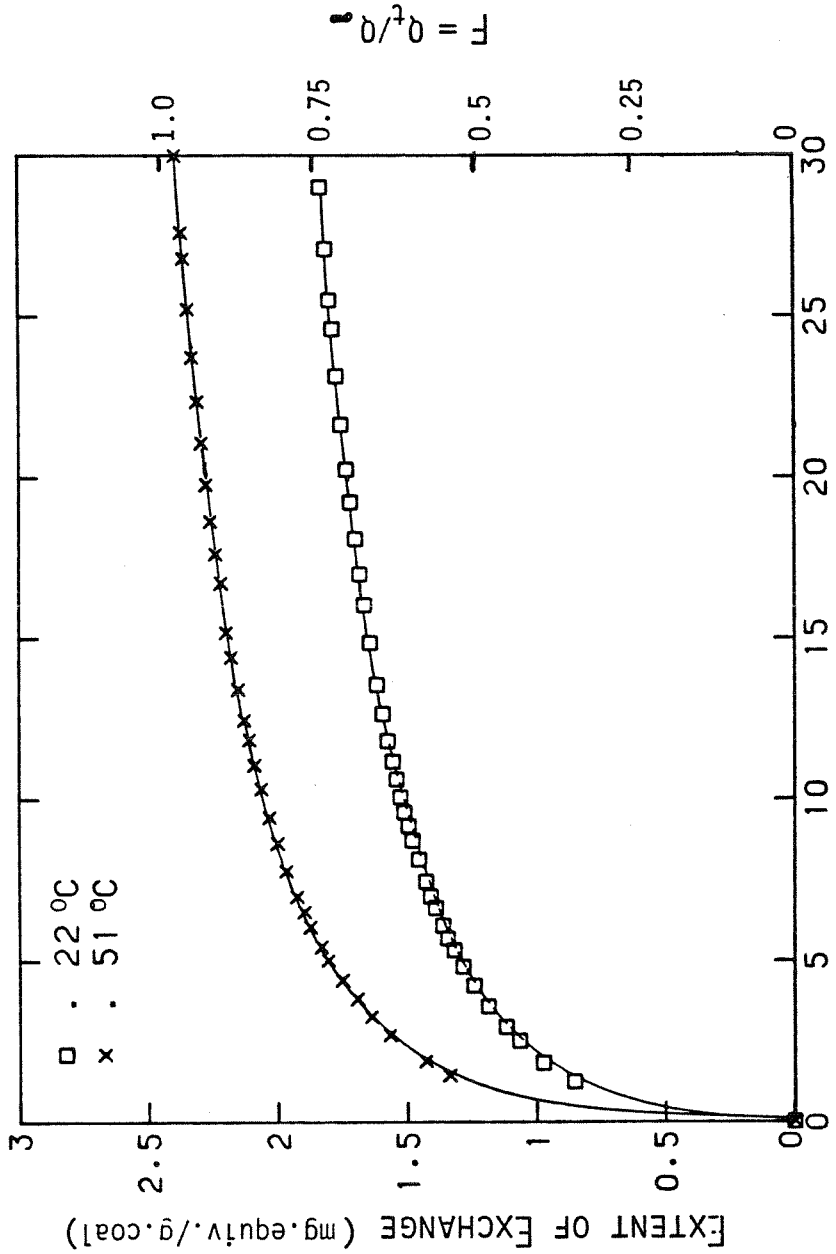

Fig. 2.6 Effect of temperature on the extent of calcium exchange of PSOC 623 (120X200 mesh) at pH 8.3 and 0.1 N [Ca^{++}].

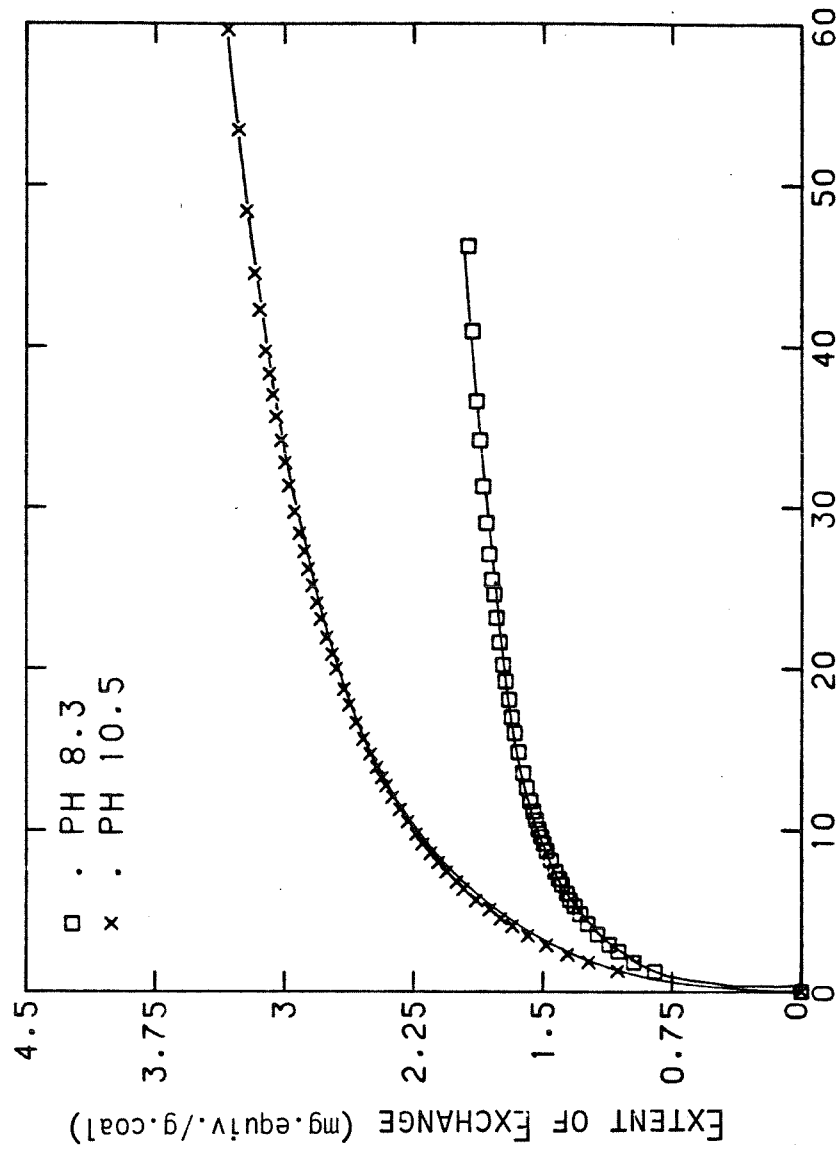

Fig. 2.7 Effect of pH on the extent of calcium exchange of PSOC 623 (120X200 mesh) at 22°C and 0.1 N [Ca^{++}].

Table 2.2

Effect of Partial Oxidation on the Content of Acidic Groups in PSOC 680

Temperature of Oxidation (°C)	Time of Oxidation (hr)	Carboxyl Groups (mg.equiv./g.)	Hydroxyl Phenolic Groups (mg.equiv./g.)	Total Acid Groups (mg.equiv./g)
-	-	0.41	2.00	2.41
195	2	0.59	2.79	3.38
195	8	2.21	3.54	5.75
195	24	2.13	4.06	6.19
260	2	2.31	3.73	6.04
260	8	1.89	3.00	4.89

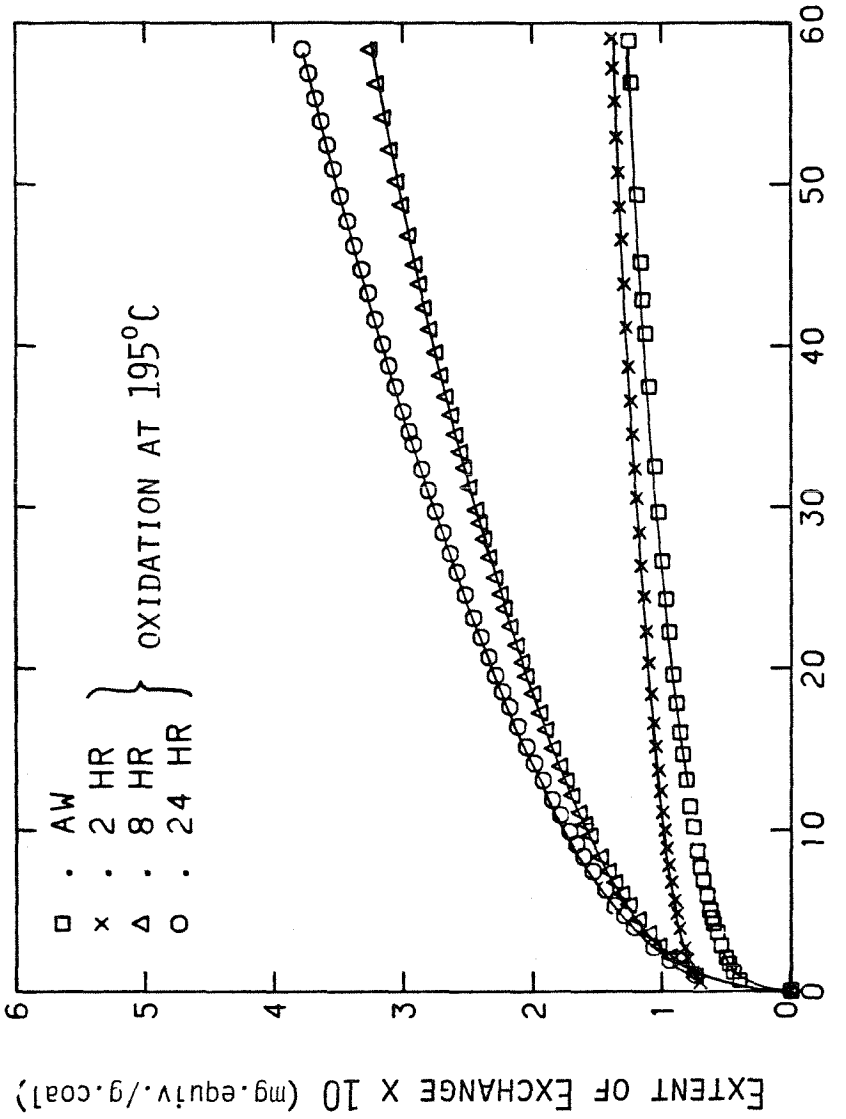

Fig. 2.8 Effect of oxidation at 195°C on the extent of calcium exchange of PSOC 680 at pH 8.3 and 0.1 N [Ca^{++}].

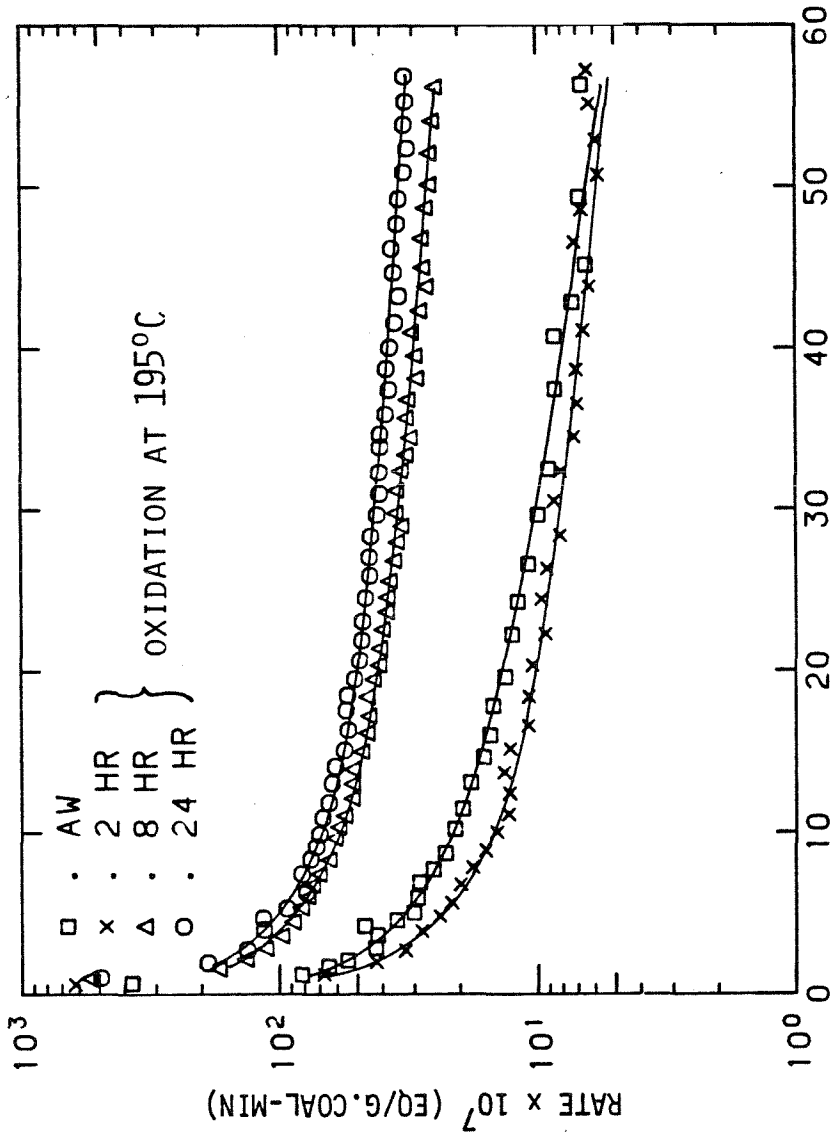

Fig. 2.9 Effect of oxidation at 195°C on the rate of calcium exchange of PSOC 680 at pH 8.3 and 0.1 N [Ca^{++}].

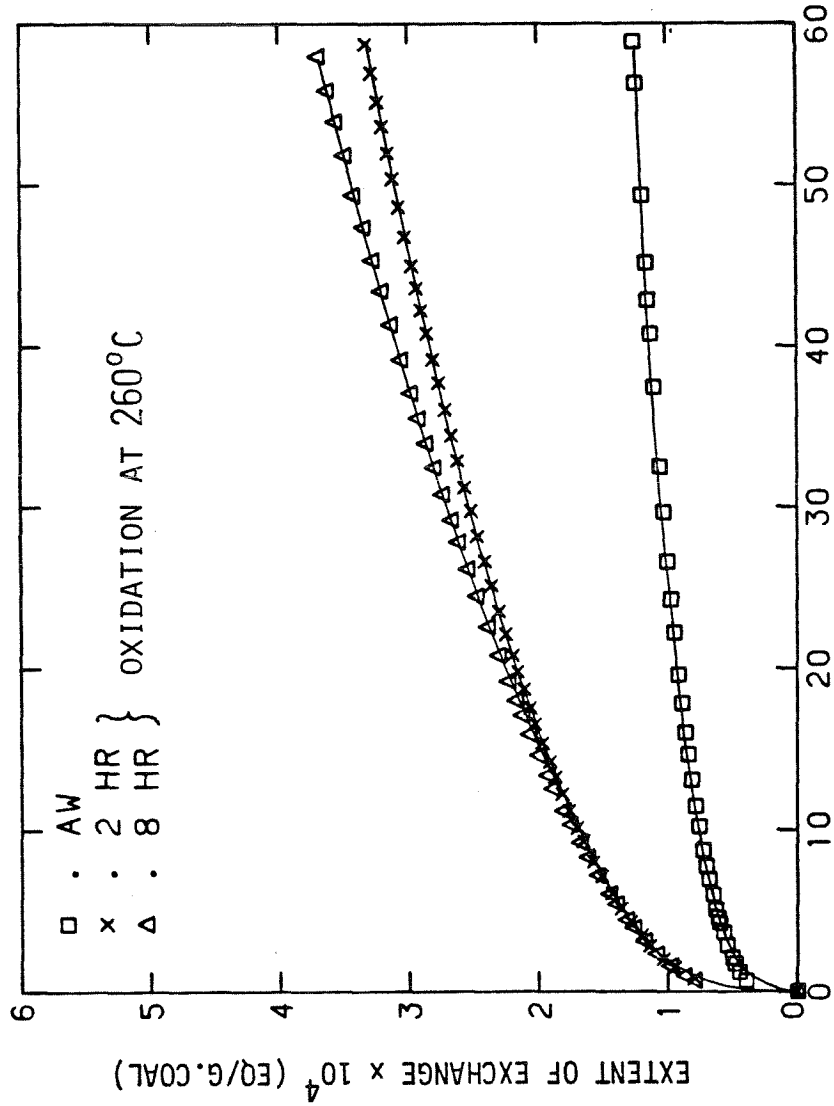

Fig. 2.10 Effect of oxidation at 260°C on the extent of calcium exchange of PSOC 680 at pH 8.3 and 0.1 N [Ca^{++}].

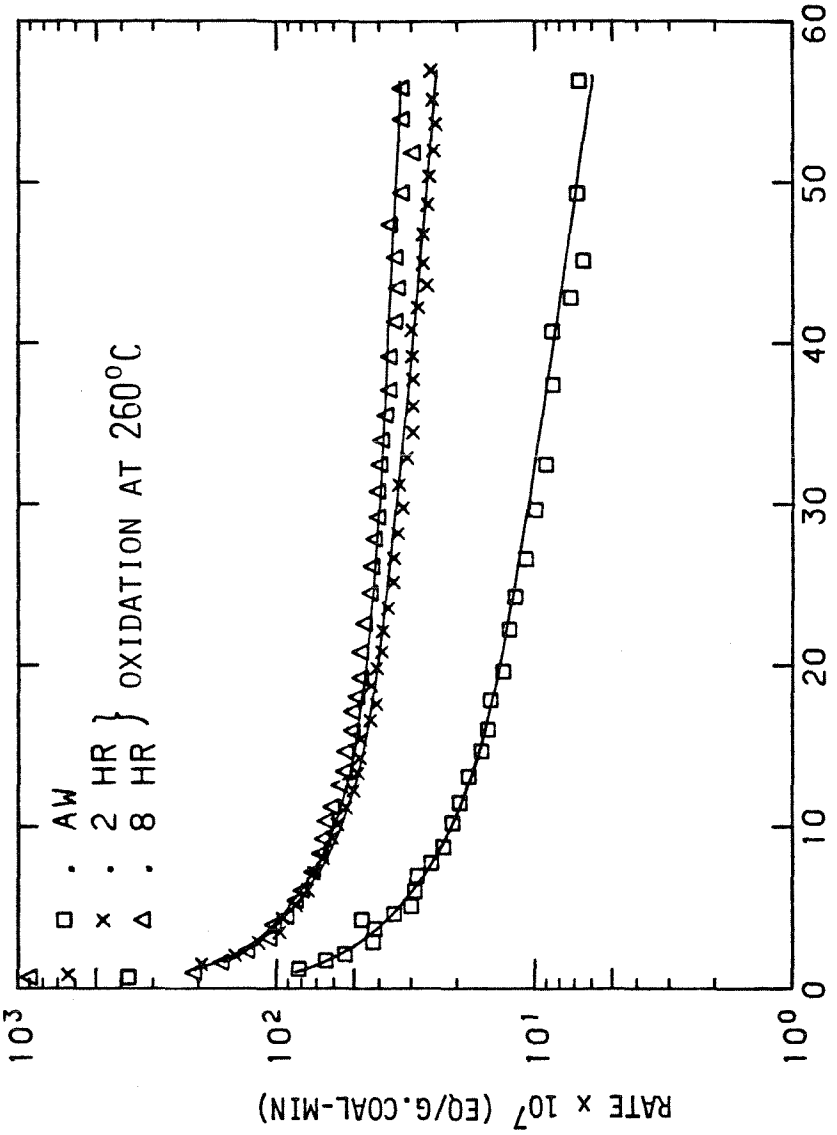

Fig. 2.11 Effect of oxidation at 260°C on the rate of calcium exchange of PSOC 680 at pH 8.3 and 0.1 N $[Ca^{++}]$.

shown to increase as the time of oxidation increases, Fig. 2.9. Similar results are observed for coal samples oxidized at 260°C as exhibited in Figs. 2.10 and 2.11.

2.4 Discussion

Calcium-ion exchange of acid groups in coal with calcium acetate may be written as a reversible chemical reaction:

$$2RH + Ca(CH_3COO)_2 \rightleftharpoons CaR_2 + 2CH_3COOH \tag{2-4}$$

where RH is either a carboxylic-acid group or a phenolic hydroxyl group. The equilibrium can be shifted toward the right by neutralizing the acetic acid formed during the reaction. If the pH value of the exchange solution is maintained at pH 8.2 to 8.3, then complete exchange of carboxyl groups may be achieved (Schafer, 1970). At pH values higher than 8.3, phenolic hydroxyl groups, weaker acids than carboxylic acids, will also undergo ion exchange. In terms of the ionic reaction, the equilibrium can be expressed as:

$$2R^-H^+(s) + Ca^{++}(aq.) \rightleftharpoons Ca^{++}(R^-)_2 + 2H^+(aq.) \tag{2-5}$$

The overall ion-exchange mechanism may be divided into five steps:

i. Diffusion of calcium ions through the solution up to the coal particles.

ii. Diffusion of calcium ions inside the coal particles.

iii. Chemical exchange between calcium ions and acid groups inside the coal particles.

iv. Diffusion of the displaced hydrogen ions out of the interior of the coal particles [reverse of step (ii)].

v. Diffusion of the displaced hydrogen ions through the solution away from the coal particles [reverse of step (i)].

Since the hydrogen ions released during ion exchange are neutralized readily

with the addition of $Ca(OH)_2$, the cation exchange resembles an acid-base reaction which is generally very fast. Thus, step (iii) is expected to be fast in comparison to diffusion processes, and the rate-controlling mechanism should be either film diffusion, steps (i) and (v), or particle diffusion, steps (ii) and (iv). Each of the diffusion mechanisms consists of two coupled processes due to conditions of electroneutrality surrounding the coal particles which cannot be violated.

2.4.1 Reaction Rate of Ion Exchange

The reaction rate for calcium-ion exchange of coal is not very well understood. If the reaction rate is assumed to follow the mass action relationship in Eq. (2-5), then the rate expression can be approximated by

$$-\frac{d[RH]}{dt} = k_f[RH]^2[Ca^{++}] - k_r[CaR_2][H^+]^2 , \tag{2-6}$$

where k_f and k_r are the forward and reverse reaction rate constants, respectively. Mass balance of the ion-exchange sites gives

$$[RH]_0 = [RH] + 2[CaR_2] , \tag{2-7}$$

where

$[RH]_0$ = initial condition concentration of exchange sites, mol/l.

$[RH]$ = concentration of exchange sites at time t, mol/l.

$[CaR_2]$ = concentration of exchanged sites, moles/l.

The ion-exchange experiments were conducted at constant pH values, thus $[H^+]$ is constant. The exchange solution also had an excess of calcium ions in order to keep $[Ca^{++}]$ relatively constant throughout each experiment.

Examination of the reaction rate terms in Eq. (2-6) reveals that the forward reaction rate is much faster than the reverse reaction rate because $[H^+]$ is

several orders of magnitude smaller than other terms in the expression. Thus, the reaction rate can be approximated by an irreversible second order reaction in $[RH]^2$ with

$$-\frac{d[RH]}{dt} = k_f^*[RH]^2 \tag{2-8}$$

where $k_f^* = k_f[Ca^{++}]$. The rate equation can be integrated to yield

$$\frac{1}{[RH]} - \frac{1}{[RH]_0} = k_f^* t\,, \tag{2-9}$$

which is rearranged to

$$\frac{1}{1-F} - 1 = k_f^*[RH]_0 t\,, \tag{2-10}$$

where $F = \dfrac{[RH]_0 - [RH]}{[RH]_0}$ is the fractional conversion of the ion-exchange sites. The ion-exchange experiments for PSOC 623 (120x200 mesh) conducted at pH 8.3 are analyzed according to the second-order rate expression given in Eq. (2-10). Figure 2.12 shows that the reaction does conform to second-order kinetics for a time interval up to about seven minutes. Analysis of the slopes of the straight line fit indicates that the second order reaction rate constant is 17 $l^2mole^{-2}sec^{-1}$ at 22°C and 49.7 $l^2mole^{-2}sec^{-1}$ at 51°C. The activation energy is estimated at approximately 7.0 kcal/mole.

The deviation of the reaction rate from second order kinetics suggests that the actual reaction rate may be more complicated than a simple second order reaction with respect to the concentration of ion-exchange sites, however chemical kinetics does not appear to be the rate-limiting process at higher time intervals. Figure 2.13 shows that the rate of ion exchange does not vary with temperature, which also supports the observation that the rate is not controlled by chemical kinetics. Experiments conducted with a larger particle size, 50x80 mesh, revealed a strong dependence of the rate on particle size, as shown in Fig.

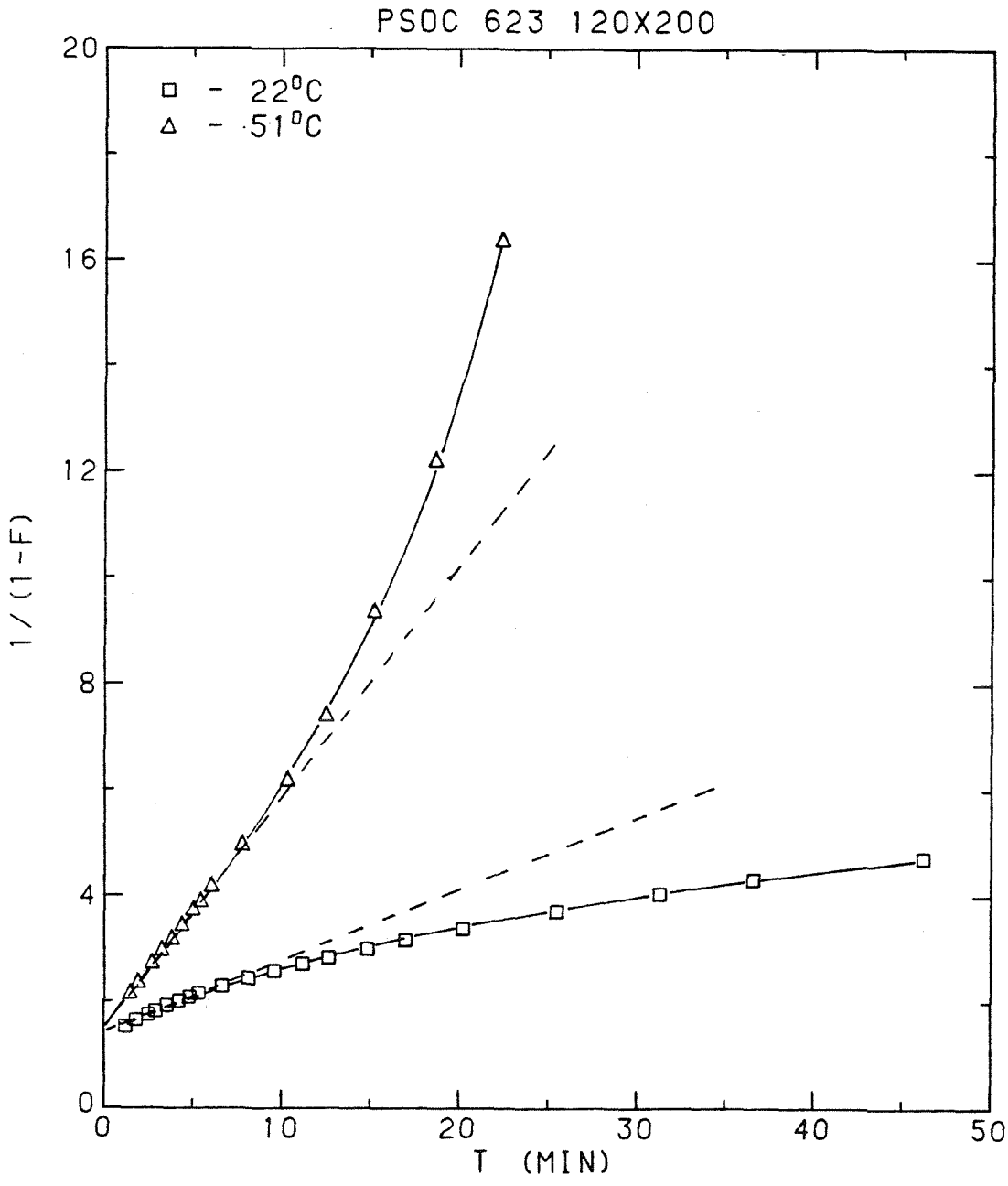

Fig. 2.12 Test of second order dependence of calcium exchange of PSOC 623 with respect to the concentration of carboxylic-acid groups.

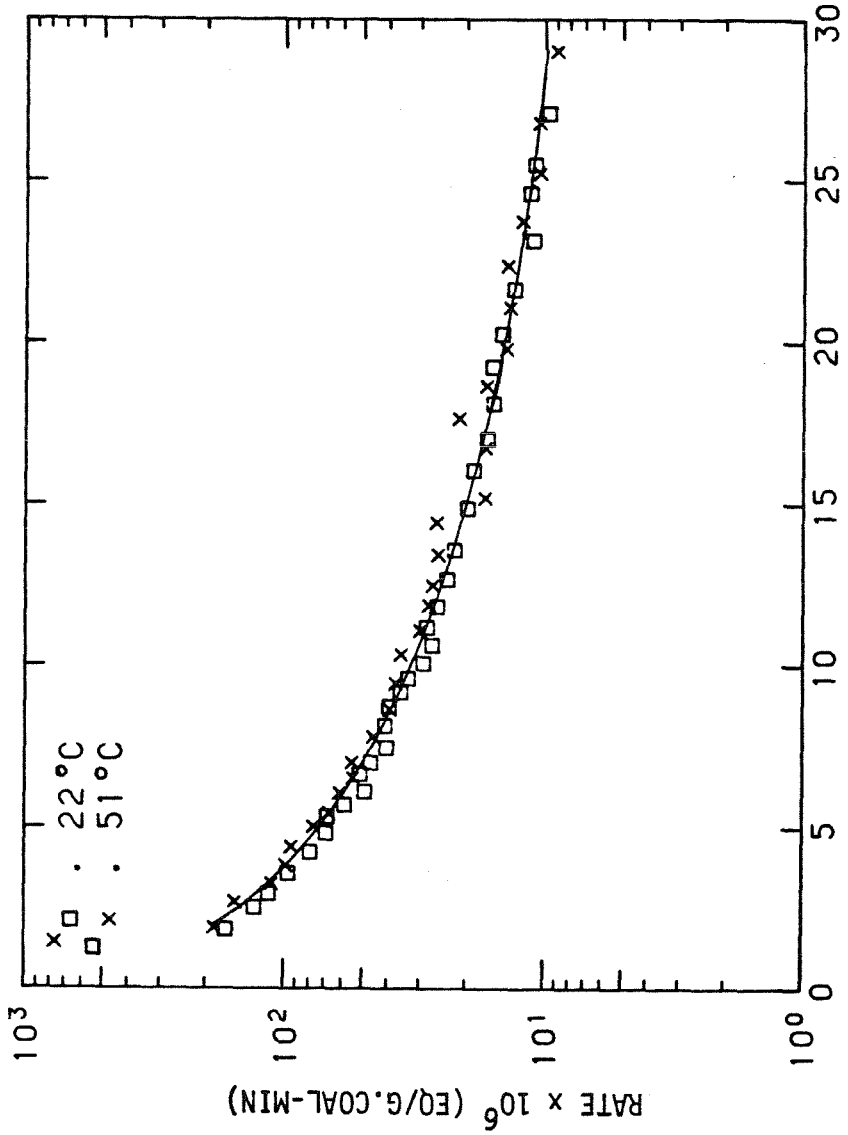

Fig. 2.13 Effect of temperature on the rate of calcium exchange of PSOC 623.

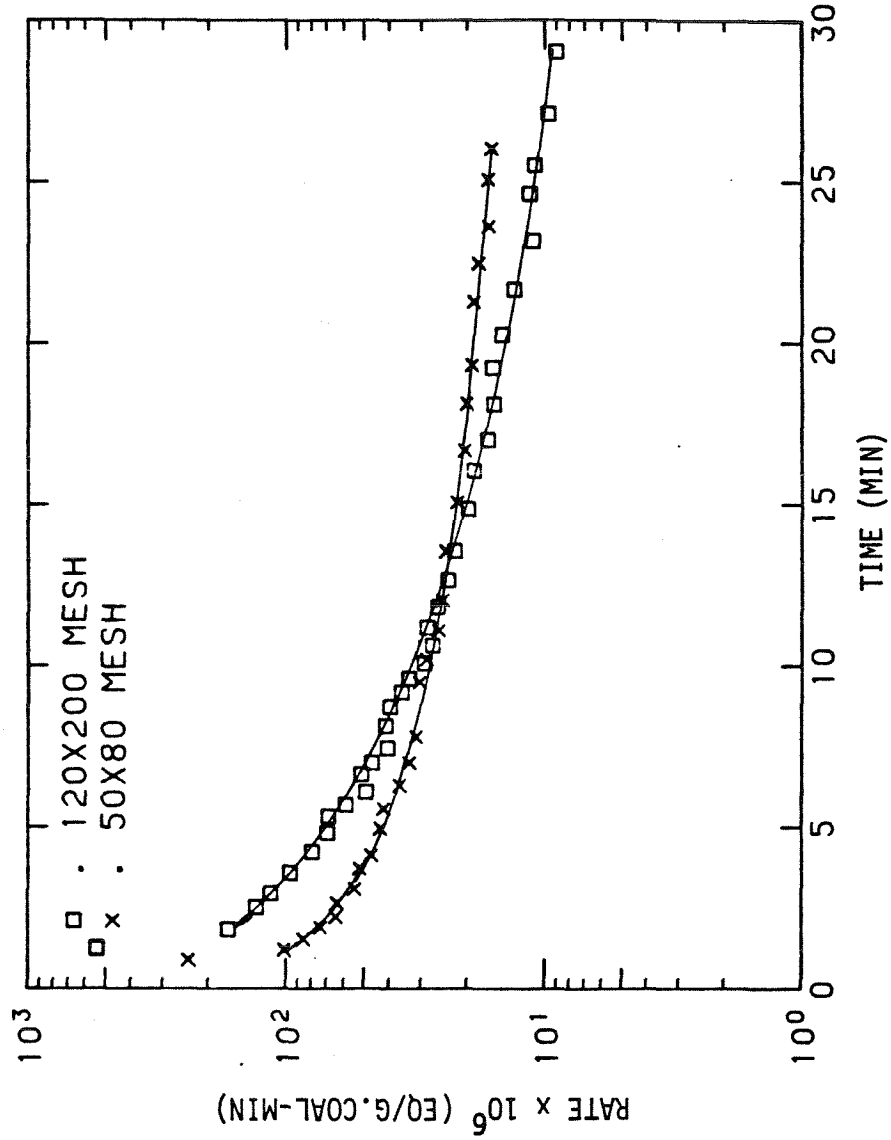

Fig. 2.14 Effect of particle size on the rate of calcium exchange of PSOC 623.

2.14. Since a chemical-reaction-controlled rate process would be independent of particle size, the observed dependence of the rate on particle size further indicates that the process of calcium-ion exchange of coal is not controlled by chemical kinetics.

2.4.2 Film Diffusion

In a film-diffusion-controlled process, there is a film of thickness δ surrounding the particles in which a concentration gradient exists. The flux of diffusing species is

$$N = -D\left[\frac{\partial C}{\partial r}\right], \tag{2-11}$$

where

D = diffusion coefficient of the diffusing species.

C = concentration of the diffusing species.

The total flowrate of diffusing species across the film is then

$$\frac{dQ_t}{dt} = 4\pi R^2 D\left[\frac{\partial C}{\partial r}\right]_{r=R}, \tag{2-12}$$

where

Q_t = total amount of diffusing species in time t.

R = radius of the spherical particles.

If the concentration gradient across the film is linear,

$$\left[\frac{\partial C}{\partial r}\right] = \frac{1}{\delta}(C_B - C_S), \tag{2-13}$$

and the concentration of the diffusing species on the surface of the particle, C_S, is equal to zero. Eq. (2-12) may be written as

$$\frac{dQ_t}{dt} = \frac{4\pi R^2 D}{\delta} C_B = \text{constant} , \qquad (2\text{-}14)$$

where

C_B = concentration of the diffusing species in the bulk solution.

Equation (2-14) suggests that the extent of ion exchange is a linear function of time. Figure 2.4 clearly exhibits a strong nonlinear dependence of the extent of exchange as a function of time, thus film diffusion is not expected to be the rate-limiting step.

The effect of film-diffusion can also be examined by evaluating the rate of mass transfer to the coal particles,

$$r = k_m A C_B , \qquad (2\text{-}15)$$

where

k_m = mass transfer coefficient,

A = surface area of the coal particles.

The mass transfer coefficient can be obtained from the expression

$$Nu = \frac{k_m d_p}{D} , \qquad (2\text{-}16)$$

where

Nu = Nusselt number, assumed to be equal to 2.

d_p = particle diameter.

The experiments were conducted with particles of 120x120 U.S. mesh size, so the average particle diameter is assumed to be 100 μm. The diffusion coefficient of calcium ions diffusing through a solution of 0.1 N calcium acetate can be estimated by (Perry and Chilton, 1973)

$$D = D_o\left[1 + \frac{m\partial \ln \gamma_{\pm}}{\partial m}\right] \frac{1}{C_w \bar{V}_w} \left[\frac{\mu_w}{\mu}\right], \qquad (2\text{-}17)$$

where

D_o = diffusivity of the diffusing species in a dilute solution.

$\gamma_{\pm}$ = mean ionic activity coefficient based on molarity.

C_w = g-mole water/cc of solution.

$\bar{V}_w$ = partial molar volume of water, cc/g·mole.

μ_w = viscosity of water.

μ = viscosity of solution.

The diffusion coefficient of calcium ions in a solution of 0.1 N calcium acetate is then estimated to be 7.1 x 10^{-6} cm^6/sec. The mass transfer coefficient is thus 1.42 x 10^{-3} cm/sec. The experiments were conducted with 0.25 g of coal with a density of approximately 1.3 g/cc. So the total external surface area of the coal particles is 115 cm^2. The estimated rate of mass transfer to the external surface of the coal particles is 4.9 x 10^{-4} moles/min, or 9.8 x 10^{-4} eq./min. This rate is far greater than the observed rates of ion exchange. Figure 2.15 also shows that the observed rate of exchange does not vary as the concentration of calcium ions is increased from 0.05 eq/l to 1.0 eq/l. Therefore, film diffusion is not the rate-limiting step for calcium-ion exchange of coal.

2.4.3 Particle Diffusion

The diffusion of calcium ions through coal particles in the presence of very fast film diffusion and reaction can be approximated by the shrinking-core model. This model assumes that reaction occurs first at the outer surface of the particle. The zone of reaction then moves into the solid, and leaves behind completely converted material and inert solid, which is referred to as ash. Thus,

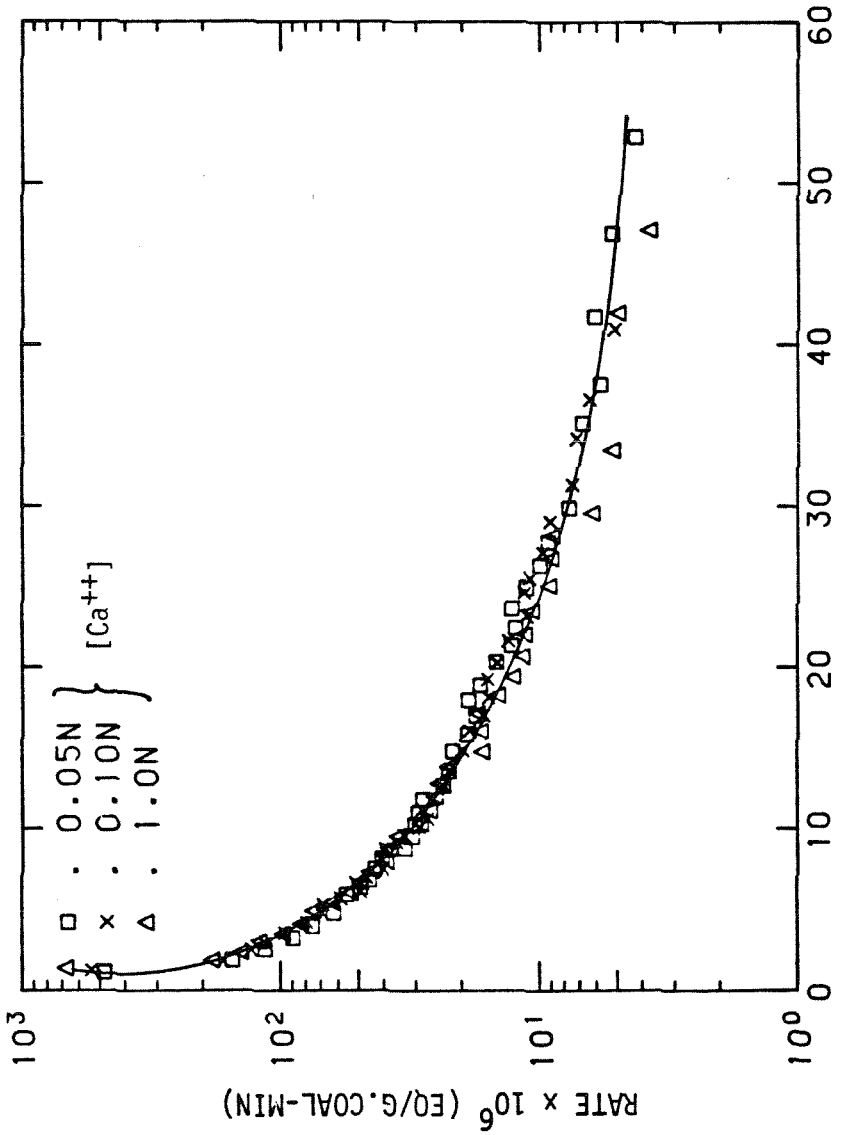

Fig. 2.15 Effect of calcium concentration on the rate of calcium exchange of PSOC 623.

at any time there exists an unreacted core of material which shrinks in size during reaction. If the shrinkage of the unreacted core is much slower than the flow rate of reactant, which is calcium ions for the case of ion exchange, toward the unreacted core, then the unreacted core can be assumed to be stationary in considering the concentration gradient of calcium ions in the ash layer at any time. The rate of reaction of calcium exchange is then given by its rate of diffusion to the reaction surface,

$$-\frac{dN_{Ca}}{dt} = 4\pi r^2 Q_{Ca} = \text{constant}\,, \tag{2-18}$$

and the flux of calcium ions within the ash layer can be expressed by Fick's law,

$$Q_{Ca} = De\,\frac{dC}{dr}\,, \tag{2-19}$$

where

De = effective diffusion coefficient.

C = concentration of calcium ions at a distance r from the center of the particle.

Integrating Eq. (2-18) across the ash layer gives

$$-\frac{dN_{Ca}}{dt}\left(\frac{1}{r_c} - \frac{1}{R}\right) = 4\pi DeC\,, \tag{2-20}$$

where

R = radius of the particle.

r_c = radius of the unreacted core.

The final solution is given by Levenspiel (1972) as

$$\frac{t}{\tau} = 1 - 3(1-F)^{2/3} + 2(1-F)\,, \tag{2-21}$$

where

F = the fractional conversion of ion exchange sites in coal.

The time required for complete conversion of ion exchange sites in a coal particle is

$$\tau = \frac{\rho_B R^2}{6bDeC}, \tag{2-22}$$

where

ρ_B = molar density of ion exchange sites in the particle.

b = stoichiometric coefficient for ion exchange sites, which is equal to 2 when the reactant is calcium ion.

The experimental data for the calcium-ion exchange of carboxylic acid groups in PSOC 623 are tested against Eq. (2-21), as shown in Fig. 2.16. The results show that the data for the 50x80 mesh coal particles follow the behavior for particle diffusion according to the shrinking-core model. The time for complete conversion of carboxylic acid groups is obtained from the slope of the linear relationship to be 6.6 hrs. The effective diffusion coefficient is then estimated to be 1.6 x 10^{-8} cm^2/sec. The data for the 120x200 mesh particles deviate from the particle diffusion expression of Eq. (2-21). However, a reasonable agreement can be obtained after the reaction has proceeded for longer than 15 minutes. The time for complete conversion based on the data in the linear region is estimated as 3.8 hrs. The corresponding effective diffusion coefficient is approximately 4.9 x 10^{-9} cm^2/sec.

The deviation of the data for ion exchange of 120x120 mesh coal particles from the prediction of the shrinking-core model may be attributed to the effect of electric fields from ionic interactions (Helfferich and Plesset, 1957). The electric potential in the particles increases as the diffusion of ions proceeds, thus resulting in a nonlinear diffusion process with a diffusion coefficient which varies

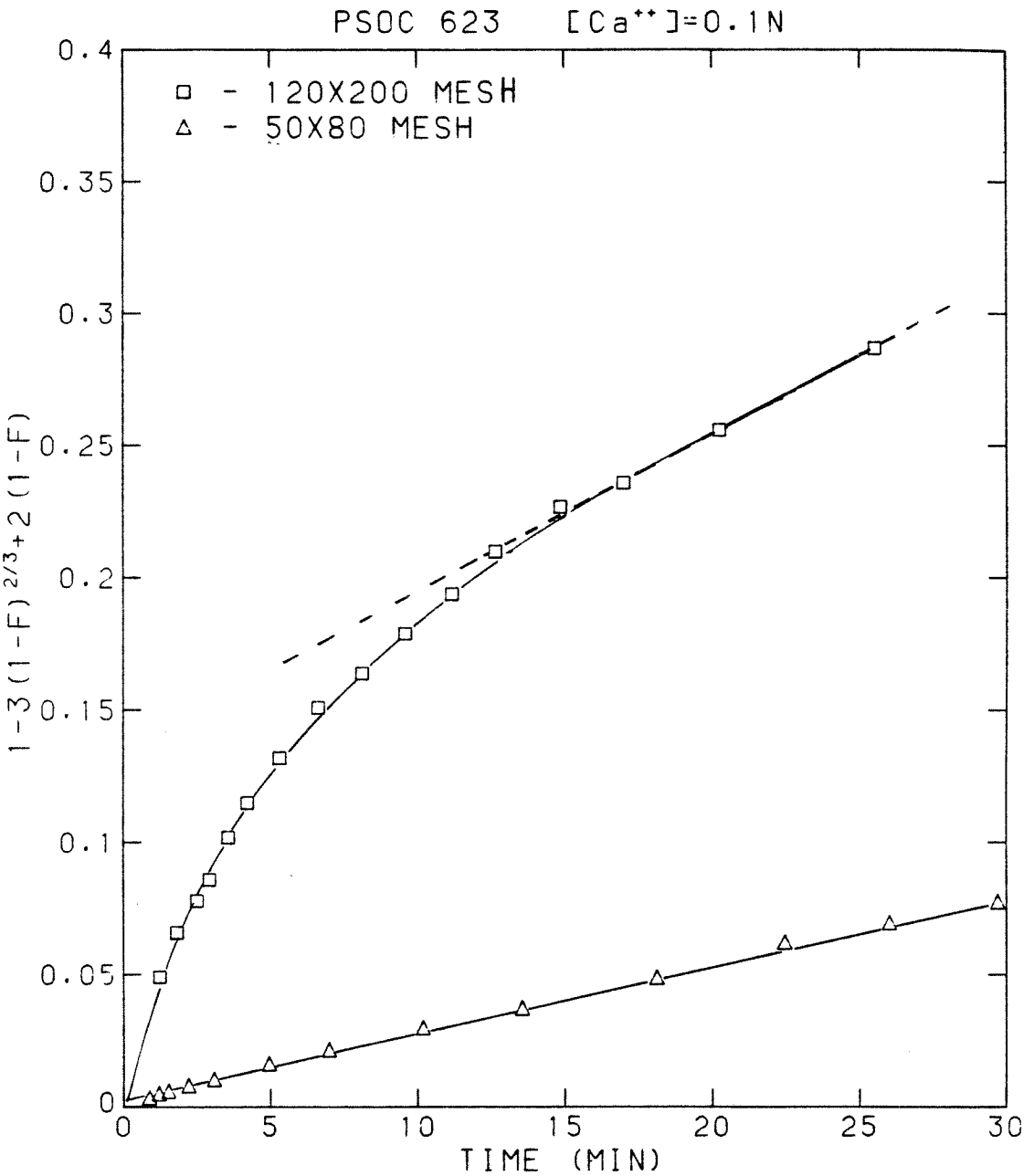

Fig. 2.16 Test of particle-diffusion limitation on calcium-ion exchange of PSOC 623.

with the concentration of ions in the particles.

2.4.4 Effect of Partial Oxidation

Partial oxidation of the bituminious coal sample, PSOC 680, at moderate temperatures in air is observed to increase the content of carboxylic-acid and phenolic hydroxyl groups in the sample as indicated in Table 2.2. The increase in the number of ion-exchange sites makes it possible to achieve higher Ca/S molar ratios in the coal for the purpose of sulfur emission control by the exchanged calcium during combustion of the coal. Table 2.3 shows that the level of Ca/S that can be obtained by exchanging carboxylic-acid groups increases from 0.18 to 1.03 simply by first oxidizing the sample at 260°C for two hours. Exchange of all the acid groups of the same sample increases the Ca/S level from 1.08 to 2.70.

The increase in the carboxylic-acid-group content results in the rates of calcium-ion exchange at pH 8.3 as shown previously in Figs. 2.9 and 2.11. However, the corresponding fractional conversions of the carboxylic groups is observed to decrease in Fig. 2.17 as the coal samples are oxidized. Analysis of the data indicates that the rates of ion exchange for the oxidized coals satisfy the criterion of particle diffusion as shown in Fig. 2.18. Table 2.4 shows that the experimentally determined diffusion coefficients for calcium and hydrogen ions in oxidized PSOC 680 are in the range of 5.0×10^{-11} to $3.5 \times 10^{-10} cm^2/sec$, which is approximately two orders of magnitude smaller than the diffusion coefficient obtained for diffusion in PSOC 623. Since the electrical field generated by the interaction of ions in the pore structure is most probably the cause of the observed low diffusivities compared to diffusivities of noncharged species (diffusion coefficients on the order of 10^{-7} to $10^{-6} cm^2/sec$), the experimental results suggest that the electrical potential in the pore structure of PSOC 680 is

Table 2.3

Effect of Oxidation on Ca/S Content Obtainable by Calcium-Ion Exchange of PSOC 680

Coal Sample	Oxidative Treatment T (°C)	Oxidative Treatment Time (hr)	Calcium Exchange of Carboxyl Groups Ca/S	Calcium Exchange of All Acid Groups Ca/S
PSOC 623	-	-	3.49	7.32
PSOC 680	-	-	0.18	1.08
PSOC 680	195	2	0.26	1.51
PSOC 680	195	8	0.99	2.57
PSOC 680	195	24	0.95	2.77
PSOC 680	260	2	1.03	2.70
PSOC 680	260	8	0.85	2.19

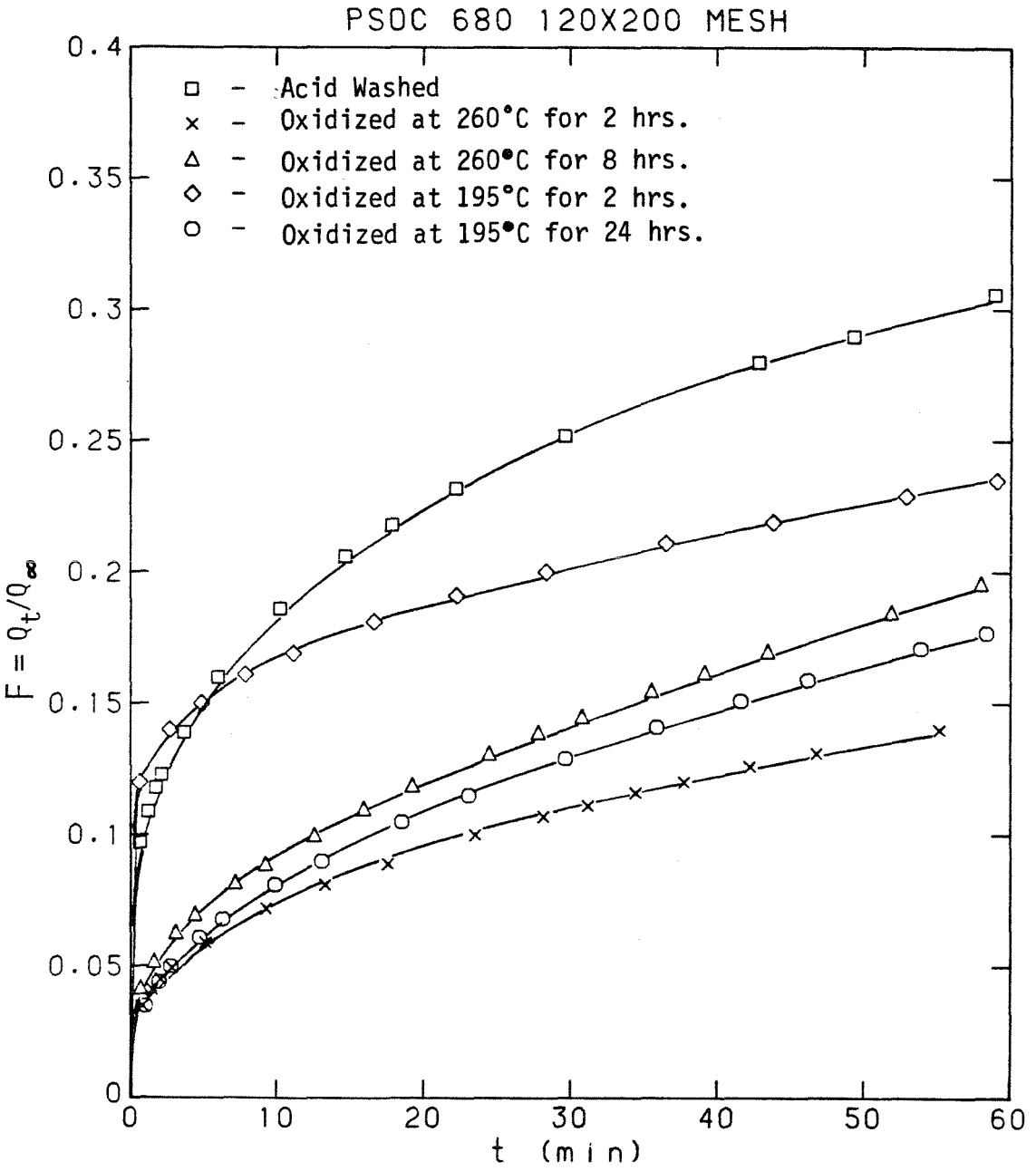

Fig. 2.17 Effect of partial oxidation on the fractional conversion of carboxylic-acid groups in PSOC 680.

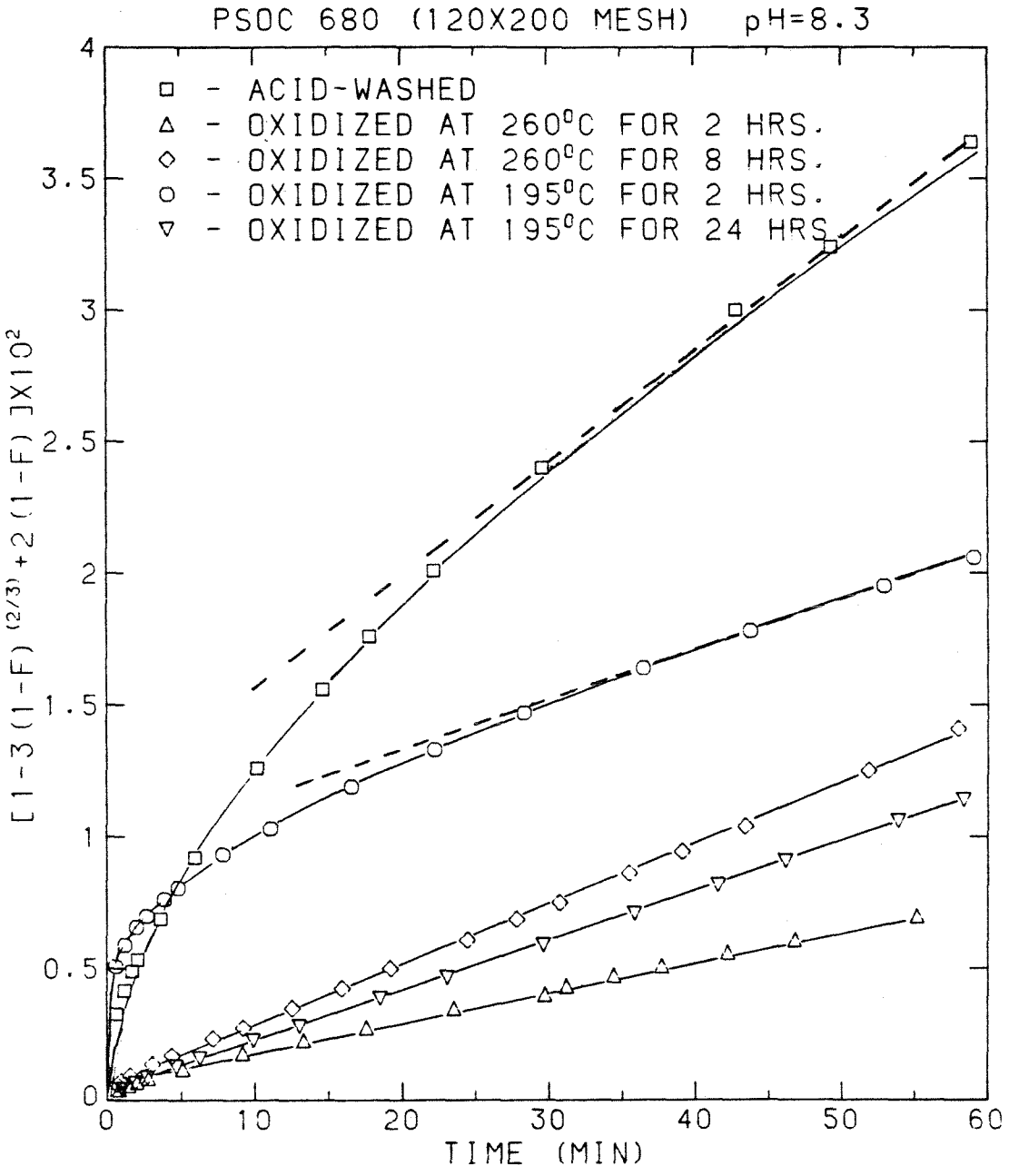

Fig. 2.18 Test of particle-diffusion limitation on calcium-ion exchange of PSOC 680.

Table 2.4

Calcium-Ion Exchange of Carboxylic-Acid Groups in Partially Oxidized PSOC 680 (120 x 200 mesh)

Oxidative Treatment			
T (°C)	Time (hr)	τ (hrs.)	$D_e \times 10^{10}$ (cm^2/sec)
-	-	40.	0.78
195	2	89.	0.50
	24	88.	3.5
260	2	145.	1.2
	8	73.	2.0

higher than in PSOC 623, which could be due to a pore-size distribution containing smaller pores.

2.5 Conclusions

The kinetics of calcium-ion exchange of coal was studied in an effort to elucidate the mechanism of ion exchange of coal. It was observed that the rate of ion exchange was dependent on particle size and pH value of the solution. Concentration of calcium ions and temperature of the exchange solution were found to affect only the initial rate of exchange. Analysis of the results indicates that particle diffusion is the rate-limiting step of the overall process of ion exchange of coal and that chemical reaction may be important in the first few minutes of reaction. Application of a particle diffusion criterion shows that the diffusion coefficient of calcium ions in 50x80 mesh PSOC 623, a lignite coal, is approximately 1.6×10^{-8} cm^2/sec. Partial oxidation of PSOC 680, a bituminous coal, was observed to increase both carboxylic-acid and phenolic hydroxyl group contents in the sample so that higher Ca/S levels may by achieved by ion exchange. Analysis of the particle diffusion behavior shows that the diffusion coefficient of calcium and hydrogen ions in partially oxidized PSOC 680 (120x200) is in the range of 5.0×10^{-11} to $3.5 \times 10^{-10} cm^2/sec$. The observed low diffusivities suggest the possible buildup of an electric field within the pore structure of coal as ion exchange progresses.

References

Blom, L., Edelhausen, L. and van Krevelen, D. W., Fuel **36**:135-153 (1957).

Boyd, G. E., Adamson, A. W. and Myers, Jr., L. S., J. Am. Chem. Soc. **69**:2836-2848 (1947)

Brooks, J. D. and Maher, T. P., Fuel **36**:51-62 (1957).

Brooks, J. D. and Sternhell, S., Aust. J. Appl. Sci. **8**:206-221 (1957).

Chang, K. K., Flagan, R. C. and Gavalas, G. R., presented at the Western States Section/The Combustion Institute, Palo Alto, October 22-23, 1984.

Freund, H. and Lyon, R. K., Comb. Flame **45**:191-203 (1982).

Fuchs, W. an Sandhoff, A. G., Fuel **12**:45-69 (1940).

Helfferich, F., "Ion Exchange", New York, N.Y. (1962).

Helfferich, F. and Plesset, M. S., J. Chem. Phys. **28**:418-428 (1958).

Kalema, W. S., "A Study of Coal Oxidation", PhD Thesis, California Institute of Technology (1985).

Kressman, T. R. E. and Kitchener, J. A., Disc. Faraday Soc. **7**:90-105 (1949).

Levenspiel, O., "Chemical Reaction Engineering", 2nd ed., N.Y., 1972.

Perry, R. H. and Chilton, C. H., ed., "Chemical Engineers' Handbook", 5th ed., 1973.

Reichenberg, D., J. Am. Chem. Soc. **75**:589-597 (1953).

Schafer, H. N. S., Fuel **49**:197-213 (1970).

Schafer, H. N. S., Fuel **49**:271-280 (1970).

Schobert, H. N., ed., "The Chemistry of Low-Rank Coals", ACS Symposium Series, No. 264 (1984).

CHAPTER 3

COMBUSTION OF CALCIUM-EXCHANGED COALS

3.1 Introduction

Sulfur emission control in coal combustion is currently practiced by various processes of post-combustion scrubbing. Because of the high cost and complex operation of these scrubbing processes, alternative methods of sulfur removal have been under active investigation. The most successful of these, fluidized combustion in a bed of calcined limestone or dolomite, is already commercial in industrial boilers and might soon become commercialized in utility boilers. At the relatively low temperatures of fluidized combustion, sulfur oxides combine with the calcium or magnesium oxide particles to form stable sulfates. Fluidized combustion has several other advantages as well, but its application is limited to new power plants. Other methods of sulfur control suitable for existing pulverized coal-fired boilers rely on injecting the calcium sorbent with the coal and removing the spent sorbent with the ash. At the high temperatures of the pulverized coal flame, calcium sulfate is not thermodynamically stable, hence sulfur oxide removal must exploit either rate limitations in the release of sulfur oxides or the capture of sulfur oxides released in the cooler post-flame part of the furnace, where the equilibrium of sulfur oxide capture becomes favorable.

Two modes of calcium sorbent injection have been investigated. The first involves the injection of ground limestone along with the coal either in a conventional furnace or in a furnace employing staged combustion (Case et al., 1982). This method has the merit of extreme simplicity and low cost but has yielded sulfur removal in the range of 40-60%, insufficient to meet existing environmental standards. Evidently, the kinetics of sulfur oxide capture in the post-flame region of the furnace are not sufficiently rapid as observed by Borgwardt (1970),

perhaps due to the slow diffusion within the partially sintered calcium oxide particles (Pigford and Sliger, 1973; Hartman and Coughlin, 1976).

Another method that has been investigated involves the calcium sorbent in closer association with the coal particles. One version is to impregnate the coal with a calcium solution and precipitate calcium carbonate right in the pores of the particles. The other method is to add calcium by exchanging acidic groups in the coal with calcium cations, using a suitable solution. This exchange may be represented by

$$2RH + CA^{++} \rightarrow R^{-}Ca^{++}R^{-} + 2H^{+} \tag{3.1}$$

where RH is a carboxylic or phenolic group in coal. Lignites have sufficient acidic groups for accepting as much as 6-8% calcium by weight. Bituminious coals do not possess sufficient acidic groups but they can acquire the required ion exchange capacity by mild oxidation (~ 200°C) at the cost of losing some heating value. Adding calcium by ion exchange produces very fine, atomic scale, dispersion in close association with the sulfur source resulting in more rapid kinetics of sulfur capture and reduced diffusional limitations due to deactivation of CaO by solid product layers.

Freund and Lyon (1982) studied the combustion of calcium-exchanged coal as a function of fuel equivalence ratio and found sulfur removal as high as 90% at sufficiently high equivalence ratios. At equivalence ratios used in conventional combustion the sulfur removal fell to 60% or lower. In view of this, they proposed this mode of calcium addition in connection with staged combustion. In the first fuel-rich stage sulfur would be captured in the form of sulfide. If this fuel-rich stage is followed by an oxygen-rich stage, the sulfide would be converted to sulfate provided the temperature remains sufficiently low.

In the present work the combustion of calcium-ion-exchanged coals was studied in a laminar flow furnace under extreme fuel-lean conditions. The purpose of this study was to determine the processes of sulfur dioxide release and recapture in the presence of finely dispersed calcium oxide. The effects of residence time, oxygen concentration, amount of calcium-additive and furnace temperature were evaluated. The results are discussed qualitatively in terms of a speculative mechanism for the release and recapture of sulfur oxide.

3.2 Experimental

3.2.1 Coal Preparation

The two coals used in this study were PSOC 623, a Texas lignite, and PSOC 680, an Indiana high volatile B bituminous. The coal samples were ground to 230 x 325 U.S. mesh size and treated with dilute acid to remove minerals from the solid. The ground coal was stirred with 1.0 N HCL in a ratio of 10 ml/g for 24 hours at 40°C. The acid treatment was sufficient for the removal of the cations of Ca, Mg, Na and K associated with carbonates, sulfates, clays and organic acid sites. Aluminosilicate material and pyrite are not dissolved but may be removed physically. After the acid wash, the slurry was filtered and rinsed with demineralized water to neutral pH. The powder was then vacuum dried at 105°C for 24 hours.

A procedure developed by Schafer (1970) for determining the carboxylic-acid-group content and the total acidity of low-rank coals was adapted to incorporate calcium ions into the coal samples by ion exchange. Each acid-washed coal sample was mixed with a 0.1 N calcium acetate solution at 25°C for 4 to 24 hours. The pH of the mixture was kept at 7.0 to 11.0 with $Ca(OH)_2$ to control the amount of calcium ion exchanged. After calcium exchange the slurry was filtered and washed with demineralized water to remove excess calcium. The

treated coal was then vacuum dried at 105°C for 24 hours. The ion-exchange capacity of the bituminous coal was insufficient to incorporate enough calcium into the coal for a meaningful Ca/S ratio. Thus the sample was prepared by first oxidizing the coal at 160°C for 65 hours in an air-fluidized-bed reactor. The oxidized coal was then acid-washed and ion exchanged.

3.2.2 Experimental Apparatus and Procedure

The experiments were conducted in a laminar flow furnace as shown in Fig. 3.1. The furnace tube was made of high purity alumina with a length of 60 cm and a diameter of 5 cm. The furnace was heated by radiation from six U-shaped molybdenum disilicide heating elements surrounding the alumina tube in a hot zone of 20 cm length. The vertical temperature profile of the furnace was obtained with a series of six thermocouples attached to the furnace wall as shown in Fig. 3.2 and with a high temperature probe inserted into the furnace from the bottom.

A coal feeder, shown in Fig. 3.3, was used to feed coal into the furnace at a rate of 0.3 g/hr via a water-cooled injector located at the top of the hot zone. A small fraction of the total gas flow entered through the injector; the balance of the gas entered in the annular region between the injector and the furnace wall. A low-density alumina disc with 40 equally spaced 0.3 mm holes was placed 5 cm above the injector tip to serve as flow straightener. The residence time of coal particles was controlled by varying the flow of gas through the straightener.

The amount of coal combusted during each 4-hour experiment was determined by weighing the test tube containing coal in the feeder before and after the experiment. The cumulative SO_2 emitted during a combustion run was determined by passing the combustion gas through two gas-washing bottles in series containing a solution of 1% H_2O_2 as shown in Fig. 3.4. In this medium SO_2

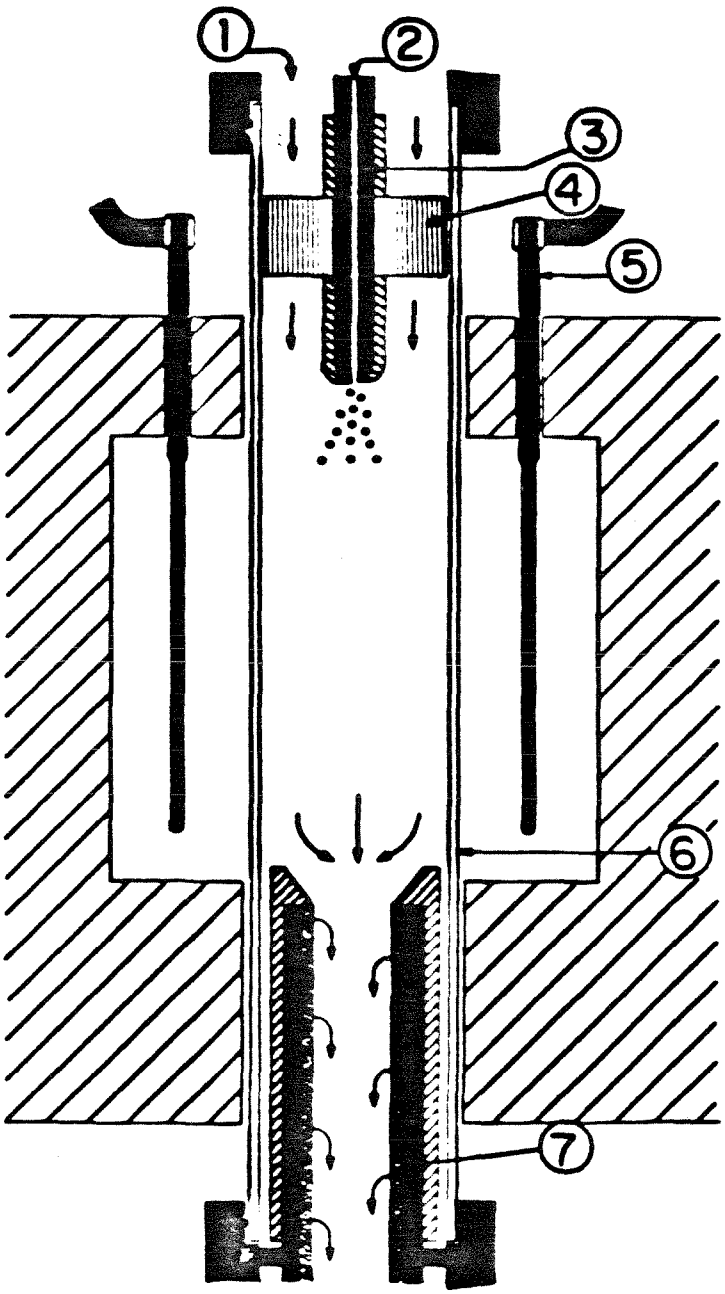

1) Main combustion air

2) Coal and gas

3) Water-cooled injector

4) Flow straightener

5) Heating element

6) Alumina furnace tube

7) Water- cooled sample probe and dilution air

Fig. 3.1 Combustion furnace (not to scale).

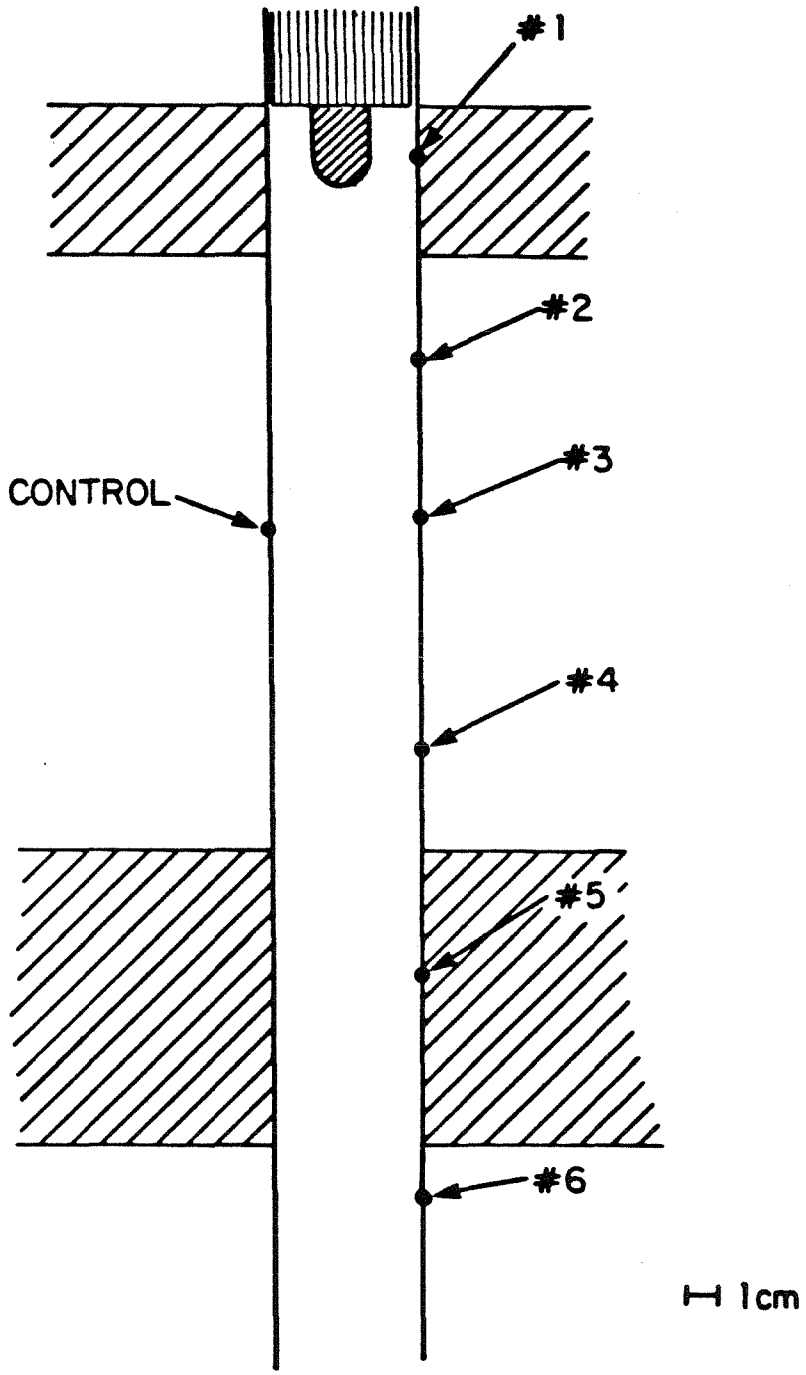

Fig. 3.2 Placement of thermocouples (to scale).

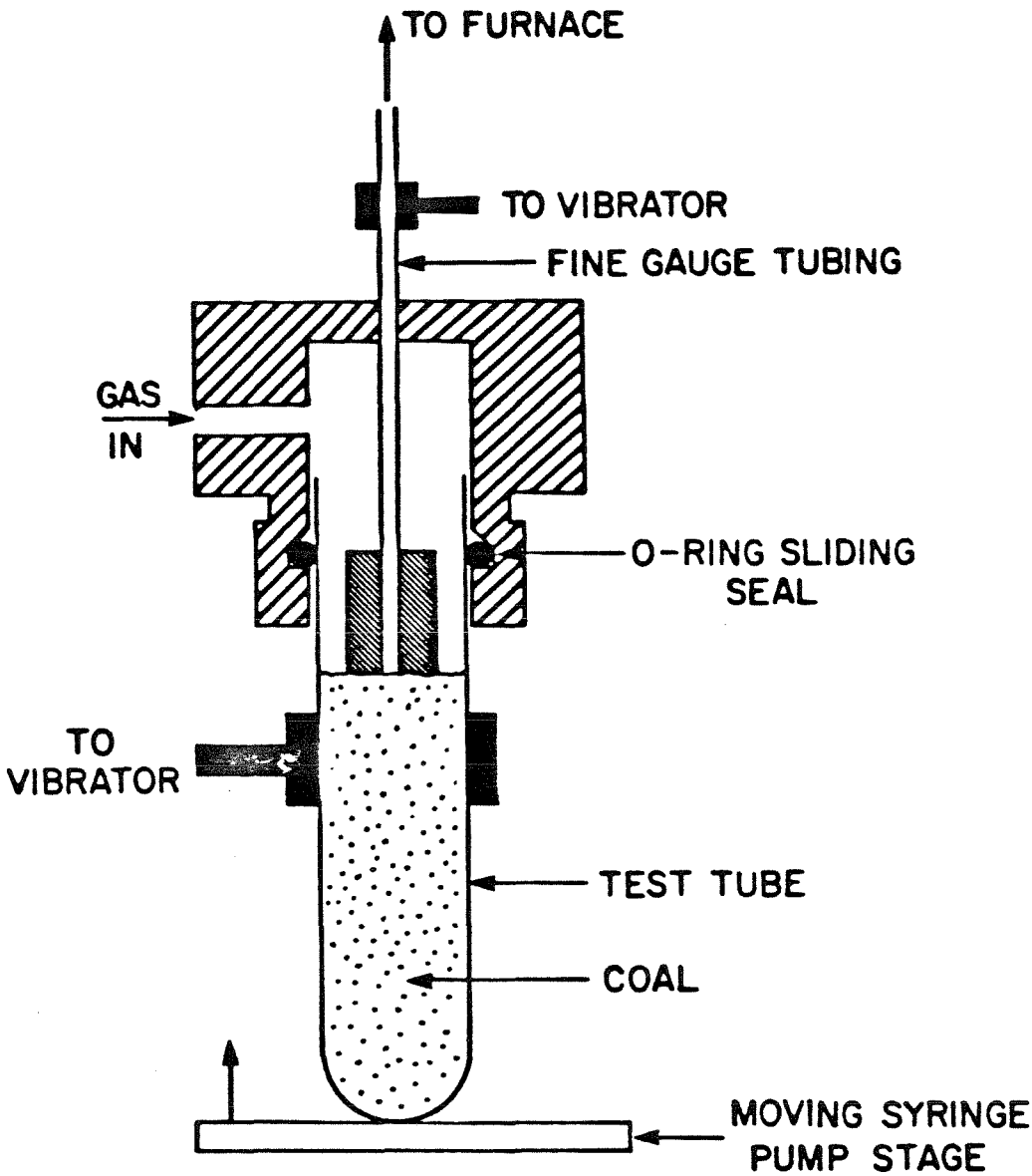

Fig. 3.3 Coal feeder
(not to scale).

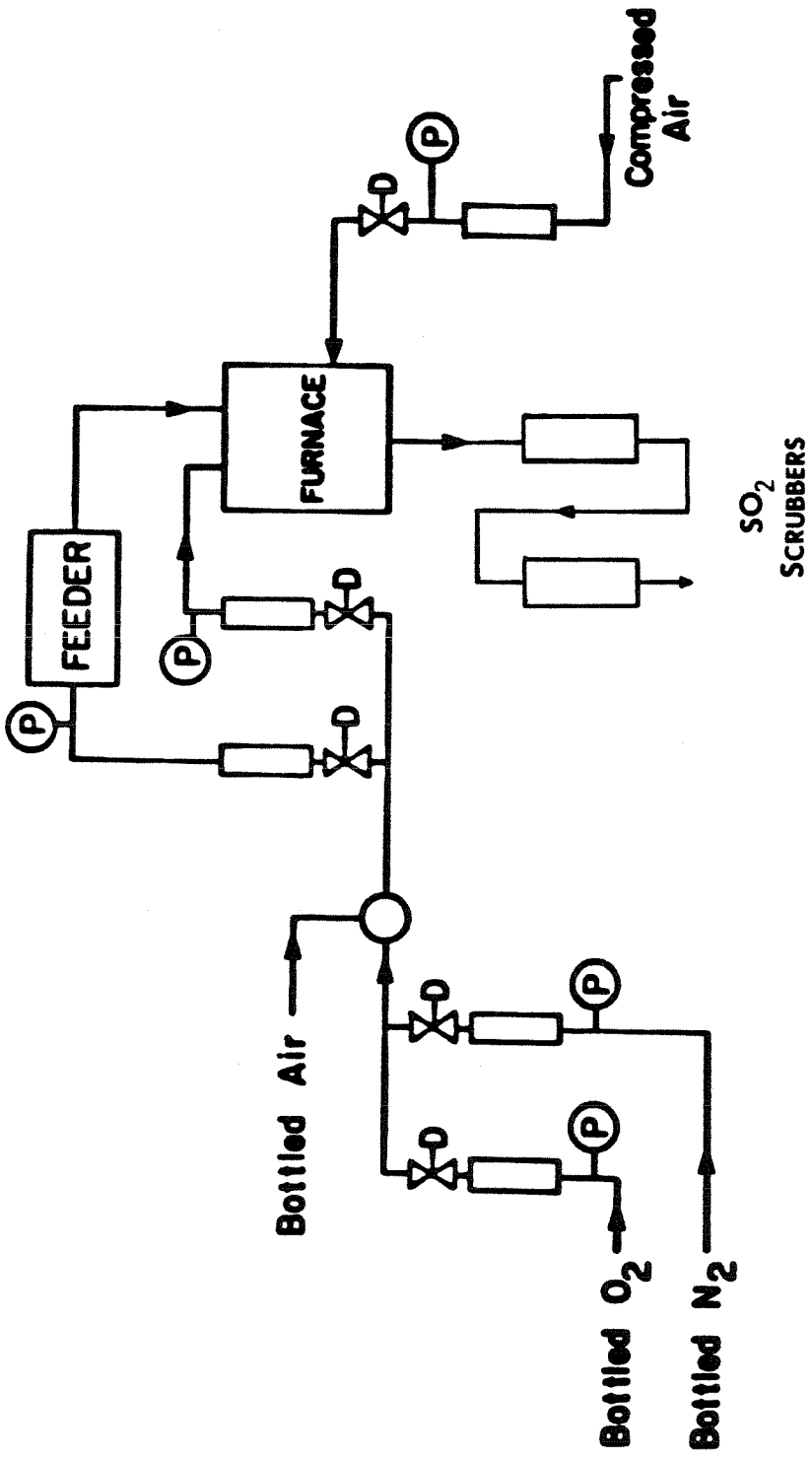

Fig. 3.4 Flow system for combustion experiments.

was converted to H_2SO_4 which was then determined potentiometrically. Sulfur content in the recovered ash was analyzed using a Leco furnace in accordance with the high temperature combustion method described in ASTM Method 3177-75.

From the bottom of the furnace an insulated and water-cooled sample collection-probe extended up into the furnace. The inner surface of the sample probe was made of porous stainless steel tube. The combustion gas was cooled and diluted with dried, filtered air through the walls of the probe. A filter assembly with quartz filter paper was placed at the end of the probe to collect ash samples.

3.2.3 Chemical Analysis of Coal

3.2.3.1 Sulfur Determination

The total sulfur content of coal and coal ash was analyzed during a Leco furnace in accordance with the high temperature combustion method described in ASTM Method 3177-75. A 0.5 g sample was measured into a boat made of refractory material and burned in the Leco furnace at 1350°C with a stream of oxygen. After 15 minutes of combustion the flow of oxygen was substituted by a stream of helium for 10 minutes. The flow of helium was added to the ASTM procedure in order to accelerate the decomposition of sulfates, in particular calcium sulfate, into SO_2 and CaO. The sulfur oxides emitted during combustion and decomposition were scrubbed with a solution of 1% hydrogen peroxide, producing sulfuric acid. The hydrogen peroxide solution was then titrated with dilute sodium hydroxide to the initial pH value of 4.5. The sulfur content of the coal or coal ash was calculated from the volume of titrant as follows:

$$S = \frac{V_{NaOH} N_{NaOH}}{w} \times 1.603 \qquad (3.2)$$

where

S = wt % sulfur in sample.

V_{NaOH} = volume of NaOH titrant, ml.

N_{NaOH} = normality of NaOH solution, g.eq/liter.

w = weight of sample, grams.

For coals that contain high levels of chlorine, HCl is evolved during combustion and contributes to the acidity of the effluent gases. Corrections for chlorine is described in the ASTM procedure. The coals used in the present study contained less than 0.02% chlorine, therefore corrections were not necessary.

The method was calibrated with reagent grade $CaSO_4 \cdot 2H_2O$, and an accuracy within 1% was obtained. Analyses of coal samples gave a standard deviation of 5%, due mainly to the inhomogeneity of samples.

3.2.3.2 Calcium Determination

The calcium content of coal was analyzed by atomic absorption spectrophotometry. Coal ash was prepared by following ASTM Method D-2795-69. The ash sample was dissolved in hydrofluoric acid, treated with concentrated sulfuric and nitric acids and then diluted to make the solution, which was employed to determine the calcium content of the ash. A series of samples was prepared with various added amounts of a standard calcium solution. The samples were then analyzed by a Varian Techtron Model AA-6 Atomic Absorption Spectrophotometer. The absorbance for each sample at a wave length of 422.7 nm and spectral band pass of 0.2 nm was obtained in an acetylene/nitrous oxide flame. In the absorbance range of 0.2-0.8, absorbance is directly proportional to con-

centration,

$$C_o = \frac{X_0}{V_o} = mA_o \tag{3.3}$$

where

Co = concentration of calcium in original sample, mg/ml

X_0 = wt of calcium in sample, mg

V_o = volume of solution in sample, ml

m = proportionality constant, mg/ml

A_o = absorbance of sample.

In samples with added standard calcium solution,

$$C_i = \frac{X_0 + \Delta X_i}{V_o + \Delta V_i} = mA_i \tag{3.4}$$

where

ΔX_i = wt of calcium in added standard solution, mg

ΔV_i = volume of added standard solution, ml.

The calcium content of the original sample X_0 can be obtained by solving the algebraic equation relating a pair of samples with different added amounts of standard calcium solution,

$$\frac{C_i}{C_j} = \frac{mA_i}{mA_j} = \frac{\left(\frac{X_0 + \Delta X_i}{V_o + \Delta V_i}\right)}{\left(\frac{X_0 + \Delta V_j}{V_o + \Delta V_j}\right)}, \tag{3.5}$$

which yields

$$X_0 = \frac{X_i(V_o + \Delta V_j) - \Delta X_j \frac{A_i}{A_j}(V_o + \Delta V_i)}{\frac{A_i}{A_j}(V_o + \Delta V_i) - (V_o + \Delta V_j)} \qquad (3.6)$$

The calcium content of the coal sample is then

$$\% \text{ Ca} = \frac{V_T(X_0/V_o)}{100w} \qquad (3.7)$$

where

V_T = total volume of the diluted ash solution, ml

w = wt of coal, mg.

3.3 Results

Table 3.1 lists the results of sulfur and calcium analyses of the calcium-ion-exchanged coals used in the combustion experiments. A comparison of the sulfur contents of the coals with the analyses provided by the Penn State University Coal Bank given in Table 3.2 shows a difference in the total sulfur contents, particularly with the bituminus coal, PSOC 680. This variation in the sulfur content is due mainly to the coal preparation procedures which involve oxidation of the bituminous coal at 160°C for 65 hours prior to acid washing and ion exchange. Since it is unlikely that appreciable amounts of organic sulfur can be removed under the mild oxidizing condition during coal preparation, therefore, the oxidative pretreatment probably oxidized pyritic sulfur to sulfates which is subsequently removed during acid washing. The agreement in the organic sulfur content of the original bituminous coal with the total sulfur content of the treated coal suggests that most of the sulfur in the calcium-ion-exchanged coal is in the form of organic sulfur species. The results of sulfur emissions observed during the combustion experiments are normalized to the total sulfur of the calcium-treated coals as given in Table 3.1.

Table 3.1

Sulfur and Calcium Analyses of Coal Samples
Used in the Combustion Experiments

	Wt% Dry Basis			Molar Ratio
	Ash	S	Ca	Ca/S
PSOC 680	21.1	1.64	7.07	3.45
PSOC 623 A	22.4	0.81	2.50	2.46
PSOC 623 B	20.2	0.81	0.82	0.81
PSOC 623 Acid-Washed	13.4	1.00	0.06	0.05

Table 3.2

Sulfur Analysis of PSOC 680 and PSOC 623
on a Dry Basis Provided by PSU Coal Bank

	% Pyritic	% Sulfatic	% Organic	% Total
PSOC 680	1.60	0.32	1.66	3.58
PSOC 623	0.19	0.12	1.01	1.35

Figure 3.5 shows the retention of sulfur during combustion of the calcium-exchanged bituminous coal, PSOC 680 (Ca/S = 3.4), at a furnace temperature of 1600°K. The extent of sulfur capture was reduced greatly as the gas flowrate increased from 0.5 l/min to 4.1 l/min corresponding to residence times of 9 seconds to 1.1 seconds in the hot zone of the furnace. The results also show that as oxygen concentration was increased from 13% to 40%, sulfur capture was increased correspondingly. In all experiments, combustion of the coal was complete since analyses of the ash samples showed no residual carbon. Sulfur analyses of ash samples from the experiments with PSOC 680 in 40% O_2 are presented in Table 3.3. Sulfur balance varied from 115.7% at a flowrate of 4.1 l/min to 86.7% at a flowrate of 0.5 l/min. The variations in sulfur may be partially due to sample inhomogeneity. Low sulfur balances may also be due to partial loss of ash deposited on the insulation for the sample probe.

Figures 3.6 and 3.7 show the effect of increasing calcium content on sulfur capture during the combustion of the lignite coal, PSOC 623. As Ca/S ratio increased from 0.81% to 2.46%, sulfur capture increased proportionally.

Figure 3.8 shows the retention of sulfur during combustion of PSOC 680 (Ca/S = 3.4) at a furnace temperature of 1400°K. The results indicate that the effect of gas flowrate on sulfur capture is not as great as at a furnace temperature of 1400°K compared to the results obtained at a furnace temperature of 1600°K.

3.4 Discussion

The evolution of sulfur during combustion of coal may be described by the following steps:

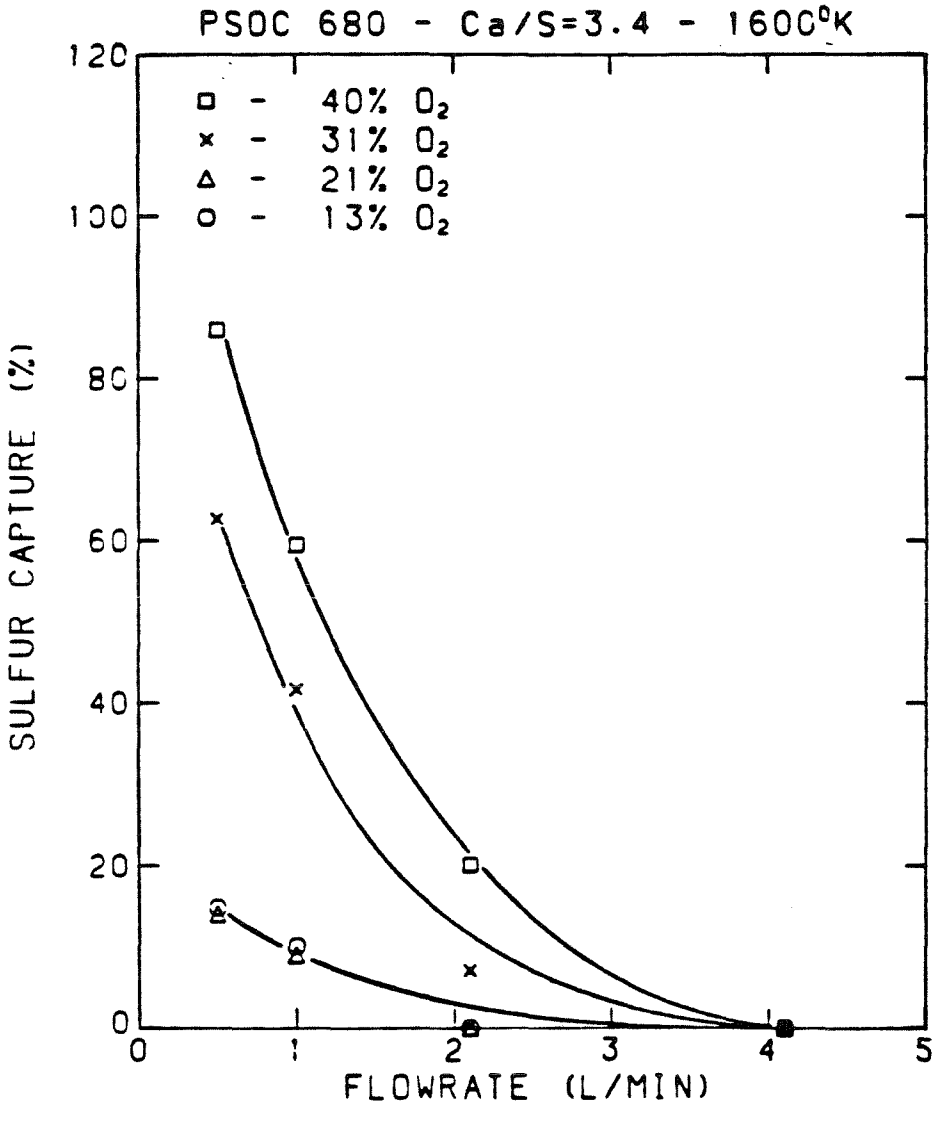

Fig. 3.5 Effect of gas flowrate and oxygen concentration on sulfur retention during combustion of calcium-ion-exchanged PSOC 680 (Ca/S = 3.4) in a laminar flow furnace.

Table 3.3

Sulfur Balance for the Combustion of PSOC 680 (Ca/S = 3.4) at 1600°K in 40% O_2

Gas Flowrate (ℓ/min)	% S in Gas as SO_2	% S in Ash	% S Balance
4.1	103.3	12.4	115.7
2.1	79.9	17.4	97.3
1.0	40.5	52.7	93.2
0.5	16.3	70.4	86.7

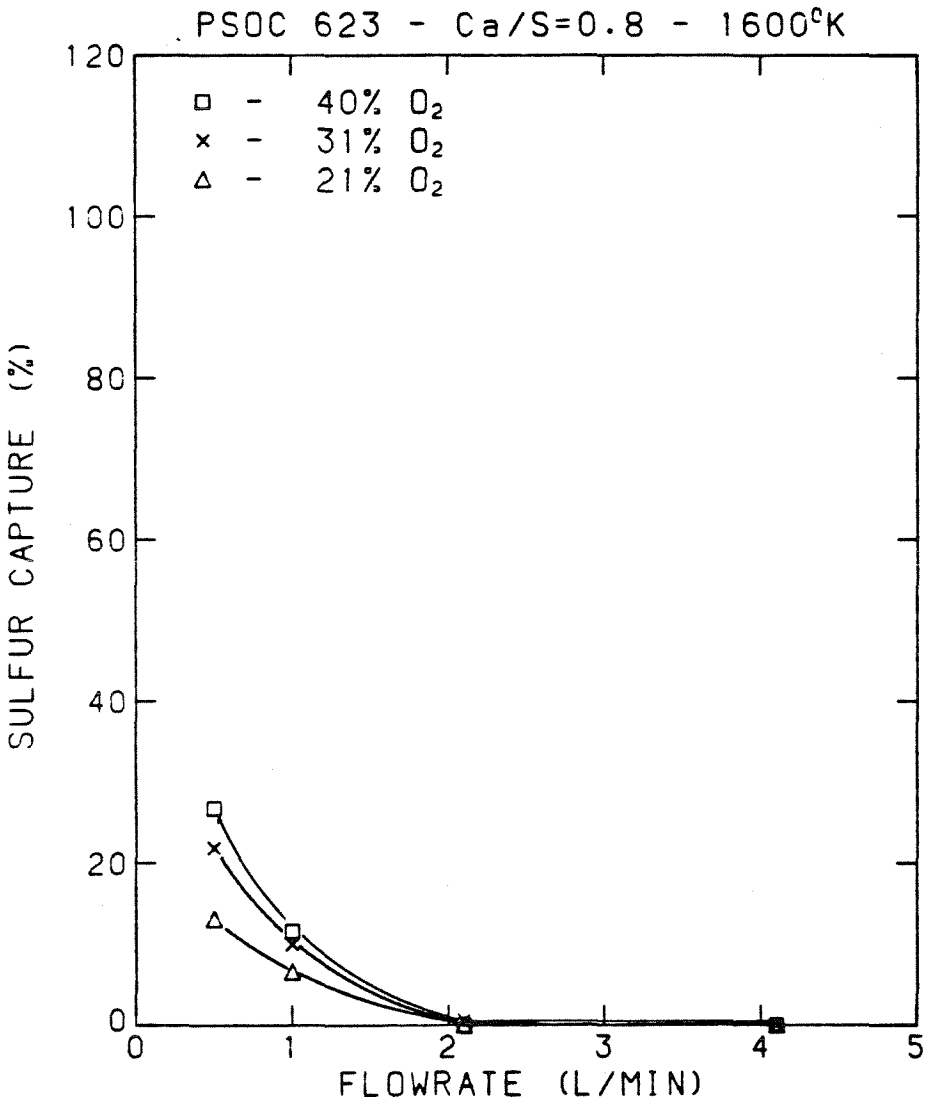

Fig. 3.6 Effect of gas flowrate and oxygen concentration on sulfur retention during combustion of calcium-ion-exchanged PSOC 623 (Ca/S = 0.8) in a laminar flow furnace.

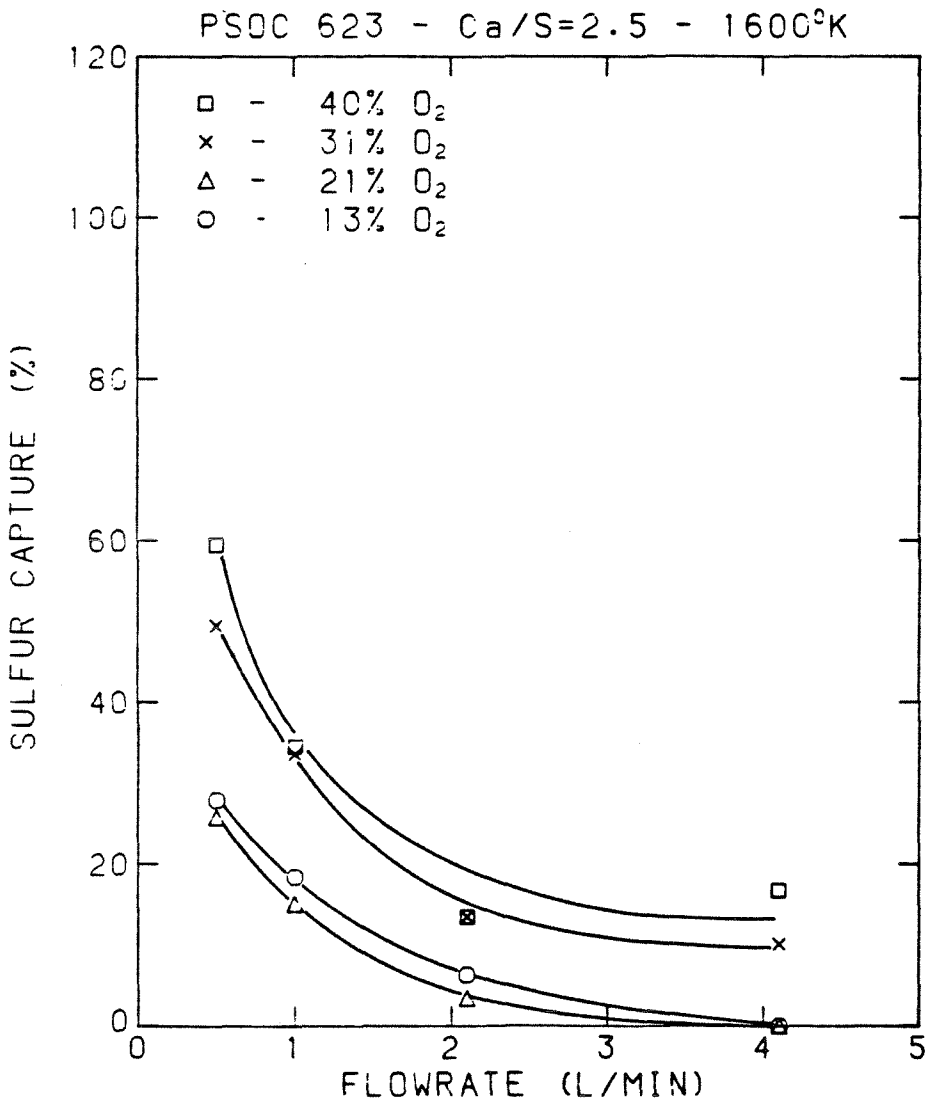

Fig. 3.7 Effect of gas flowrate and oxygen concentration on sulfur retention during combustion of calcium-ion-exchanged PSOC 623 (Ca/S = 2.5) in a laminar flow furnace.

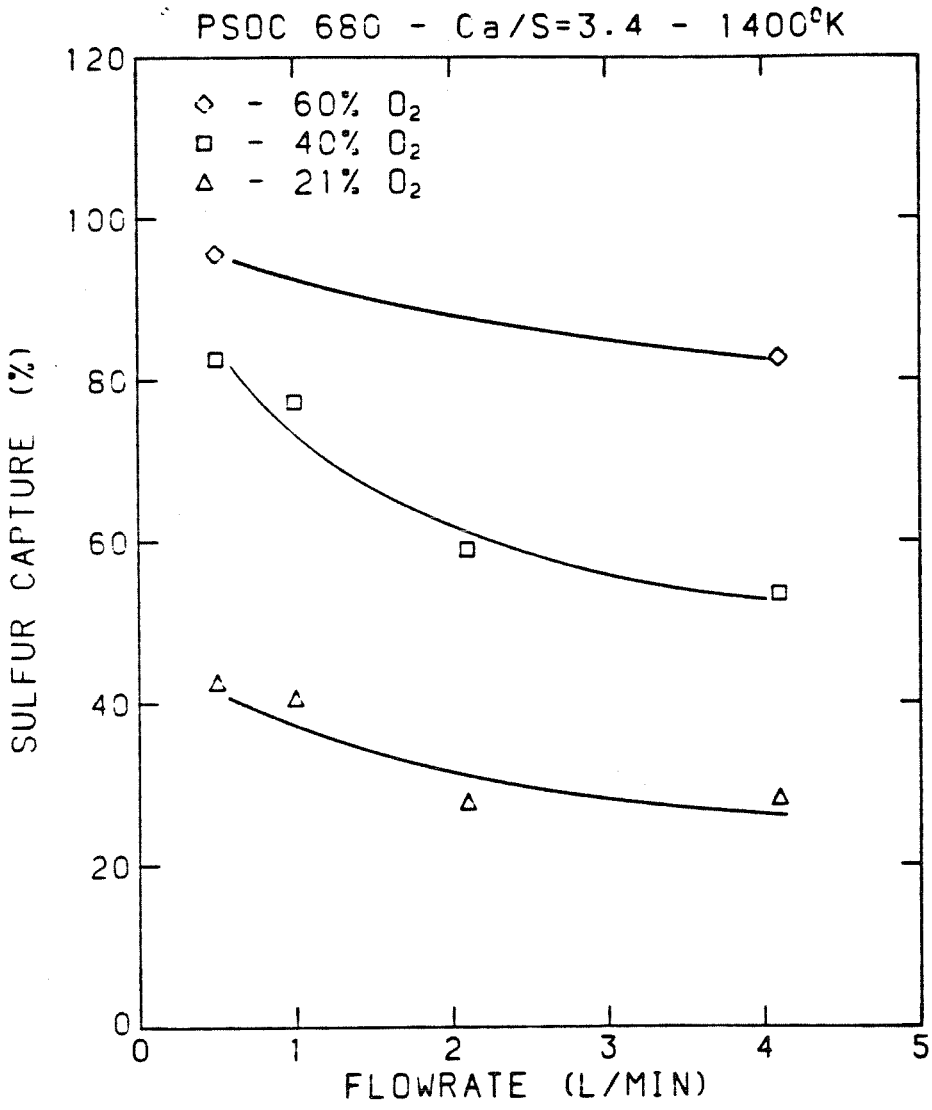

Fig. 3.8 Effect of gas flowrate on sulfur retention during combustion of PSOC 680 (Ca/S = 3.4) at a furnace temperature of 1400°K.

i. Reducing Conditions:

$$R\text{–}S \rightarrow H_2S^{\dagger} + R' \tag{3.8}$$

$$R\text{–}Ca \rightarrow CaO + R'' \tag{3.9}$$

$$CaO + H_2S \rightarrow CaS + H_2O \tag{3.10}$$

$$CaO + SO_2 + 3CO \rightarrow CaS + 3CO_2 \tag{3.11}$$

$$CaO + COS \rightarrow CaS + CO_2 \tag{3.12}$$

ii. Oxidizing Conditions:

$$H_2S + \frac{3}{2}O_2 \rightarrow SO_2 + H_2O \tag{3.13}$$

$$R\text{–}S^{\ddagger} + O_2 \rightarrow SO_2 + CO \tag{3.14}$$

$$CaS + 2O_2 \rightarrow CaSO_4 \tag{3.15}$$

$$COS + \frac{3}{2}O_2 \rightarrow SO_2 + CO_2 \tag{3.16}$$

$$CaO + SO_2 + \frac{1}{2}O_2 \rightleftarrows CaSO_4 \tag{3.17}$$

During devolatilization and early stages of combustion, the interior of the char particles is under reducing conditions, thus sulfur may be evolved as volatile sulfur species or may form calcium sulfide through steps (3-10) to (3-12). As oxygen penetrates the char particles, gaseous sulfur species are oxidized to SO_2 and calcium sulfide is oxidized to calcium sulfate. Calcium sulfate may also be formed by the reaction of CaO and SO_2 in an oxygen-rich environment.

Reaction (3-17) can proceed in either direction depending on the temperature and the partial pressures of SO_2 and O_2. The calculated equilibrium SO_2 partial pressures based on reaction (3-17) is plotted against 1/T in Fig. 3-9.

† *May also be volatile organic sulfur species such as mercaptans and carbonyl sulfide.*

‡ *May also be inorganic sulfur species.*

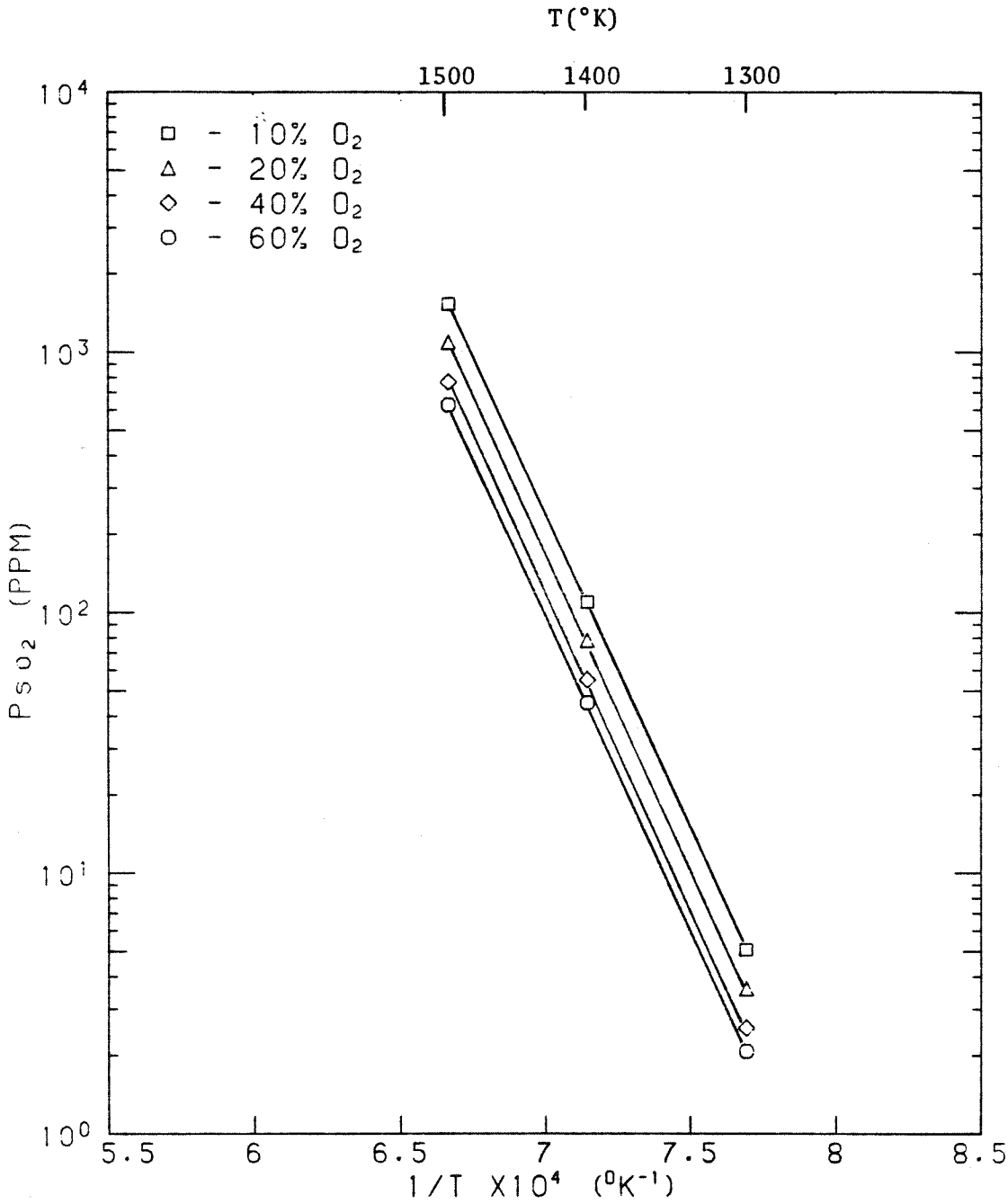

Fig. 3.9 Calculated equilibrium SO_2 partial pressure for the reaction $CaO + SO_2 + \frac{1}{2} O_2 \rightleftharpoons CaSO_4$.

During combustion experiments with a fixed coal feedrate of 1.2 g/hr, the SO_2 partial pressures ranged from 20 ppm at a gas flowrate of 4.1 *l* /min to 160 ppm at a gas flowrate of 0.5 *l* /min. Thus the formation of $CaSO_4$ will be unfavorable thermodynamically at temperatures above 1350°K to 1450°K as flowrates vary from 4.1 *l* /min to 0.5 *l* /min. Figure 3.9 also shows that as oxygen partial pressure increases, equilibrium SO_2 partial pressure decreases correspondingly. At the heated section of the furnace the wall temperature is maintained at 1600°K and the particle temperature is considerably higher. At these temperatures all sulfur species would be released as SO_2 under conditions of equilibrium, thus sulfur capture probably occurs when the particles are cooled downstream of the hot zone such that the formation of $CaSO_4$ is thermodynamically favorable.

3.4.1 Effect of Residence Time

The temperature profiles of the furnace at the experimental flowrates are presented in Fig. 3-10. The thermodynamically favorable zone for the formation of $CaSO_4$ begins as the furnace temperature falls below 1400°K, which is approximately 27 cm from the injector. The zone ends as the particles reach the sample collector which is 34 cm from the injector. The reaction rate for the formation of $CaSO_4$ from CaO and SO_2 decreases rapidly as temperature decreases below 750°C (Borgwardt, 1970). Thus the introduction of cool dilution air through the sample probe serves to quench further reactions as the furnace temperature is lowered to 1000°K and SO_2 concentration is reduced.

The relevant temperature for the formation or decomposition of $CaSO_4$ is the particle temperature. Calculations of the particle temperature were made with a coal combustion model developed by C. L. Senior (1984) based on the work of Libby and Blake (1979). The calculated peak particle temperatures are plotted against oxygen concentration in Fig. 3.11. The times required for 95% burnout

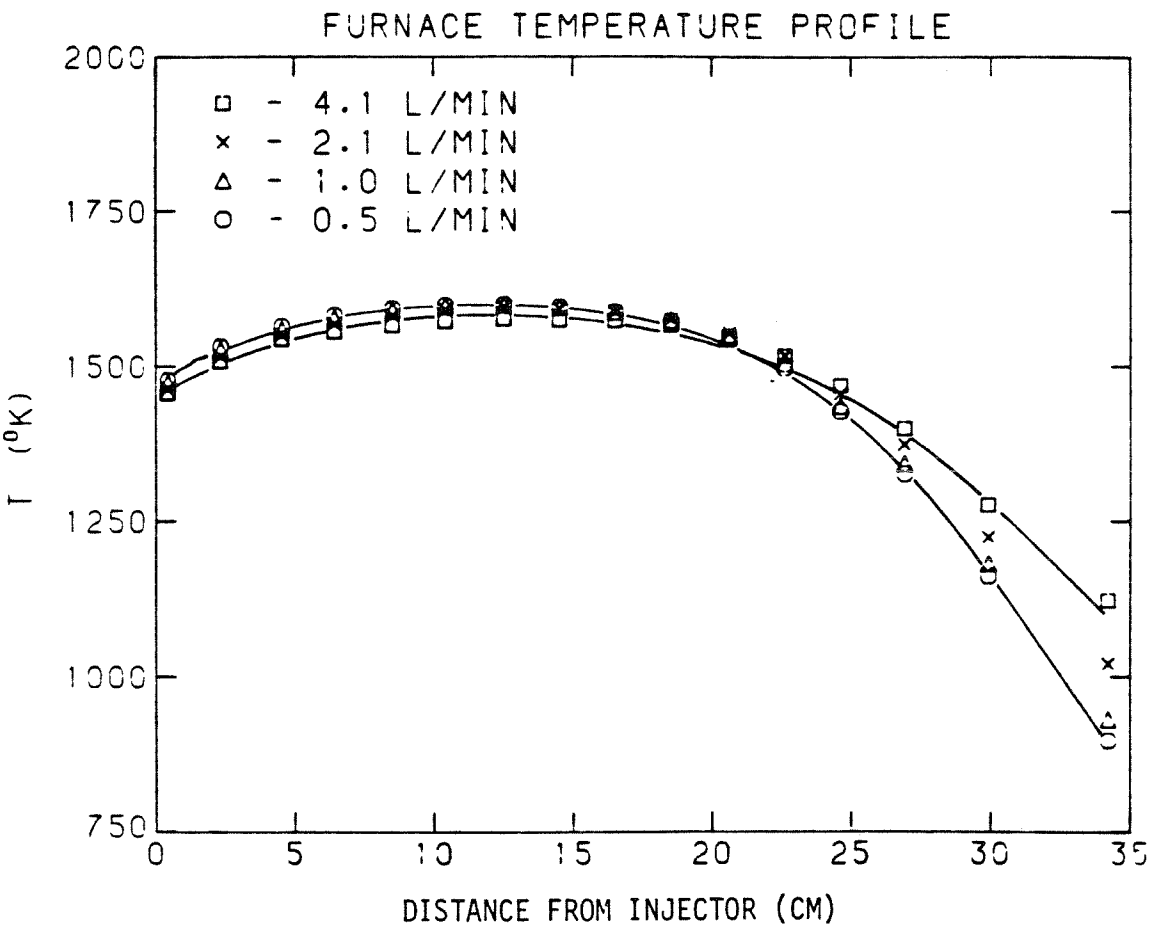

Fig. 3.10 Furnace temperature versus distance from coal injector.

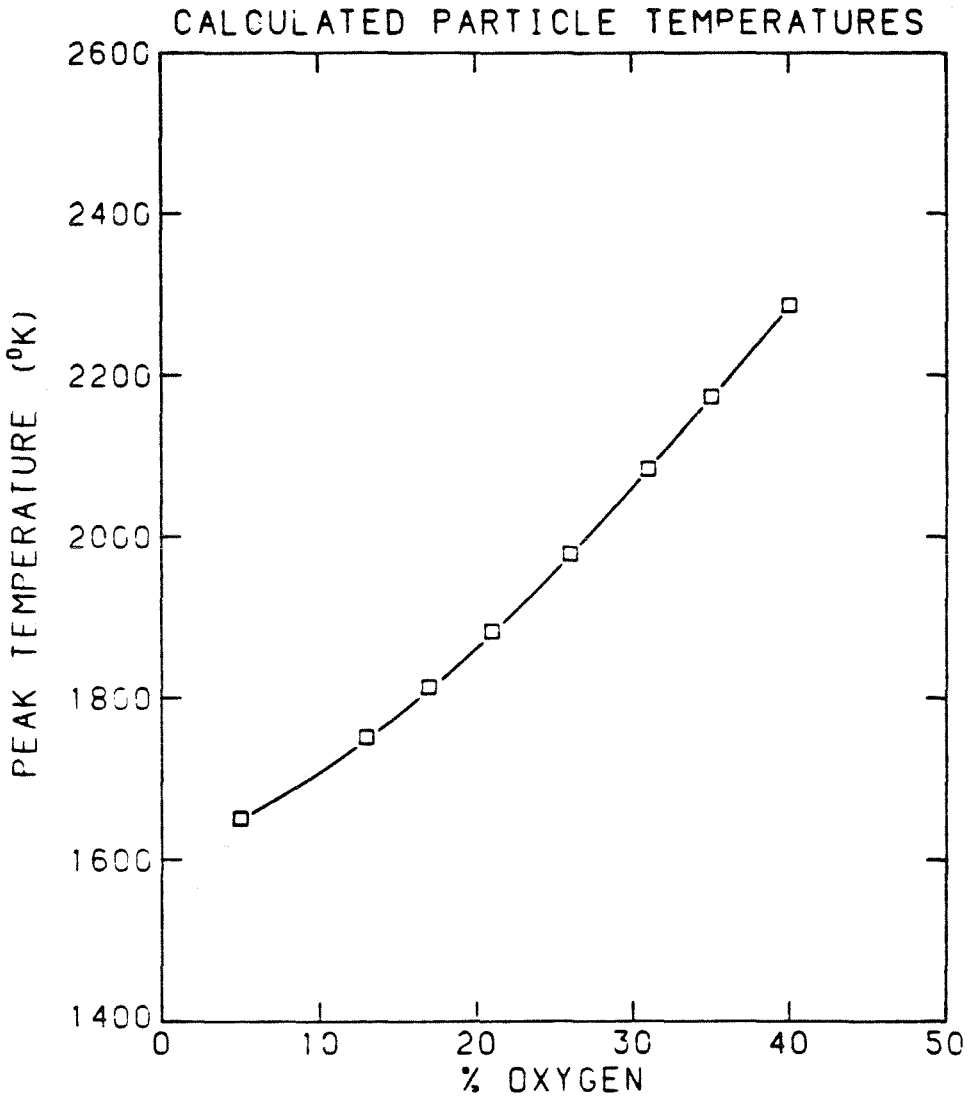

Fig. 3.11 Theoretical calculation of particle temperature for the combustion of a bituminous coal at a furnace temperature of 1600°K.

of carbon were calculated to be 25 msec for combustion with 40% O_2 to 68 msec with 13% O_2 at a furnace temperature of 1600°K. The particles are combusted completely and cooled to the furnace temperature in approximately 100 msec to 200 msec, only a fraction of the particle residence time in the hot zone which ranges from 1.1 sec to 9 sec. Therefore, the particle temperature through the lower portions of the furnace was assumed to be similar to the furnace temperature as illustrated in Fig. 3.12.

The particle residence time through the zone where the temperature favors capture of SO_2 by CaO was calculated for each of the flowrates. The results for the combustion experiments conducted at a furnace temperature of 1600°K showing the effects of the redefined particle residence time are presented in Figs. 3.13 - 3.15. In all cases, the extent of sulfur capture increases with a corresponding increase in particle residence time.

Figure 3.12 shows that the furnace and particle temperatures range from 1400°K to 1000°K in the reactive zone of the furnace which is approximately 7 cm long, as designated by D' where the temperatures are lowered to 1400°K, and D'' where cool dilution air is introduced through the sample probe. Thus the observed sulfur capture is the cumulative result of the reaction of SO_2 and CaO with O_2 over a temperature range of 400°K.

In the case of strongly fuel-lean conditions, the oxygen concentration is in excess and remains relatively constant throughout the furnace. Thus if the reaction between the gas and CaO is of first order with respect to SO_2 (McClellan et al., 1970), then the reaction rate can be expressed as

$$-\frac{dC_{SO_2}}{dt} = k^* C_{SO_2}, \tag{3-18}$$

which gives

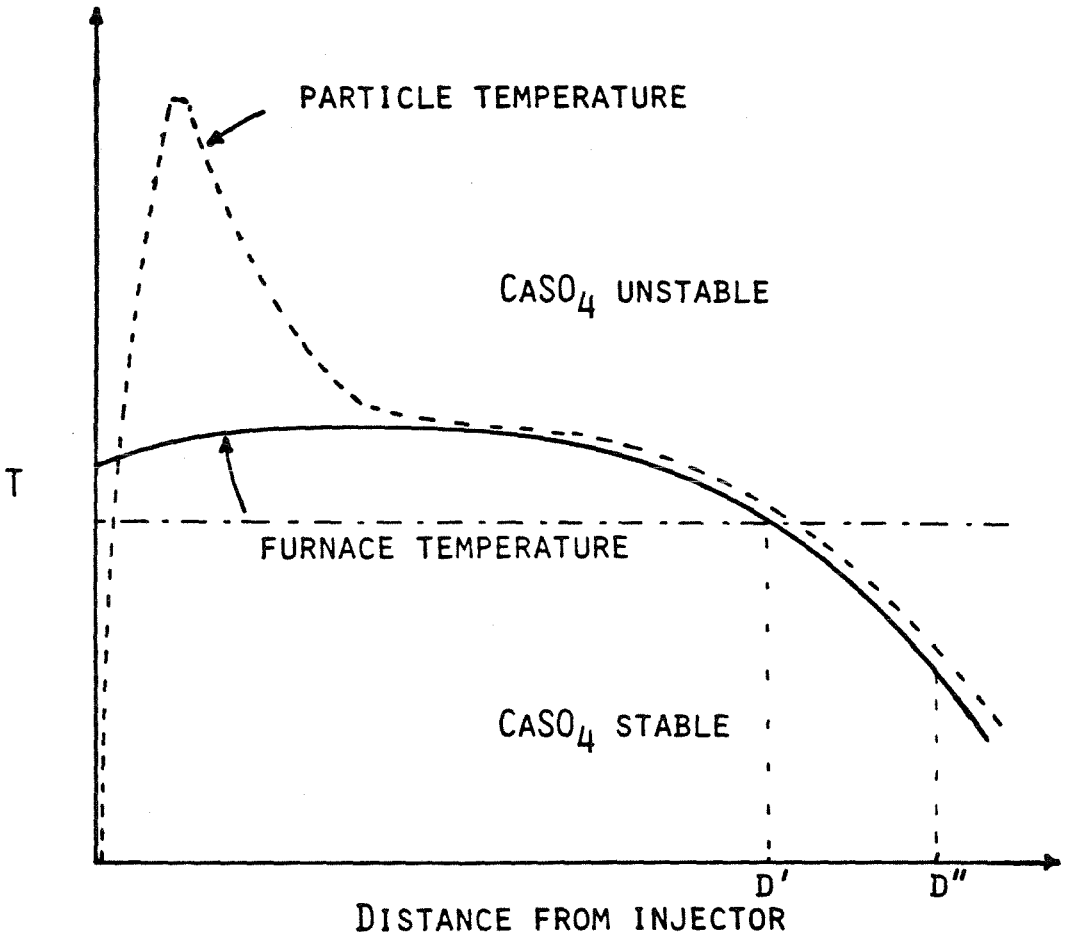

Fig. 3.12 Illustration of particle temperature profile.

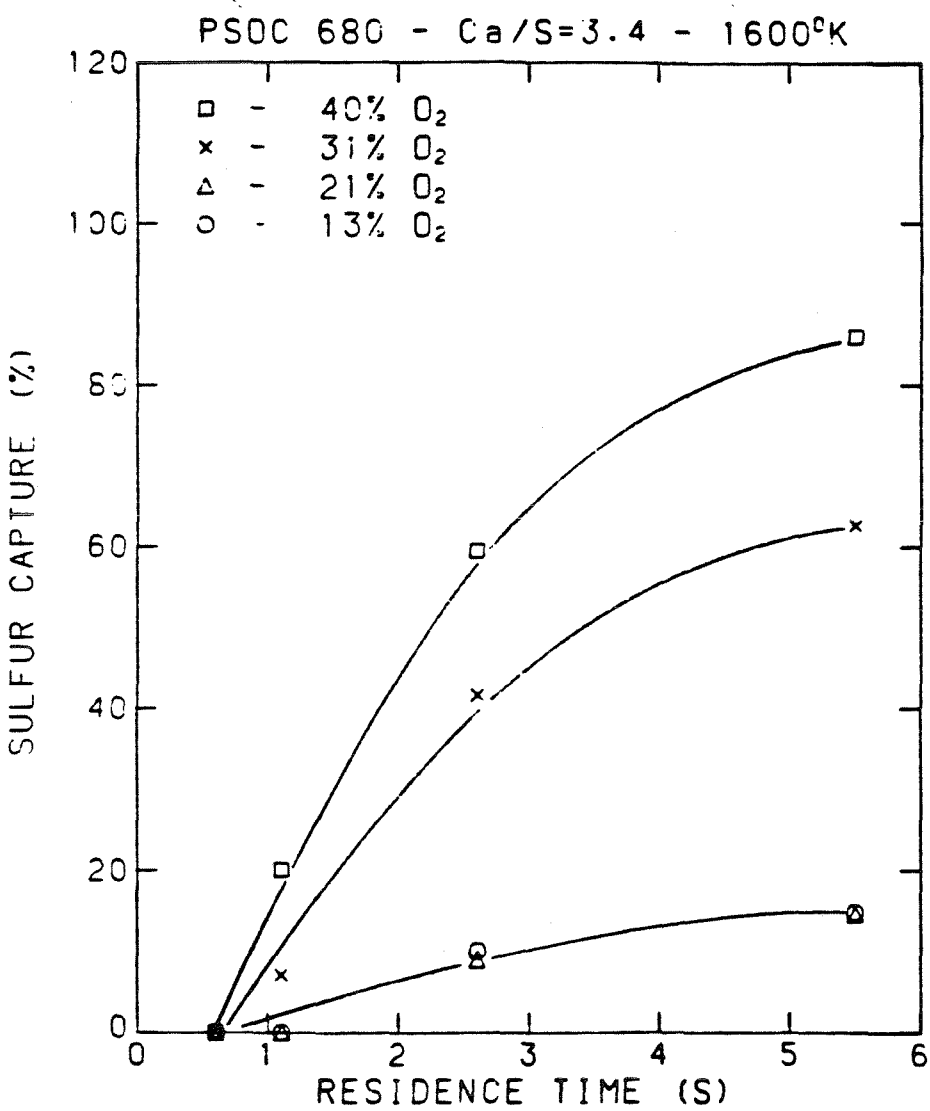

Fig. 3.13 Effect of particle residence time on sulfur retention for the combustion of PSOC 680 (Ca/S = 3.4) at various oxygen concentration.

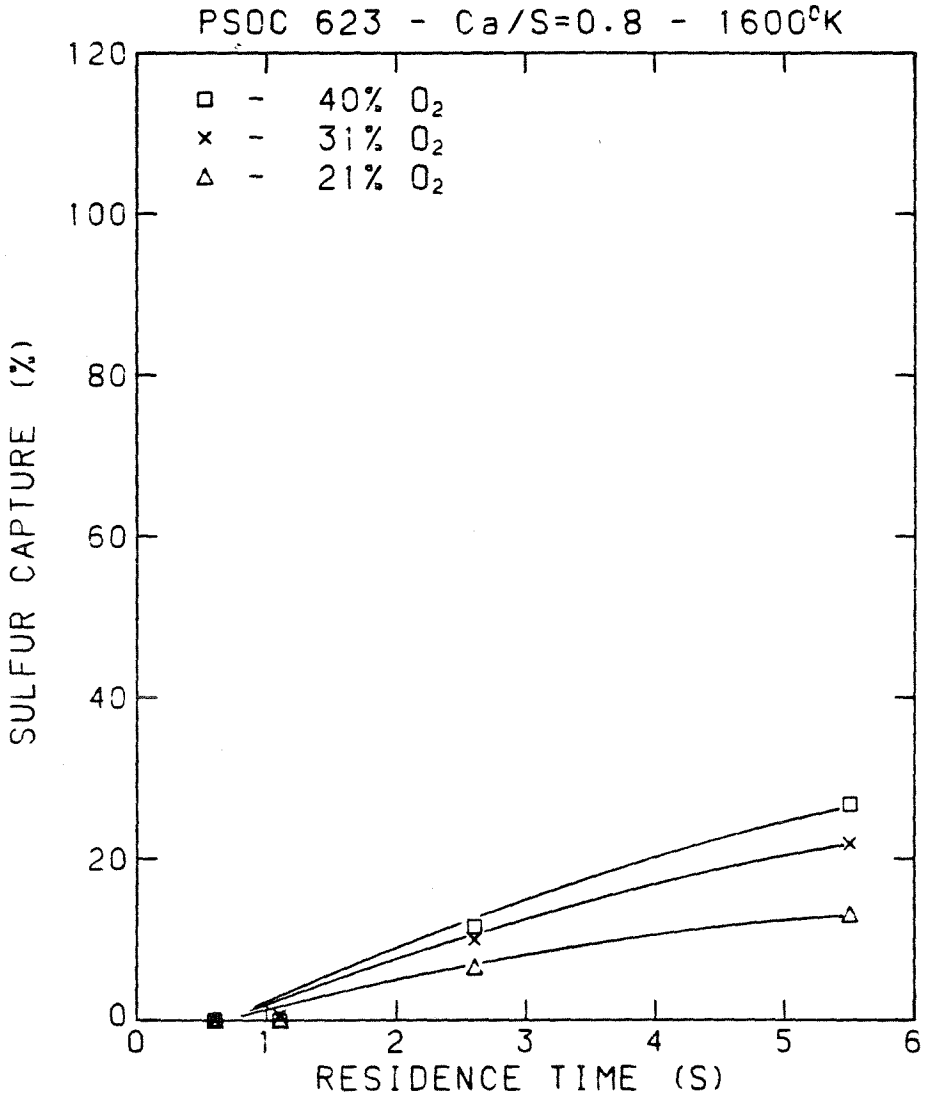

Fig. 3.14 Effect of particle residence time on sulfur retention for the combustion of PSOC 623 (Ca/S = 0.8) at various oxygen concentration.

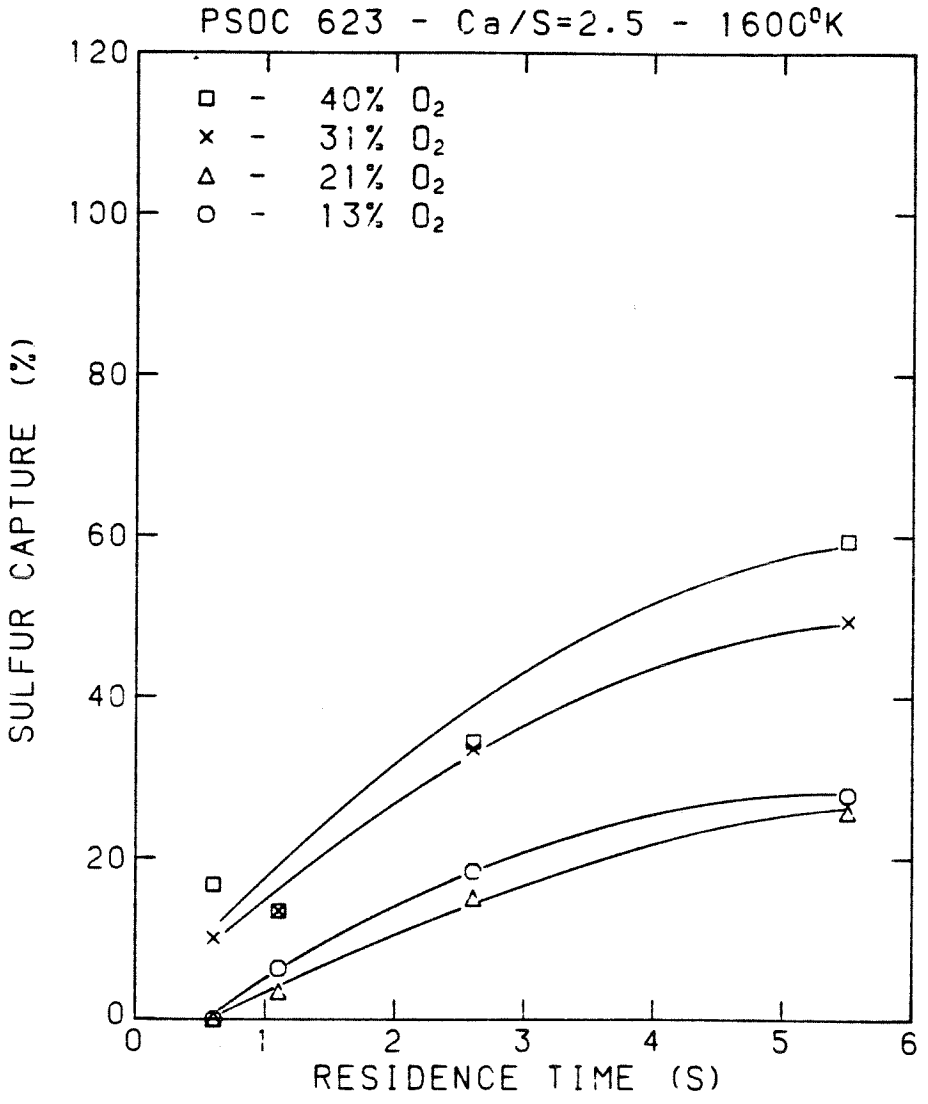

Fig. 3.15 Effect of particle residence time on sulfur retention for the combustion of PSOC 623 (Ca/S = 2.5) at various oxygen concentration.

$$\ln \frac{C_{SO_2}}{C^0_{SO_2}} = -k^* t \,, \tag{3-19}$$

where

C_{SO_2} = the concentration of SO_2 in the gas.

k^* = the first order reaction rate constant which includes the effect of oxygen concentration, the properties of the ash particles (e.g. calcium content in the ash), and is averaged over the temperature range of the reactive zone —from 1400°K to 1000°K.

The observations at high flowrates, or low residence times, show little or no sulfur capture. This result suggests that all the sulfur in the original coal sample is in the form of SO_2, therefore the concentration of SO_2 in the gas before recapture occurs, $C^0_{SO_2}$, can be calculated from the rate of coal combusted and the flowrate of gas through the furnace. The SO_2 analyzed in the exit gas gives the concentration at the quench point, assuming reaction does not continue beyond the sample probe.

Figure 3.16 shows a linear dependence of $\ln(C_{SO_2}/C^0_{SO_2})$ with respect to time for sulfur capture during combustion of PSOC 680 (Ca/S = 3.4). Figures 3.17 and 3.18 indicate similar linear relationships during combustion of PSOC 623 (Ca/S = 2.5) and PSOC 623B (Ca/S = 0.8), respectively. These results show that sulfur capture is a first order reaction with respect to SO_2 in the gas.

According to Eq. (3-19), the slope of the straight line of $\ln(C_{SO_2}/C^*_{SO_2})$ versus time is the negative value of k^*, the first order reaction rate constant. The experimentally determined first order reaction rate constants are tabulated in Table 3.4. There is no variation in the reaction rate constant at 13% and 21% O_2 concentration, suggesting a zeroth order dependence on oxygen at low oxygen

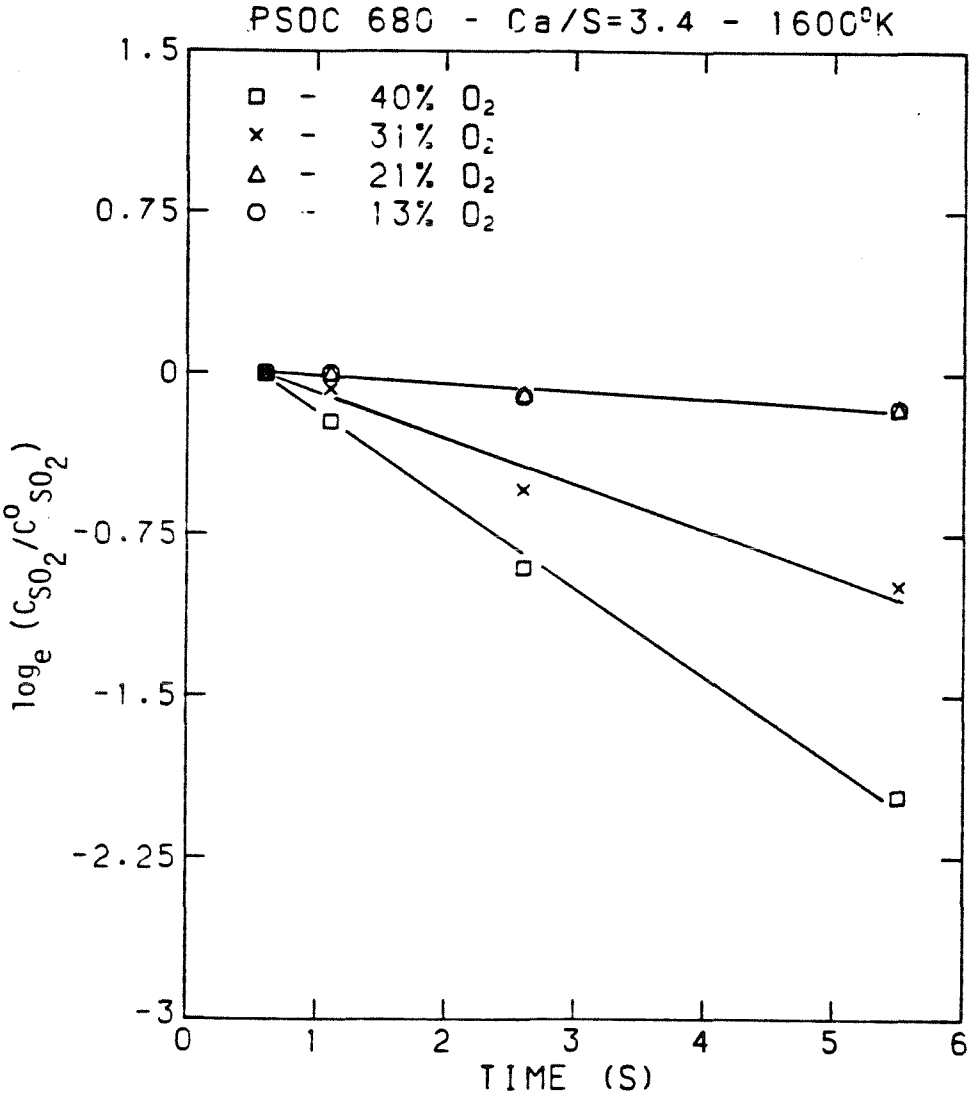

Fig. 3.16 First order dependence of sulfur capture with respect to SO_2 concentration during combustion of PSOC 680 (Ca/S = 3.4) at 1600°K.

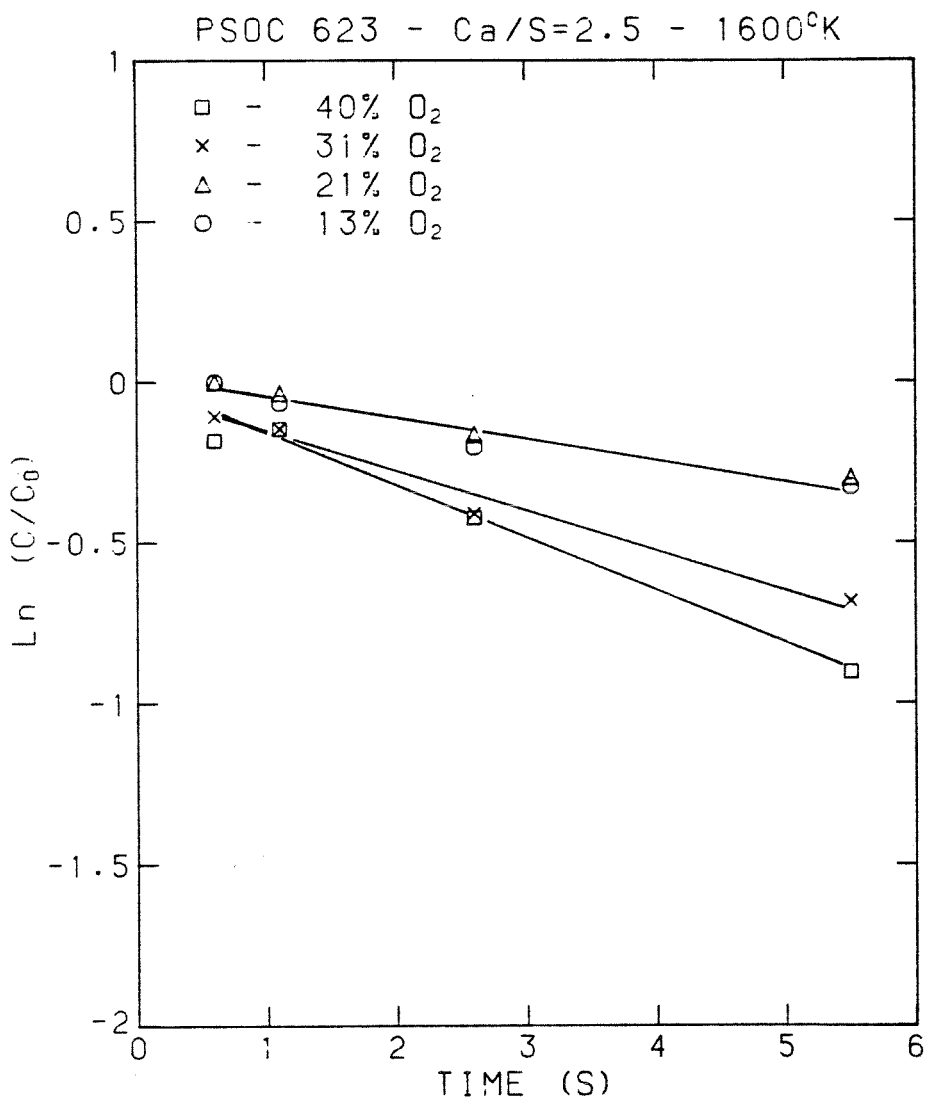

Fig. 3.17 First order dependence of sulfur capture with respect to SO_2 concentration during combustion of PSOC 623A (Ca/S = 2.5) at 1600°K.

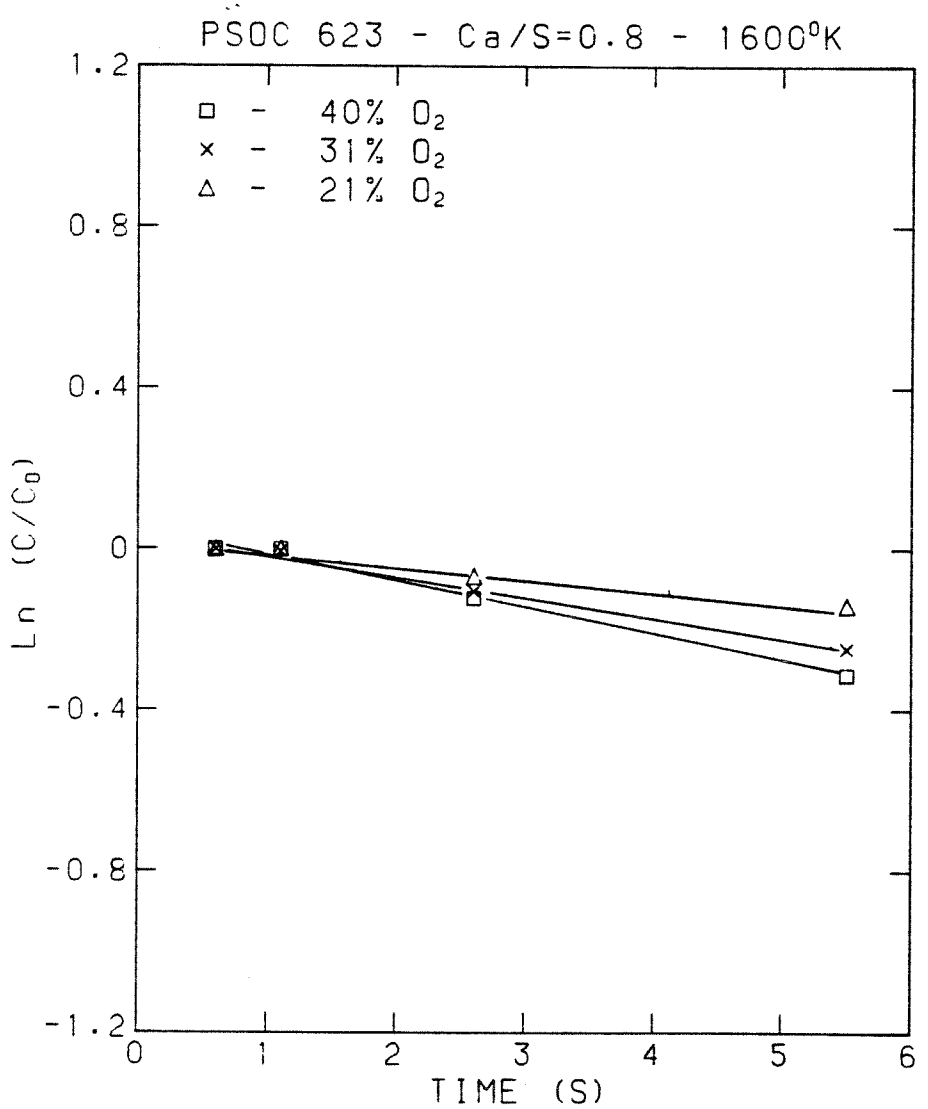

Fig. 3.18 First order dependence of sulfur capture with respect to SO_2 concentration during combustion of PSOC 623B (Ca/S = 0.8).

Table 3.4

First order reaction rate constants for the retention of SO_2 during combustion of coals at 1600°K.

P_{O_2} (atm)	PSOC 680 (Ca/S = 3.4) K^*, (sec^{-1})	PSOC 623A (Ca/S = 2.5) K^*, (sec^{-1})	PSOC 623B (Ca/S = 0.8) K^*, (sec^{-1})
0.40	0.40	0.17	0.067
0.31	0.21	0.12	0.052
0.21	0.034	0.061	-
0.13	0.035	0.065	0.030

levels. As oxygen concentration increases above 21%, the reaction rate constant also increases. The observed trends of reaction rate constant and oxygen concentration suggest that the order of reaction is not constant with respect to oxygen concentration at higher oxygen concentrations.

The effective reaction time for the formation of calcium sulfate in the present study ranges from 0.6 seconds to 5.5 seconds. The short reaction times for all of the experiments combined with the the observed results of little or no sulfur capture at 0.6 second raise the possibility of diffusional resistances for the reaction of SO_2 with CaO dispersed in the coal ash. The diffusional processes are: the diffusion of SO_2 through the bulk gas, the diffusion of SO_2 through the pores of the ash particles, and possibly the diffusion of SO_2 through a shell of solid reaction product which forms on the active solid surface as the reaction proceeds.

The characteristic time for the diffusion of SO_2 through the bulk gas to the ash particles can be approximated by

$$t_D \cong \frac{\lambda^2}{D}. \tag{3-20}$$

where

λ = the distance that SO_2 has to diffuse through the bulk gas to reach the ash particles.

D = the mass diffusivity of SO_2 through the bulk gas.

An upper limit on t_D can be estimated by examining the experimental conditions at a gas flowrate of 4.1 l /min. In an average experiment, 1.3 g of coal is fed into the furnace over a period of 4 hours. The average particle size is 50 μm in diameter, thus there are approximately 1.5×10^7 particles fed through the furnace along with 9×10^5 cm^3 of gas. If we assume the particles do not break up and

the particles are distributed uniformly in the furnace, then an upper limit for λ is approximately 0.2 cm. The mass diffusivity for binary mixtures of gases can be calculated by the Chapman-Enskog formula for gaseous state at low density (Hirschfelder et al., 1954),

$$D_{AB} = 0.0018583 \frac{\sqrt{T^3 \left[\frac{1}{M_A} + \frac{1}{M_B}\right]}}{p\sigma_{AB}^2 \Omega_{D,AB}} \qquad (3\text{-}21)$$

in which

D_{AB} = the diffusivity of A in B.

p = the pressure of the system.

σ_{AB} = the Lennard-Jones collision diameter.

$\Omega_{D,AB}$ = a dimensionless function of the intermolecular potential field for one molecule of A and B.

For SO_2 in air, D varies from 1.05 cm^2/sec at 1000°K to 1.84 cm^2/sec at 1400°K. The upper limit of the bulk gas diffusional characteristic time is then 38 msec, which is considerably faster than the reaction time scale. This result suggests that the diffusion of SO_2 through the bulk gas does not pose a resistance to the formation of $CaSO_4$ if the assumption of uniform distribution of particles is valid.

Diffusion of SO_2 within a spherical particle of ash in the absence of chemical reaction may be expressed as:

$$\frac{\partial c}{\partial t} = \frac{D_e}{r^2} \frac{\partial}{\partial r}\left[r^2 \frac{\partial c}{\partial r}\right], \qquad (3\text{-}22)$$

where

c = the concentration of SO_2 at time t and radial position r in the spherical particle.

D_e = the effective diffusivity.

If the concentration of SO_2 is assumed to be uniform at the surface of the particle, then the boundary and initial conditions can be approximated by:

$$c = c_s \quad \text{at} \quad r = R \quad (t \geq 0)$$

$$c = 0 \quad \text{for} \quad t < 0 \quad (0 \leq r \leq R)$$

where

c_s = the concentration of SO_2 at the surface of the particle.

R = the radius of the particle.

The equations may be non-dimensionalized to give:

$$\frac{\partial \bar{c}}{\partial \bar{t}} = \frac{1}{\bar{r}^2} \frac{\partial}{\partial \bar{r}} \left[\bar{r}^2 \frac{\partial \bar{c}}{\partial \bar{r}} \right], \tag{3-23}$$

$$\bar{c} = 1 \quad \text{at} \quad \bar{r} = 1 \quad (\bar{t} \geq 0)$$

$$\bar{c} = 0 \quad \text{at} \quad \bar{t} < 0 \quad (0 \leq \bar{r} \leq 1),$$

with

$$\bar{c} = \frac{c}{c_s}, \bar{r} = \frac{r}{R} \quad \text{and} \quad \bar{t} = \frac{t}{t_{D_e}},$$

where $t_{D_e} = \frac{R^2}{D_e}$, the characteristic time for intraparticle diffusion.

The solution of Eq. (3-23) is (Crank, 1956):

$$\bar{c}(\bar{r},\bar{t}) = \frac{c(r,t)}{c_s} = 1 + \frac{2}{\pi \cdot \bar{r}} \sum_{n=1}^{\infty} \frac{(-1)^n}{n} \sin(n\pi\bar{r}) e^{-n^2\pi^2\bar{t}}. \tag{3-24}$$

At the center of the particle ($\bar{r} = 0$), the solution reduces to:

$$\bar{c}(0,\bar{t}) = \frac{c(0,t)}{c_s} = 1 + 2\sum_{n=1}^{\infty}(-1)^n e^{-n^2\pi^2}\left[\frac{t}{t_{D_e}}\right]. \qquad (3\text{-}25)$$

The concentration of SO_2 at the center of the particle reaches 99% of the value at the surface when $t \cong 0.55\ t_{D_e}$. The effective diffusivity of SO_2 through the ash particle can be estimated by applying the parallel-pore model for a monodisperse system:

$$D_e = \frac{\varepsilon \cdot D}{\sigma} \qquad (3\text{-}26)$$

where

ε = porosity of the ash particle.

σ = tortuosity factor.

D = diffusivity of SO_2 in the ash particle.

If the diffusion of SO_2 in ash particles can be approximated by the diffusion of SO_2 in calcined limestone, then the value of D/δ at 900°C was calculated by Hartman and Trnka (1980) to be 0.081 cm^2/sec, based on the data of Campbell et al. (1970) for the Knudsen diffusion of carbon dioxide in porous limestone with a tortuosity factor of 1.5. The ash from the combustion of 50 μm coal particles is present either in discrete particles of up to 5 μm in diameter or in an agglomerate of many individual particles of approximately 40 μm in diameter as observed under a Scanning Electron Microscope. The porosity of individual particles is very low due to melting of ash under high temperatures. On the other hand, the porosity of agglomerates is much higher due to void spaces between particles. If the general physical properties of ash are assumed to be similar to those of calcined limestone, then the porosity can be estimated as 0.5. The effective diffusion coefficient of SO_2 through ash is then $D_e \cong 0.041$ cm^2/sec. The characteristic time for diffusion of SO_2 in a 40 μm ash agglomerate is then

estimated to be $t_{D_e} \cong 10^{-4}$ sec. A similar characteristic time for diffusion in a 5 μm ash particle would put the porosity at 0.03, which is possibly within order of magnitude of the actual porosity of ash particles.

The diffusion of SO_2 through a layer of solid reaction products in the sulfation of calcined limestone was determined by Pigford and Sliger (1973) to be negligible for particles smaller than 100 μm. Since the ash particles in the combustion of coal are generally smaller than 50 μm, it is assumed that diffusion of SO_2 through solid product layer is negligible.

The small characteristic times for diffusion suggest that chemical reaction is the rate-limiting step for the capture of SO_2 in the case of uniformly distributed ash particles.

Examination of the ash samples collected in the absence of dilution air revealed a nonuniform distribution of ash deposited on the quartz filters. The majority of the ash particles appeared to be located near the center of the filter in a circular pattern. Thus it is possible that the distribution of ash particles is not radially uniform throughout the furnace, but is actually concentrated in a cylinder extending from the coal injector to the sample collector. This pattern of ash distribution does not affect the characteristic times for diffusion of SO_2 through ash particles, however it does change the characteristic time for diffusion of SO_2 in the bulk gas.

The diffusion of SO_2 through the bulk gas of the furnace in the absence of chemical reaction can be expressed in cylindrical coordinates as:

$$\frac{\partial c}{\partial t} = D \frac{1}{r} \frac{\partial}{\partial r} \left[r \frac{\partial c}{\partial r} \right] \qquad (3\text{-}27)$$

where

c = concentration of SO_2 at a distance r from the centerline of the furnace in time t.

D = mass diffusivity of SO_2 through the bulk gas.

If chemical reaction is fast relative to gas diffusion (a simplifying assumption in order to examine characteristic time of gas diffusion), then the initial and boundary conditions are:

I.C.: $c = C^0_{SO_2}$ at $t = 0$.

B.C.1: $c = 0$ at $r = R_1$ $(t > 0)$.

B.C.2: $\partial c/\partial r = 0$ at $r = R_f$ $(t > 0)$.

where

$C^0_{SO_2}$ = concentration of SO_2 in gas phase before entering reaction zone.

R_f = radius of the furnace tube.

R_1 = radius of cylinder in which ash particles are concentrated.

Using the method of separation of variables gives:

$$c(r,t) = R(r)T(t) . \tag{3-28}$$

Equation (3-27) is transformed into

$$RT' = D(R''T + \frac{1}{r}R'T) . \tag{3-29}$$

or

$$\frac{T'}{DT} = \frac{R''}{R} + \frac{1}{r}\frac{R'}{R} = -\lambda^2 \tag{3-30}$$

where λ is an eigenvalue. The time dependence of the solution can be obtained from

$$T' + D\lambda^2 T = 0 \tag{3-31}$$

which yields

$$T(t) = a_1 e^{-D\lambda^2 t} , \tag{3-32}$$

where a_1 is a constant of integration. The other half of Eq. (3-30) gives

$$r^2R'' + rR' + \lambda^2 r^2 R = 0 , \tag{3-33}$$

the solution of which is:

$$R(r) = a_2 J_0(\lambda r) + a_3 Y_0(\lambda r) , \tag{3-34}$$

where a_2 and a_3 are integration constants.

The boundary conditions give

$$\text{B.C.1: } a_2 J_0(\lambda R_1) + a_3 Y_0(\lambda R_1) = 0 , \tag{3-35}$$

and

$$\text{B.C.2: } -a_2 \lambda J_1(\lambda R_f) + a_3 \lambda Y_1(\lambda R_f) = 0 , \tag{3-36}$$

which yields the spatial dependence of the solution:

$$R(r) = -a_3 \left\{ \frac{Y_0(\lambda R_1)}{J_0(\lambda R_1)} J_0(\lambda r) - Y_0(\lambda r) \right\} . \tag{3-37}$$

The general solution is obtained by combining Eqs. (3-32) and (3-37),

$$c(r,t) = \sum_{n=1}^{\infty} A_n \left\{ \frac{Y_0(\lambda_n R_1)}{J_0(\lambda_n R_1)} J_0(\lambda_n r) - Y_0(\lambda_n r) \right\} e^{-D\lambda_n^2 t} \tag{3-38}$$

The furnace radius R_f is 2.5 cm and if R_1 is assumed to be 1 cm, then the eigenvalues can be solved from Eqs. (3-35) and (3-36). The first two eigenvalues are $\lambda_1 \cong 0.9$ cm^{-1} and $\lambda_2 \cong 3.1$cm^{-1}. Since λ_2^2 is sufficiently larger than λ_1^2, the general solution can be approximated by the first term in the series:

$$c(r,t) \cong A_1 \left\{ \frac{Y_0(\lambda_1 R_1)}{J_0(\lambda_1 R_1)} J_0(\lambda_1 r) - Y_0(\lambda_1 r) \right\} e^{-D\lambda_1^2 t} \tag{3-39}$$

The initial conditions yield

$$c(r,o) = C^{o}_{SO_2} = A_1 \left\{ \frac{Y_0(\lambda_1 R_1)}{J_0(\lambda_1 R_1)} J_0(\lambda_1 r) - Y_0(\lambda_1 r) \right\}. \tag{3-40}$$

Combining Eqs. (3-39) and (3-40) gives the relative concentration of SO_2 as a function of time,

$$\frac{c(r,t)}{C^{o}_{SO_2}} = e^{-0.81Dt} \tag{3-41}$$

The decrease in SO_2 concentration is plotted versus time in Fig. 3.19, which covers the range of temperatures in the reaction zone. At an average temperature of 1200°K, the concentration of SO_2 in the annular region between the cylinder of ash particles and the furnace wall decreases 50% in 0.6 second and 90% in 2.0 seconds. Since the reaction time for $CaSO_4$ formation in the combustion experiments ranges from 0.6 second to 5.5 seconds, the diffusion of SO_2 in the gas phase can present a resistance to the reaction rate if the distribution of ash particles is centered in the inner region of the furnace.

3.4.2 Effect of Oxygen Concentration

The effects of varying oxygen concentration on sulfur capture are also exhibited in Figs. 3.13-3.15. The results show that as oxygen concentration increases, there is a corresponding increase in the observed sulfur capture. The experimentally determined first order reaction rate constants for reaction (3-18) are plotted in Fig. 3.20. For the three coal samples examined in this study, the first order rate constants remain constant as oxygen concentration is increased from 13% to 21%. This trend suggests that sulfur capture is zeroth order with respect to oxygen in the range of 13% to 21% oxygen. However, at oxygen levels above 21%, the first order rate constant increases as oxygen concentration in the gas increases. Analysis of the effect of oxygen reveals that the order of reaction is not constant with respect to oxygen concentration.

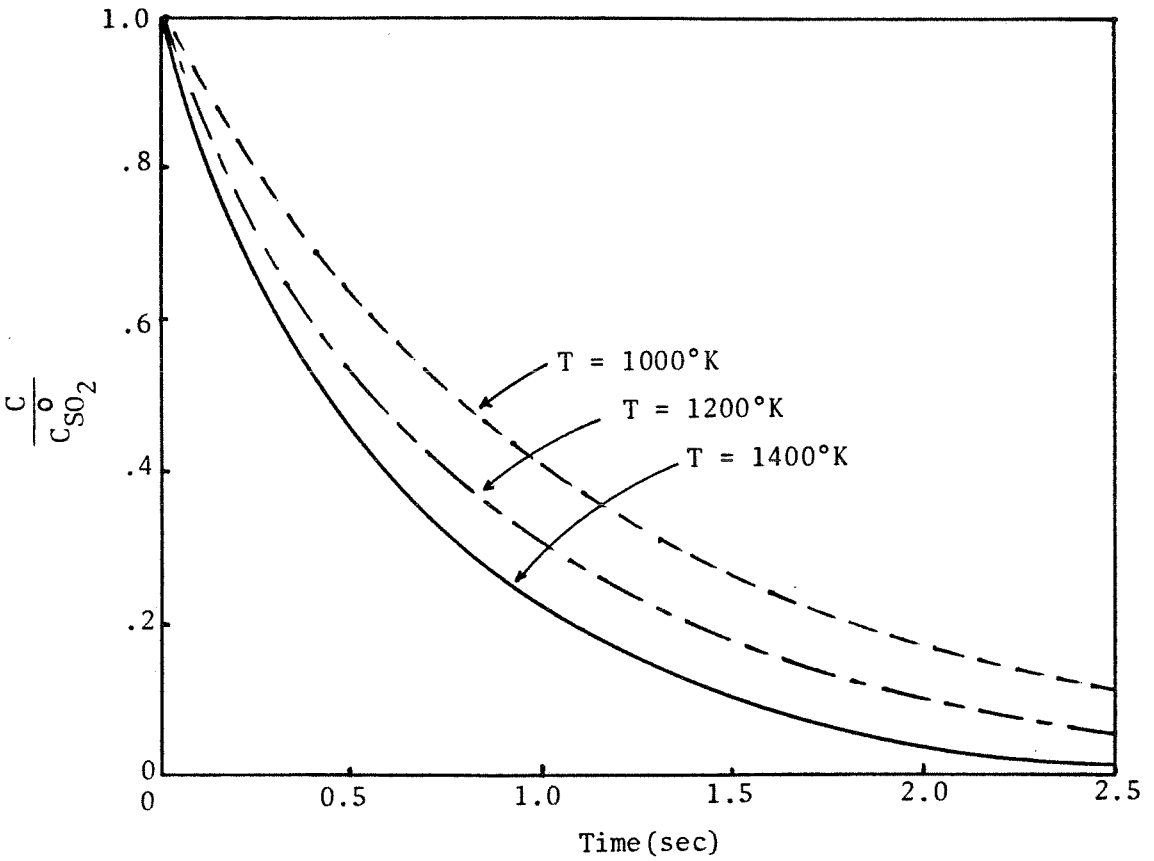

Fig. 3.19 Relative concentration ($C/C^{o}_{SO_2}$) of SO_2 as a function of time for the diffusion of SO_2 through bulk gas as described in equation (3-41).

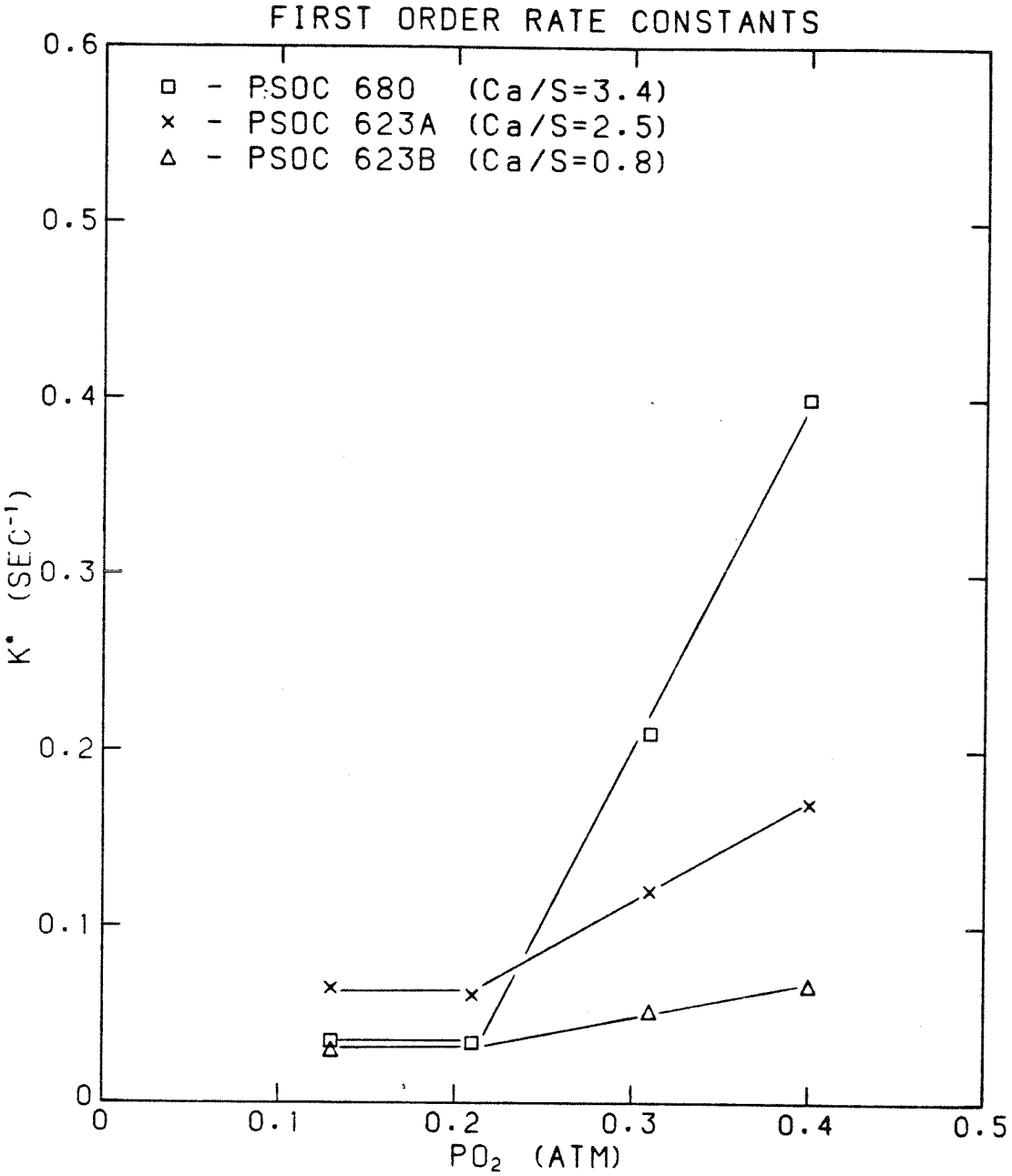

Fig. 3.20 The effect of oxygen on first order reaction rate constants.

Although SO_2 absorption on CaO in the ash according to reaction (3-17) appears to be the dominant mechanism of sulfur capture, other mechanisms may also occur. One possibility is the vaporization of calcium in a high-temperature environment such as that surrounding a burning char particle (Quann and Sarofim, 1982). The calcium vapors diffusing outside the particle would reoxidize to form CaO aerosol particles of very high surface area that would be effective in capturing SO_2.

Calcium vaporization can occur by the reduction of calcium oxide in a reducing environment during the combustion of char particles,

$$CaO(s) + CO(g) \rightleftharpoons Ca(g) + CO_2(g) . \tag{3-42}$$

The equilibrium partial pressure of calcium is determined from the equilibrium constant

$$K = \frac{P_{CO_2} P_{Ca}}{P_{CO}} . \tag{3-43}$$

At high temperatures, the primary product of carbon combustion is carbon monoxide (Mulcahy and Smith, 1969). Thus if the only source of CO_2 is from reaction (3-42), the partial pressure of CO_2 can be assumed to be equal to the partial pressure of calcium. The equilibrium partial pressure of calcium is then

$$P_{ca} = (KP_{CO})^{1/2} . \tag{3-44}$$

To estimate the amount of calcium vaporized, it was assumed that the rate of vaporization is limited by diffusion from the particle surface to the free stream. In this case the rate of calcium vaporization can be calculated by (Senior and Flagan, 1982)

$$R_{Ca} = \frac{y_{Ca} R_c}{1 - e^{-P_e}} , \tag{3-45}$$

where

R_c = rate of carbon combustion,

y_{Ca} = mass fraction of calcium vapor at the particle surface,

and the Peclet number, P_e, at the particle surface is defined as

$$P_e = \frac{R_c}{4\pi r_p c D}, \tag{3-46}$$

where

r_p = radius of the coal particle.

c = gas concentration at the particle surface.

D = diffusivity of gas at the particle surface.

A particle combustion model developed by C. L. Senior (1984) was used to calculate the transient particle temperature, partial pressure of CO at the particle surface and the combustion rate. The equilibrium constant K was calculated at the average particle temperature T_p with thermodynamic data from the JANAF Tables (Dow Chemical Company, 1971) and Stern and Weise (U.S. National Bureau of Standards, 1966). The calcium mass fraction Y_{Ca} was then calculated from (3-45). The rate of calcium vaporization was integrated with respect to time from ignition to 95% burnoff to obtain the total amount vaporized during combustion.

The calculated calcium vaporization is summarized in Fig. 3.21 by plotting the cumulative percent of calcium vaporized as a function of oxygen during combustion of a coal containing 2.5% calcium. The estimated calcium vaporization is in good agreement with observed data reported by Quann (1982), Fig. 3.22, during combustion of a lignite. The extent of vaporization increases with oxygen content since higher particle temperatures at high oxygen concentra-

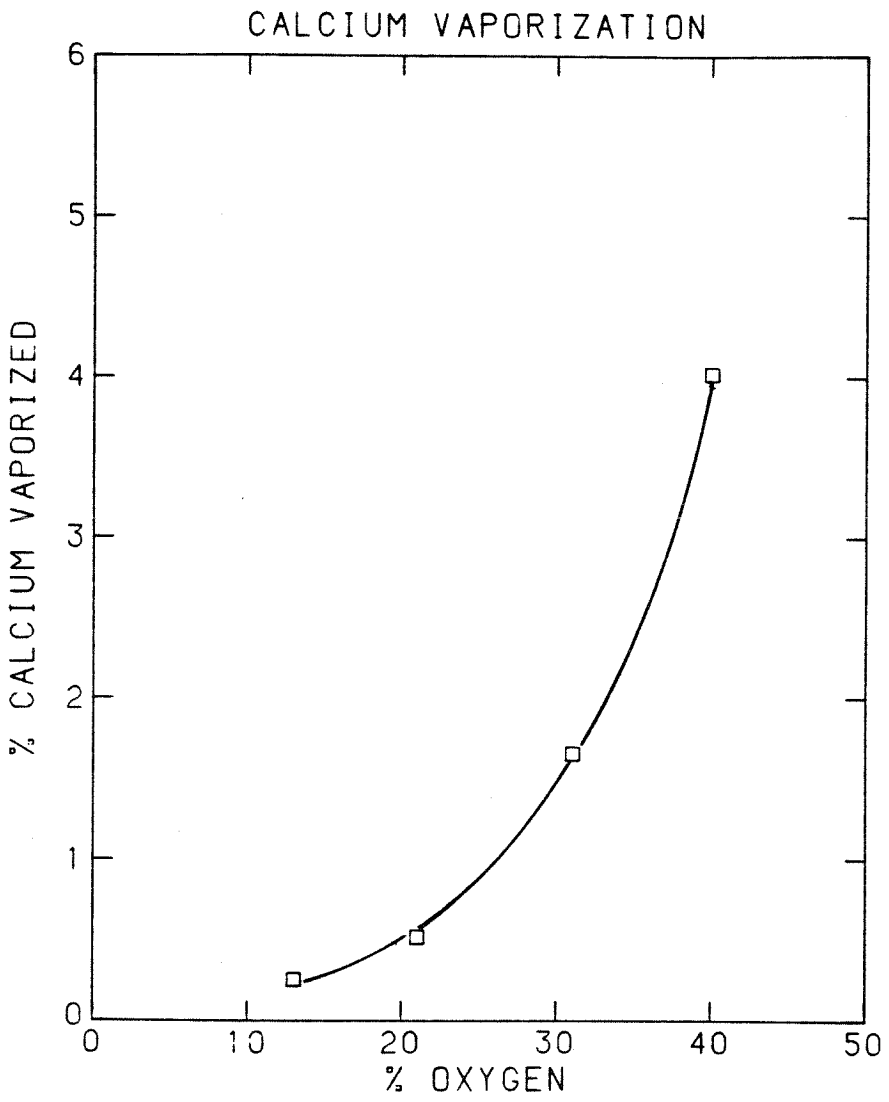

Fig. 3.21 Calculated calcium vaporization during combustion of a coal with 2.5% Ca at a furnace temperature of 1600°K.

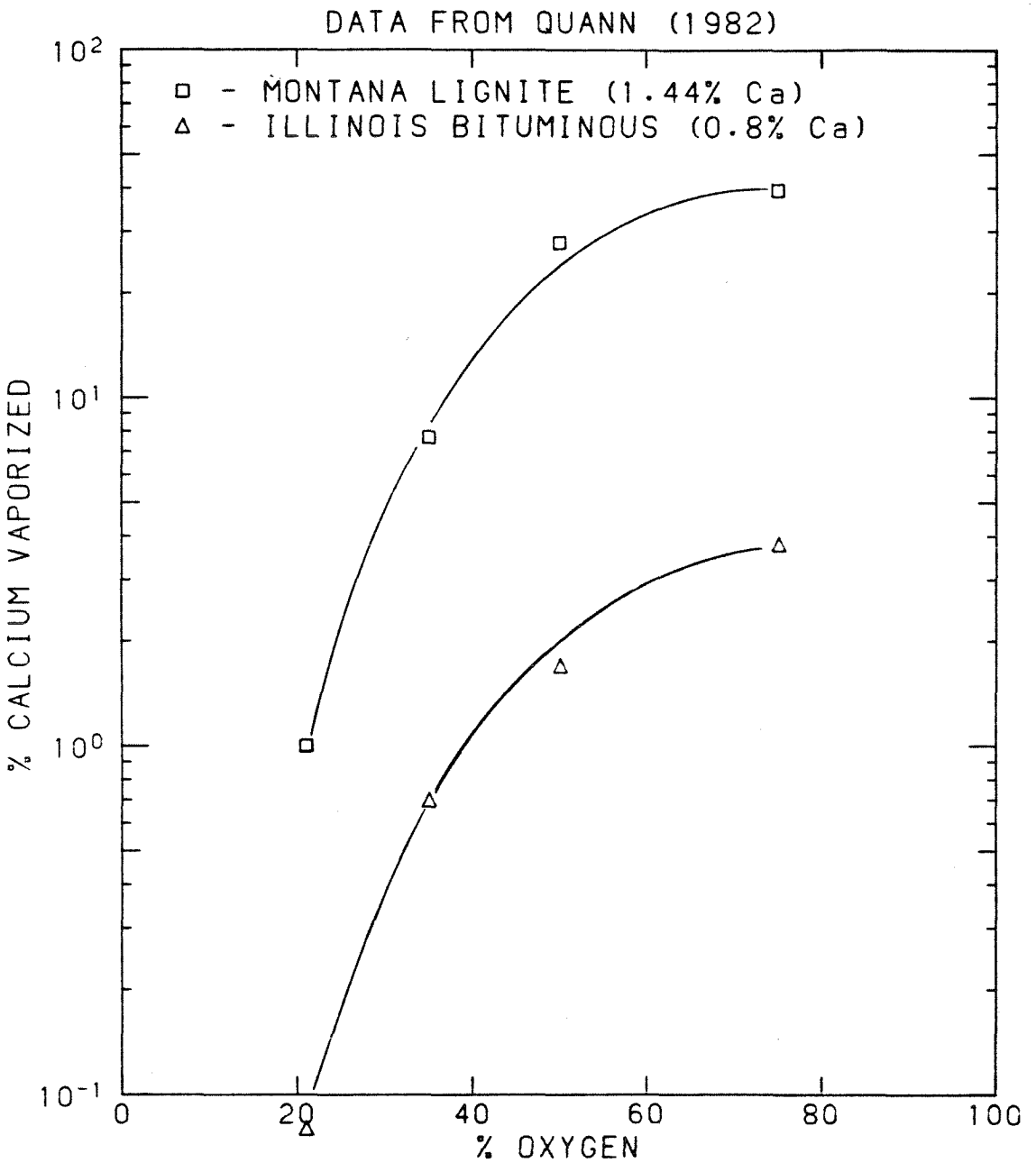

Fig. 3.22 The effect of oxygen on vaporization of calcium during combustion of pulverized coals at a furnace temperature of 1750°K (data of Quann).

tions accelerate the vaporization. However, the total amount of calcium vaporized under experimental conditions examined in this study is in all cases less than 5%. This analysis shows that the effect of calcium vaporization on sulfur capture is relatively small.

3.4.3 Effect of Calcium Content

The three coal samples used for this study were prepared with varying amounts of calcium to examine the effect of Ca/S ratio on sulfur retention and the efficiency of the ion-exchanged calcium in capturing sulfur. The results for combustion experiments conducted with 40% O_2 are compared in Fig. 3.23. The extent of sulfur capture is observed to increase approximately proportional to the increase in the Ca/S ratio of the coal sample, although there does not appear to be any noticeable difference due to coal types other than the effect of Ca/S content of the coal. This same trend is also apparent in the experiments conducted with 31% O_2 as shown in Fig. 3.24.

Earlier discussions have indicated that the capture of SO_2 by CaO in coal ash is chemical reaction-rate limited during combustion of 50 μm coal particles. Thus theoretically, the extent of sulfur capture should be independent of calcium content in the coal if there is a sufficient excess of calcium. The observed dependence of sulfur capture on calcium content suggests that the efficiency of calcium is rather low, possibly due to the inaccessibility or deactivation of part of the calcium content.

Huffman et al. (1981) reported that calcium in coal acts as a fluxing agent in accelerating the melting of ash under reducing conditions at 1200°K to 1400°K and under oxidizing conditions at 1500°K to 1700°K. The particle temperatures achieved in this study far exceeded the melting temperature of calcium-enriched ash, and the glassy, spherical appearance of the ash particles when

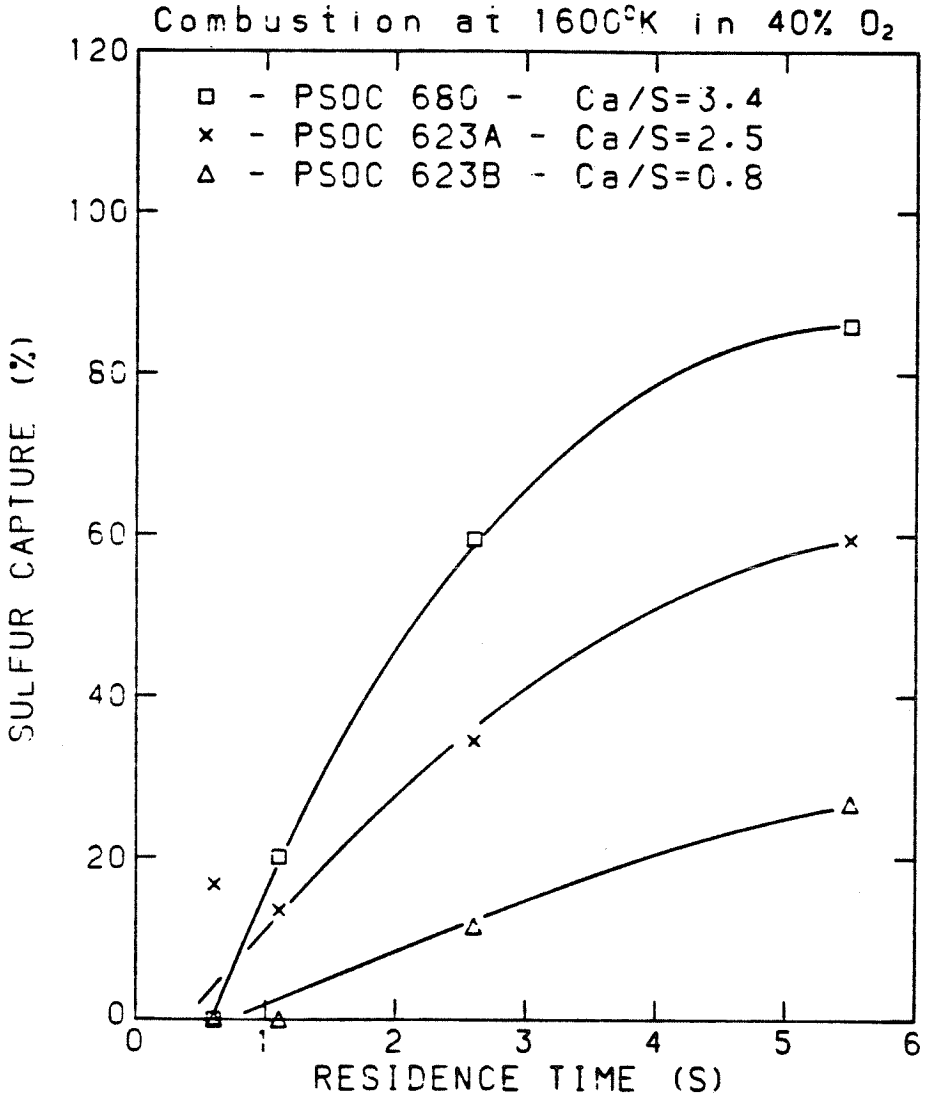

Fig. 3.23 Effect of calcium content on sulfur retention for combustion of coal in 40% O_2.

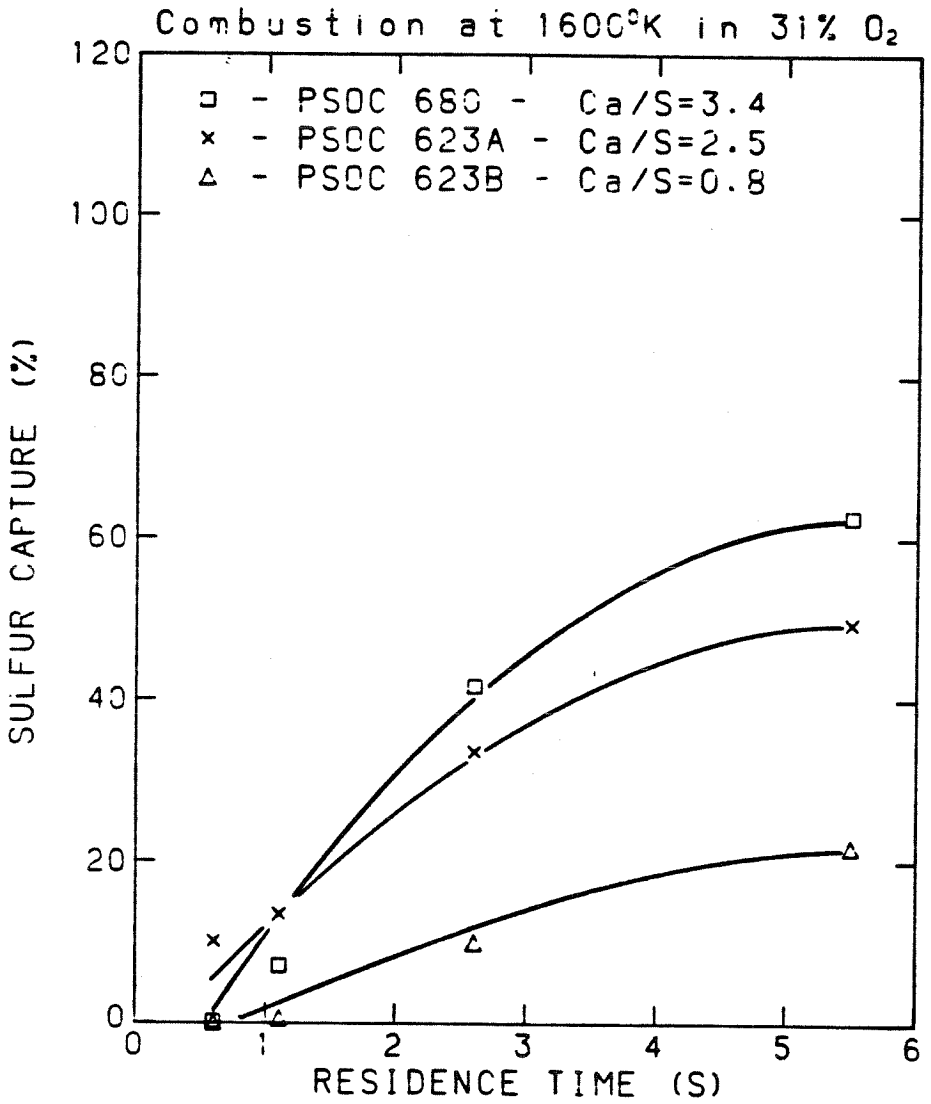

Fig. 3.24 Effect of calcium content on sulfur retention for combustion of coal in 31% O_2.

examined under a microscope indicate that a considerable extent of ash melting occurs, thereby consuming part of the calcium. Calcium oxide has also been found to react with alumina and silica to form aluminate and silicate at approximately 1500°K (Cobb, 1910). In the presence of both alumina and silica, calcium aluminosilicates are formed. Since the major components of coal ash are alumina and silica, thus a fraction of the calcium is lost due to the formation of aluminosilicates and becomes unavailable for sulfur capture (Raask, 1982). Baker and Attar (1981) and Newman (1941) further found that $CaSO_4$ decomposes faster when mixed with silica and aluminosilicates, thus suggesting an even lower efficiency of sulfur capture by the calcium in coal. The possible loss of calcium due to the formation of aluminosilicates is consistent with the observed dependence of sulfur capture on the calcium content of coal samples. However, calcium deactivation cannot be quantified without knowledge of the extent of formation of calcium aluminosilicates.

3.4.4 Effect of Furnace Temperature

The effect of furnace temperature on sulfur capture during combustion of PSOC 680 (Ca/S = 3.4) is shown in Fig. 3.25. At the most favorable conditions for sulfur capture, 0.5 l/min gas flow rate and 40% O_2, there is virtually no difference in the results for experiments conducted at furnace temperatures 1400°K and 1600°K. This is because at sulfur capture levels of above 90%, any actual difference would be relatively small. However, as gas flowrate increases, the extent of sulfur capture for experiments at 1400°K increases rapidly compared to experiments conducted at 1600°K. This observed trend is most probably due to the combined effects of longer reaction times and lower particle temperatures at the lower furnace temperature.

The reaction time was defined earlier as the residence time of particles

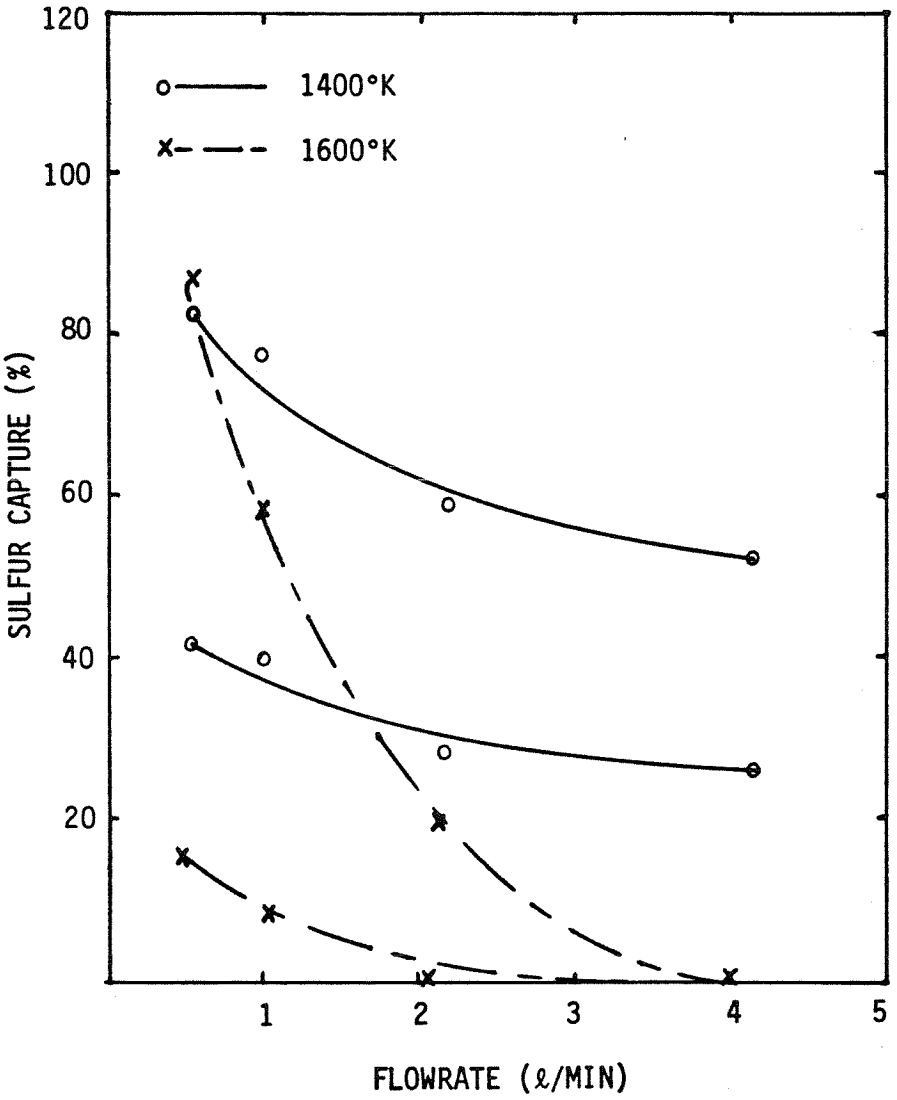

Fig. 3.25 Effect of furnace temperature on sulfur retention during combustion of PSOC 680 (Ca/S = 3.4).

through the furnace zone where the temperatures favor capture of SO_2 by CaO. Since the furnace temperature of 1400°K is approximately the temperature at which the formation of $CaSO_4$ becomes thermodynamically favorable, the reaction time for sulfur capture with a furnace temperature of 1400°K is then the residence time of the particle in the furnace from the location where the particle temperature approaches that of the furnace to the point where dilution air is introduced. The results of the experiments conducted at a furnace temperature of 1400°K showing the effects of the redefined particle residence time are presented in Fig. 3.26. Analysis of the data according to first order kinetics with respect to SO_2 gives first order reaction rate constants of 0.067 sec^{-1} at 40% O_2 and 0.016 sec^{-1} at 21% O_2. The observed rate constants are smaller than those obtained at a furnace temperature of 1460°K due to the difference in the temperature-time history of the particles, particularly since the reaction rate is time averaged over the entire temperature range. The maximum reaction rate of the sulfation of calcined limestone was reported to be approximately at 1220°K (Borgwardt, 1970; Borgwardt and Harvey, 1982). The reaction rate decreases as temperatures diverge from 1220°K. Thus, increasing the overall reaction time by increasing the particle residence time at 1400°K would effectively decrease the average reaction rate.

The particle temperatures attained during pulverized combustion at 1400°K are much lower than at 1600°K, as illustrated by the calculated temperatures in Fig. 3.27. The lower particle temperatures and the higher levels of sulfur capture at low reaction times for experiments conducted at 1400°K suggest possible effects from other mechanisms of sulfur capture than just the recapture of SO_2 by CaO in the ash. Under reducing conditions during the early stages of combustion, CaS is formed by the reaction of CaO with gaseous sulfur species (Freund and Lyon, 1982) as indicated by reactions (3-10) to (3-12). The sulfide is

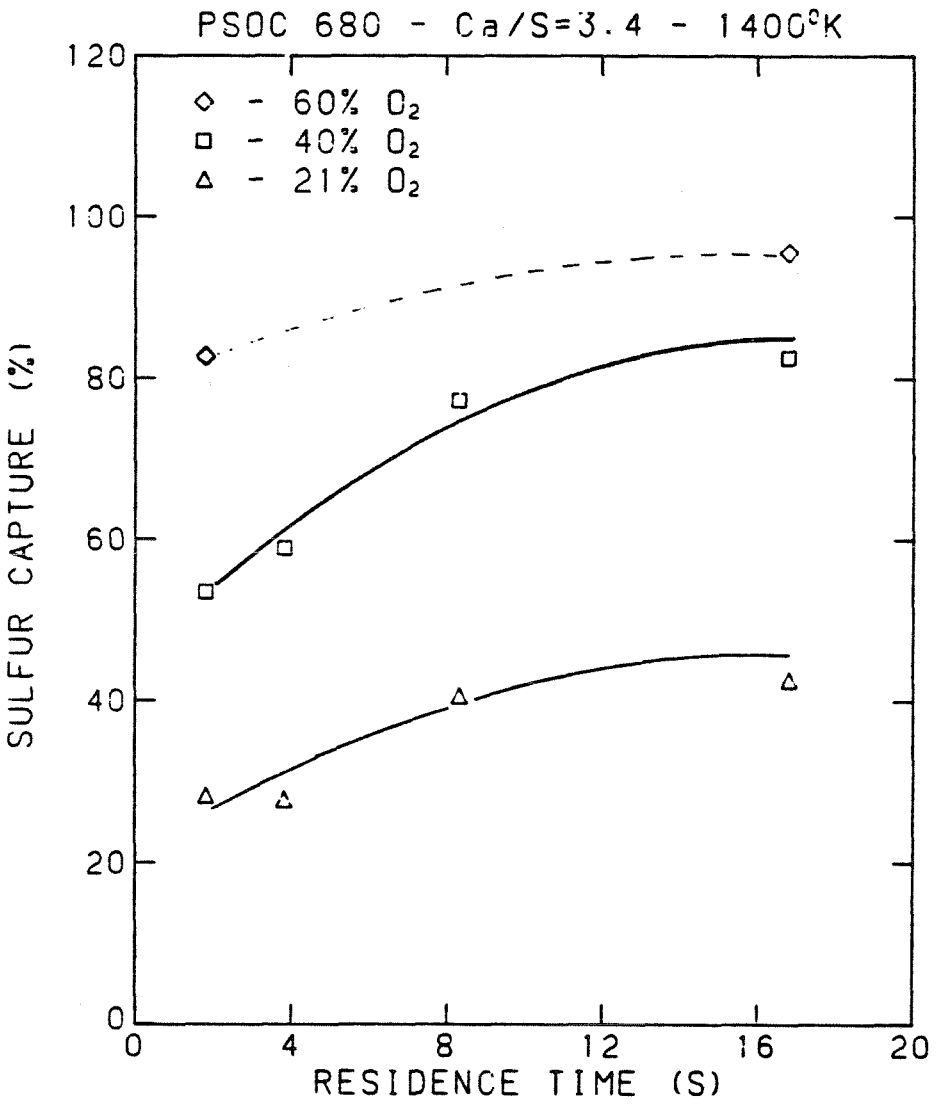

Fig. 3.26 Effect of residence time on sulfur retention during combustion of PSOC 680 (Ca/S = 3.4) at a furnace temperature of 1400°K.

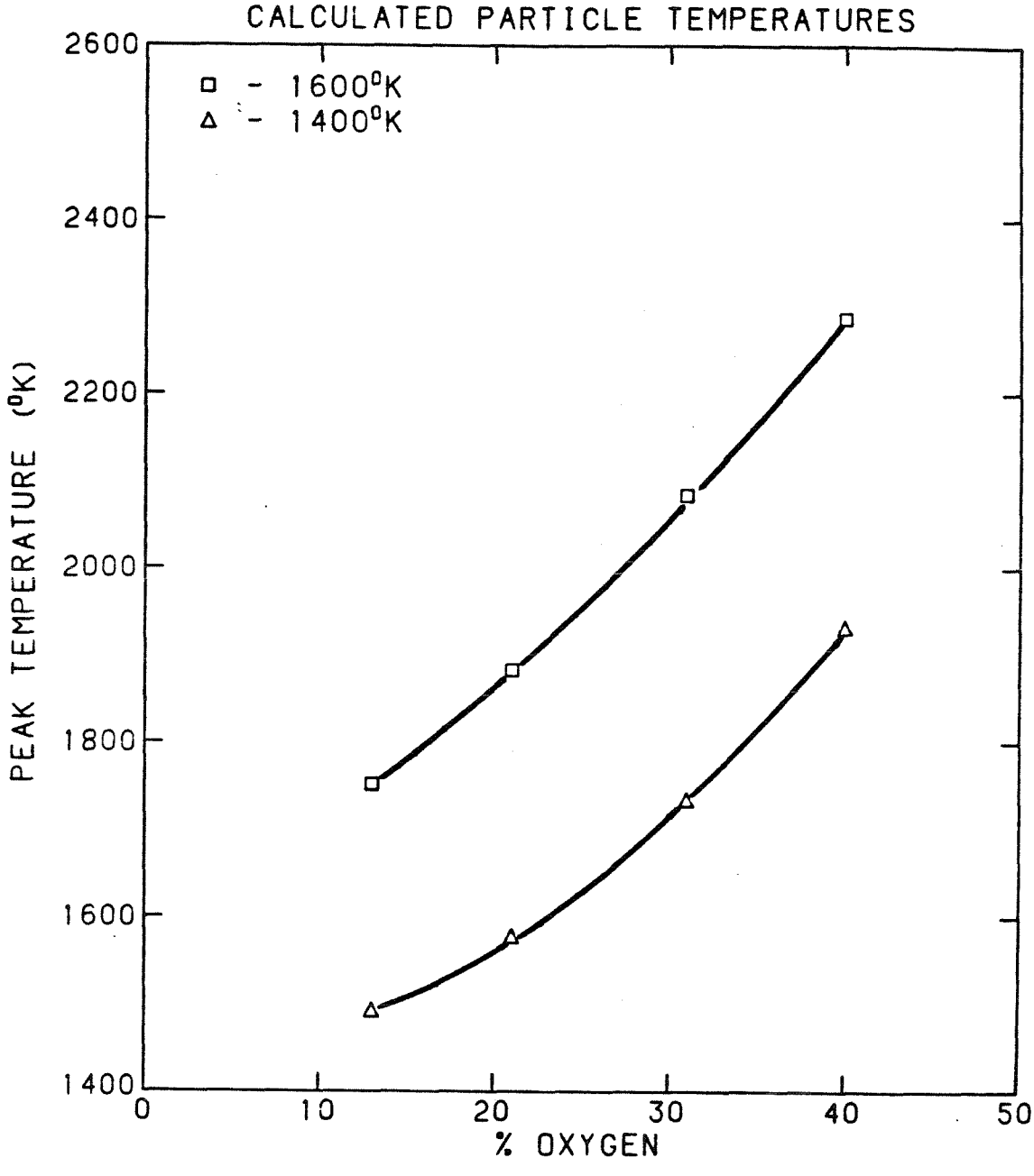

Fig. 3.27 Theoretical calculation of particle temperature for the combustion of a bituminous coal with a diameter of 50 μm.

subsequently oxidized to $CaSO_4$. In the case of higher furnace temperature of 1600°K, the $CaSO_4$ formed readily decomposes to CaO and SO_2. In the case of the lower furnace temperature of 1400°K, the rate of $CaSO_4$ decomposition would be considerably slower at lower particle temperatures. Thus the overall sulfur capture would be due to the capture of sulfur during combustion of coal and the post-combustion recapture of SO_2 by CaO in the ash particles.

3.5 Conclusions

The retention of sulfur during the combustion of calcium-ion-exchanged coals was studied in a laminar flow furnace under strongly fuel-lean conditions. It was observed that the extent of sulfur retained in coal ash increased with increasing particle residence time and increasing oxygen concentration in the combustion gas. Sulfur capture was also observed to increase in proportion to an increase in the Ca/S content of the coal. Analysis of the results indicates that chemical reaction is the rate-limiting step in the capture of SO_2 by CaO in coal ash to form $CaSO_4$. Diffusion of SO_2 through the combustion gas was also found to have a possible effect on the reaction rate due to the inhomogeneity of the distribution of coal ash.

The findings of this study suggest that in the reducing environment generated during early stages of combustion, a fraction of the sulfur in coal may react with CaO to form CaS. As the particle environment becomes oxidizing, CaS is oxidized to $CaSO_4$ which then readily decomposes to release SO_2. However, if the furnace temperature is sufficiently low, e.g. 1400°K or lower, then the rate of decompostion is slower, thus part of the sulfur is never released into the combustion gas. At the high temperatures attained during combustion, CaO or $CaSO_4$ can react with alumina and silica present in the ash, therefore removing a portion of the calcium from further reactions and decreasing the efficiency of

the original calcium content from capturing sulfur. The major fraction of sulfur retention is derived from the recombination of SO_2 and O_2 with CaO in the lower region of the furnace where temperatures are favorable for the stability of $CaSO_4$.

References

Baker, D. C. and Attar, A., Env. Sci. Tech. **15**:288-293 (1981).

Borgwardt, R. H., Env. Sci. Tech. **4**:59-63 (1970).

Borgwardt, R. H. and Harvey, R. D., Env. Sci. Tech. **6**:351-360 (1972).

Campbell, F. R., Hills, A. W. D. and Paulin, A., Chem. Eng. Sci. **25**:929 (1970).

Case, P. L., Heap, M. P., McKinnon, C. N., Pershing, D. W. and Payne, R., Prepr. ACS Fuel Chemistry Division **27**:158-166 (1982).

Cobb, J. W., J. Soc. Chem. Ind. **29**:250-259 (1910).

Crank, J., "Mathematics of Diffusion", Oxford University Press (1956).

Dow Chemical Company, Thermal Research Laboratory, JANAF Tables, 2nd ed., National Bureau of Standards, Washington, D.C.

Freund, H. and Lyon, R. K., Comb. Flame **45**:191-203 (1982).

Hartman, M. and Coughlin, R. W., AIChE J. **22**:490-498 (1976).

Hartman, M. and Trnka, D., Chem. Eng. Sci. **35**:1189-1194 (1980).

Hirschfelder, J. O., Curtiss, C. F. and Bird, R. B., "Molecular Theory of Gases and Liquids", Wiley, New York (1954).

Huffman, G. P., Huggins, F. E. and Dunmyre, G. R., Fuel **60**:585-597 (1981).

Libby, P. A. and Blake, T. R., Comb. Flame **36**:139-169 (1979).

McClellan, G. H., Hunter, S. R. and Scheib, R. M., Spec. Tech. Publ., No. 472, p. 32, ASTM (1970).

Mulcahy, M. F. R. and Smith, I. W., Rev. Pure Appl. Chem. **19**:81-107 (1969).

Newman, E. S., Journal of Research of the NBS **27**:9-196 (1941).

Pigford, R. L. and Sliger, G., Ind. Eng. Chem. Proc. Des. Dev. **12**:85-91 (1973).

Quann, R. J. and Sarofim, A. F., 19th Symp. (Int.) Combustion Institute, Pittsburg, pp. 1429-1440 (1982).

Quann, R. J., "Ash Vaporization under Simulated Pulverized Coal Combustion Conditions", PhD Thesis, Massachusetts Institute of Technology (1982).

Raask, E., Prog. Energy Comb. Sci. **8**:26-276 (1982).

Schafer, H. N. S., Fuel **49**:197-213 (1970).

Schafer, H. N. S., Fuel **49**:271-280 (1970).

Senior, C. L. and Flagan, R. C., Aerosol Sci. Tech. :371-383 (1982).

Senior, C. L., "Submicron Aerosol Formation during Combustion of Pulverized Coal", PhD Thesis, California Institute of Technology (1984).

Stern, K. H. and Weise, E. L., "High Temperature Properties and Decomposition of Inorganic Salts", NSRDS-NBS 7, U. S. National Bureau of Standards, Washington, D.C. (1966).

CHAPTER 4

CONCLUSIONS AND RECOMMENDATIONS

4.1 Conclusions

1. Lignite coal possesses significant ion-exchange capacity which can be used to introduce calcium ions into the coal matrix in a molecular scale, uniform distribution. The ion-exchange capability is due to the presence of carboxyl and phenolic hydroxyl groups in the coal. For exchange of the lignite, coal can achieve Ca/S ratios greater than 7. Bituminous coal contains a considerably lower ion-exchange capacity than lignite coal. The concentration of available carboxyl and phenolic groups was increased by oxidation in air at 195°C and 260°C. Ion exchange of the oxidized bituminous coal could result in Ca/S contents greater than 2.5.

2. The initial rate of ion exchange increased as the calcium-ion concentration or temperature of the reaction was raised. This higher initial rate could be due to faster reaction rate and higher driving force for diffusion of ions across a liquid film surrounding coal particles.

3. The rate of ion exchange increased appreciably as the pH value of the exchange solution was increased. The increase in rate at higher pH values is due mainly to the higher ion-exchange capacity as more acidic groups readily undergo cation exchange.

4. Particle diffusion was found to be the rate-determining step for the process of ion exchange. Analysis of the results with a simple model for particle diffusion indicated that the diffusion coefficient of calcium ions was approximately 1.6×10^{-8} cm^2/sec for diffusion in PSOC 623. The diffusion coefficient in PSOC 680 was estimated at 5.0×10^{-11} to 3.5×10^{-10} cm^2/sec. This difference could probably be due to the different electric potentials in the

pore structures generated by ionic interactions.

5. Emission of SO_2 during fuel-lean combustion of calcium-ion-exchanged coals was observed to decrease with increasing particle residence time. Analysis of the results suggested that SO_2 was released during combustion of the coal samples and was captured by CaO in the cooler region of the furnace where thermodynamics together with kinetics favor the formation of $CaSO_4$.

6. Chemical reaction was found to be the rate-determining step in the capture of SO_2 by CaO in coal ash. Diffusion of SO_2 from the gas phase to the ash particles could also affect the reaction rate due to the inhomogeneity of the radial dispersion of coal ash in the combustion furnace.

7. Sulfur retention was observed to increase as oxygen concentration in the combustion gas was increased. This trend may be partially due to vaporization of calcium at the high particle temperatures attained during combustion in higher oxygen concentrations, which would then result in CaO aerosol particles of high surface area that would be effective in capturing SO_2.

8. The efficiency of sulfur capture by the exchanged calcium was found to be lower than theoretically possible. This result could be due to a loss of calcium from the formation of aluminosilicates and thus becoming unavailable for sulfur capture.

4.2 Recommendations

1. The present study examined the kinetics of ion exchange of carboxylic-acid groups in coal. A further study examining the kinetics of exchange of all acid groups in coal would be informative.

2. The diffusivity of ions in coal were found to be several orders of magnitude slower than in an electrolyte solution. A study of the surface area and pore

size distribution of the coal as a function of extent of ion exchange can be useful in the understanding of the diffusion process.

3. The efficiency of sulfur capture by exchanged calcium was affected by the presence of alumina and silica in the coal. The interference can be eliminated by preparing synthetic coals in which ion-exchanged calcium is the only mineral present. The particle temperature and vaporization of calcium should also be measured to fully understand the role and efficiency of calcium in the retention of sulfur.

4. A detailed surface area study of the coal and ash from combustion should be conducted in order to examine the effect of particle surface area on the efficiency of sulfur capture. The temperature profile of the reaction zone should also be incorporated into the analysis of the results so that kinetic parameters may be obtained.

APPENDIX

FURNACE CALIBRATION

The overall SO_2 balance in the combustion furnace was determined by a series of calibration runs with a gas of known SO_2 concentration under experimental conditions. At each flowrate, the SO_2 concentration in the gas was set by a mixture of air and 1005 PPM SO_2 in air to simulate the SO_2 concentration in the furnace during combustion of coal. At the start of a run, the flow of air was introduced into the furnace through the inlet for main combustion gas, while the flow of 1005 PPM SO_2 was fed through the coal injector. The exit gas mixture was scrubbed through two gas-washing bottles containing a solution of 1% H_2O_2. The total amount of SO_2 collected in a four-hour run was analyzed by titration of the H_2O_2 solution.

The first calibration run was conducted with the furnace at room temperature. The overall SO_2 balance obtained was 99.7%, which suggested that there were no leaks in the system. The results for the calibration runs conducted at experimental temperatures are as follows:

Flowrate (l/min)	**%SO_2 Balance**
4.1	92
2.1	89
1.0	88
0.5	84

The results of the calibration runs show that there is a loss of SO_2 through the furnace at high temperatures. Since the system is closed and has no leaks, the

losses can only be due to the lower part of the furnace where the alumina-insulated sample collector is located. If the recombination of SO_2 with CaO to form $CaSO_4$ occurs in the cooler region of the furnace and the reaction is negligible as the combustion gases are cooled and diluted with air entering the sample probe, then the actual sulfur emission can be calculated as

$$S^* = \frac{S}{\varphi}, \tag{A-1}$$

where

S^* = corrected sulfur emission.

S = measured sulfur emission.

φ = correction factor as determined by calibration experiments.

Tables A.1 to A.4 summarize the results of the combustion experiments taking into consideration the losses of SO_2 in the furnace. In several cases, the correction results in sulfur balances exceeding unity, which could be due to several factors: experimental error, inhomogeneity of coal samples and a simplification of the correction. Duplicate runs conducted at most cases showed the results to be reproducible to approximately 5%.

Table A.1

Corrected data for retention of sulfur during combustion of PSOC 623A (Ca/S = 2.5) at a furnace temperature of 1600°K

% O_2	Flowrate (l/min)	% S emission (measured)	% S emission (corrected)	% S capture
40	4.1	76.6	83.3	16.7
	2.1	77.0	86.5	13.5
	1.0	57.6	65.5	34.5
	0.5	34.0	40.5	59.5
30.6	4.1	82.7	89.9	10.1
	2.1	77.0	86.5	13.5
	1.0	58.4	66.4	33.6
	0.5	42.4	50.5	49.5
21	4.1	94.7	102.9	0
	2.1	86.0	96.6	3.4
	1.0	74.7	84.9	15.1
	0.5	62.3	74.2	25.8
13.1	4.1	93.8	102.0	0
	2.1	83.4	93.7	6.3
	1.0	71.8	81.6	18.4
	0.5	60.6	72.1	27.9

Table A.2

Corrected data for retention of sulfur during combustion of PSOC 623B (Ca/S = 0.8) at a furnace temperature of 1600°K

% O_2	Flowrate (l/min)	% S emission (measured)	% S emission (corrected)	% S capture
40	4.1	96.0	104.3	0
	2.1	93.5	105.1	0
	1.0	77.8	88.4	11.6
	0.5	61.5	73.2	26.8
30.6	4.1	99.3	107.9	0
	2.1	88.5	99.4	0.6
	1.0	79.2	90.0	10.0
	0.5	65.6	78.1	21.9
21	4.1	117.5	127.7	0
	2.1	92.3	103.7	0
	1.0	82.2	93.4	6.6
	0.5	73.0	86.9	13.1

Table A.3

Corrected data for retention of sulfur during combustion of PSOC 680 (Ca/S = 3.4) at a furnace temperature of 1600°K

% O_2	Flowrate (l/min)	% S emission (measured)	% S emission (corrected)	% S capture
40	4.1	95.0	103.3	0
	2.1	71.1	79.9	20.1
	1.0	35.6	40.5	59.5
	0.5	11.8	14.0	86.0
30.6	4.1	91.9	99.9	0.1
	2.1	82.7	92.9	7.1
	1.0	51.3	58.3	41.7
	0.5	31.3	37.3	62.7
21	4.1	97.0	105.4	0
	2.1	98.6	110.8	0
	1.0	80.1	91.0	9.0
	0.5	71.7	85.4	14.6
13.1	4.1	94.1	102.3	0
	2.1	94.1	105.7	0
	1.0	79.1	89.9	10.1
	0.5	71.6	85.2	14.8

Table A.4

Corrected data for retention of sulfur during combustion of PSOC 680 (Ca/S = 3.4) at a furnace temperature of 1400°K

% O_2	Flowrate (l/min)	% S emission (measured)	% S emission (corrected)	% S capture
60	4.1	15.9	17.3	82.7
	0.5	3.7	4.4	95.6
40	4.1	42.8	46.5	53.5
	2.1	36.5	44.0	59.0
	1.0	20.0	22.7	77.3
	0.5	14.6	17.4	82.6
21	4.1	66.0	71.7	28.3
	2.1	64.3	72.2	27.8
	1.0	52.2	59.3	40.7
	0.5	48.1	57.3	42.7
30.7	0.5	43.6	51.9	48.1